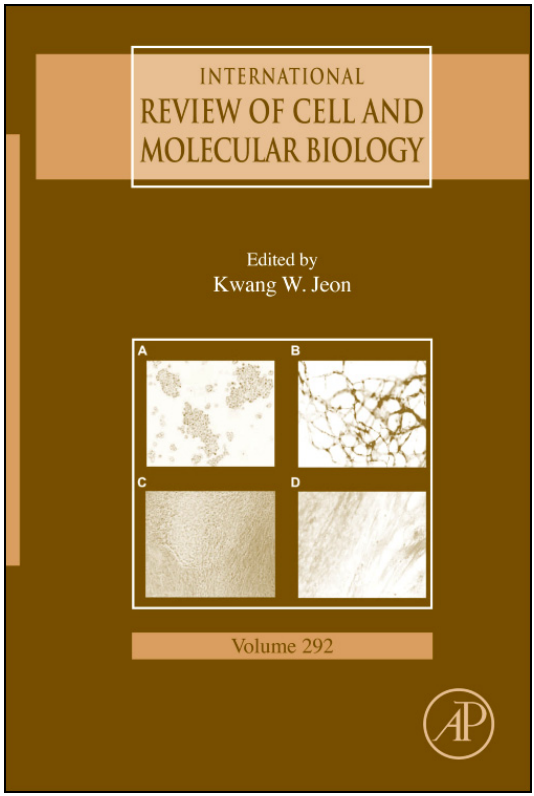

From: Christopher H.S. Aylett, Jan Löwe, and Linda A. Amos, New Insights into the Mechanisms of Cytomotive Actin and Tubulin Filaments. In Kwang W. Jeon, editor: International Review of Cell and Molecular Biology, Vol. 292, Burlington: Academic Press, 2011, pp. 1-71.
ISBN: 978-0-12-386033-0

CHAPTER ONE

New Insights into the Mechanisms of Cytomotive Actin and Tubulin Filaments

Christopher H.S. Aylett, Jan Löwe, *and* Linda A. Amos

Contents

1. Introduction 2
2. Mechanisms of Directed Movement 3
   2.1. Treadmilling 4
   2.2. Dynamic instability 4
   2.3. Choice of mechanism is determined by subtle differences 4
   2.4. Membrane shaping and remodeling 5
3. The Tubulin/FtsZ Family 6
   3.1. Evolutionary gap in living organisms 6
   3.2. Filaments and tubes 11
   3.3. Conformational changes in protofilaments 12
   3.4. Atomic structures of tubulin family 14
   3.5. Assembly and the nucleotide hydrolysis cycle 19
   3.6. New insights from TubZ filaments 20
   3.7. Lateral interactions in the tubulin family 25
   3.8. Roles of the C-termini 30
   3.9. Tubulin-binding drugs 31
   3.10. EB proteins 34
   3.11. So, what is the initial state of GTP-bound protofilaments? 36
   3.12. Control of microtubule dynamics by accessory proteins 38
   3.13. γ-Tubulin complexes 39
   3.14. Less well-known tubulin family members 40
   3.15. Microtubules are flexible in spite of being stiff 41
4. The Actin Family 42
   4.1. Actin family filament complexes 43
   4.2. Atomic structures of the actin family 43
   4.3. Nucleotide hydrolysis 48
   4.4. Lateral interactions in actin filaments 49
   4.5. Filament dynamics in the actin family 52

MRC Laboratory of Molecular Biology, Cambridge, UK

International Review of Cell and Molecular Biology, Volume 292
ISSN 1937-6448, DOI: 10.1016/B978-0-12-386033-0.00001-3

5. Concluding Remarks and Future Directions 56
5.1. Conformational changes associated with nucleotide hydrolysis cycles 56
5.2. Subunit conformations at filament ends 57
5.3. Cooperativity 57
5.4. Relationships between family members help trace the course of evolution 58
Acknowledgments 58
References 59

Abstract

Dynamic, self-organizing filaments are responsible for long-range order in the cytoplasm of almost all cells. Actin-like and tubulin-like filaments evolved independently in prokaryotes but have converged in terms of many important properties. They grow, shrink, and move directionally within cells, using energy and information provided by nucleotide hydrolysis. In the case of microtubules and FtsZ filaments, bending is an essential part of their mechanisms. Both families assemble polar linear protofilaments, with highly conserved interfaces between successive subunits; the bonding at these longitudinal interfaces is nucleotide dependent. Better understanding of the mechanisms by which nucleotide hydrolysis affects the bonding between subunits in filaments, and other structural changes related to the nucleotide hydrolysis cycles, has emerged from recent X-ray crystallographic and electron microscopic structures, showing eukaryotic or prokaryotic protofilaments in various states. Detailed comparisons of the structures of related proteins from eubacteria, archaea, and eukaryotes are helping to illuminate the course of evolution.

Key Words: Cytoskeleton, Filaments, Microtubules, F-actin, Tubulin, Actin, FtsZ, TubZ, MreB, ParM, Treadmilling, Dynamic instability, Membrane shaping, Nucleotide hydrolysis, Evolution.

1. Introduction

The interiors of cells need to be continuously rearranged in order for the cell to undergo reproducible cell cycles without mishap and carry out a wide variety of functions. This dynamic spatial organization depends crucially on filaments that are assembled and disassembled, often quite rapidly. To understand the processes involved will require detailed information about the structures and properties of each type of filament and the accessory proteins that modulate their activities.

The cytoplasmic filaments that are absolutely essential to cells are polar assemblies that self-organize, driving their own arrangement; we have

termed these filaments cytomotive (Löwe and Amos, 2009) because they can produce motility without assistance from other proteins. The primary cytomotive filaments, those of the actin and tubulin families, seem to have originated quite independently in prokaryotes but to have converged toward similar solutions to the problem of producing directed and controlled movement (Erickson, 2007; Löwe et al., 2004). Many other proteins form filaments in the cytoplasm, such as the coiled-coil intermediate filaments, but are incapable of self organization; they may be able to assemble once, in the required positions, but will not disassemble and reassemble without help.

The difficulties in using the techniques of modern molecular biology to investigate actin and tubulin include their requirement for several specific folding factors, providing a barrier to the expression in prokaryotes of the native or modified proteins. Eukaryotic actins and tubulins are also compatible between eukaryotic species, so expression of mutants there is fraught with difficulty due to the dominant negative effect of the mutant on host systems. Thus, a major source of recent insight comes from comparing the highly conserved eukaryotic filament proteins with their more variable bacterial counterparts; this is especially useful since prokaryotic proteins can more readily be genetically modified to test ideas about structure and function. As we discuss in detail, although the filaments originated separately and each have diverged to evolve family members that perform slightly different tasks, the level of structural similarity is remarkable. In particular, the interactions responsible for the formation of protofilaments are nucleotide dependent and strongly conserved within each family; this turns out to be of overriding importance, since it suggests that the basic mechanism has been conserved in each case. It seems that crucial conformational changes associated with assembly and disassembly occur between different domains within a subunit in actin family filaments but such changes take place at the interface between subunits in the tubulin family.

Important new insights into these filament proteins have come from crystals studied by X-ray crystallography and also from advances in the processing of electron micrographs. The latter have made the production of high-resolution images of large complexes, such as assembled filaments, more routine. X-ray scattering analyses of functional complexes, including assembled filaments, have also made important new contributions to our understanding of how cytomotive filaments assemble and disassemble.

2. Mechanisms of Directed Movement

Cytomotive filaments move and self-organize by mechanisms that depend on binding and hydrolysis of nucleotide by individual subunits. Thus, the growing or shrinking filament ends can be thought of as

molecular machines (Howard and Hyman, 2003; Kovar and Pollard, 2004; McIntosh et al., 2010). The two main mechanisms by which polar polymers assembling autonomously from free subunits achieve directed movement are known as "treadmilling" and "dynamic instability." For these activities to be useful to a cell, it is essential that the growing or shrinking ends provide binding sites that are specifically recognized by their "cargo" molecules. The cargos may help to ensure their own transport by promoting or inhibiting filament growth or shrinkage, depending on the particular system.

2.1. Treadmilling

This behavior was first predicted by Wegner (1976) for eukaryotic actin filaments, when it became clear that conformational changes related to nucleotide hydrolysis led to differences in the association of subunits at the two ends. The differences affect the on-rate, the off-rate, and the critical concentration of free subunits that marks the boundary between net addition of subunits to the polymer or net loss. If the critical concentrations are higher at one end of a filament than at the other, an intermediate concentration of free subunits will result in continuous addition to one end (the "plus" end) and continuous loss from the other (the "minus" end).

2.2. Dynamic instability

This was first discovered by Mitchison and Kirschner (1984) as a property of microtubules reassembled *in vitro* from purified tubulin. If the concentration of free subunits is sufficient, a filament may continue to grow at either end as long as the end is stabilized by the presence of a "cap" of subunits with unhydrolyzed nucleotide bound. If, on the other hand, subunits that have hydrolyzed nucleotide are exposed at an end by chance, a "catastrophe" may lead to the rapid loss of a large number of subunits. Shrinkage may proceed completely or the filament may be rescued and regrow. This stochastic behavior means that each end of a filament can grow or shrink independently and, as was observed, individual microtubules may shorten even in the presence of a high concentration of free tubulin subunits. It means that microtubules can search a wide region of cytoplasm by growing, shrinking, and growing out again, until a growing end contacts, and is stabilized by, its target, such as the kinetochore of a condensed chromosome.

2.3. Choice of mechanism is determined by subtle differences

Some prokaryotic members of the actin superfamily (such as the ParM group of plasmid proteins; Gerdes et al., 2010; Salje et al., 2010) naturally exhibit dynamic instability, rather than treadmilling, and members of the tubulin/FtsZ superfamily (notably the TubZ group of proteins found on

some eubacterial plasmids; Larsen et al., 2007) steadily treadmill, rather than exhibiting instability at both ends. Conversion from one form of behavior to the other may depend only on subtle changes in the amino acid sequences and ensuing structural folds. Moreover, studies of F-actin in cells or under cell-like *in vitro* conditions suggest that eukaryotic actin filaments under the influence of accessory proteins undergo catastrophic bursts of disassembly (Diez et al., 2005; Kueh et al., 2008; Staiger et al., 2009). Conversely, microtubules with their ends under the control of suitably sophisticated protein complexes are able to treadmill; for example, this appears to be the case for kinetochore microtubules in mitotic spindles during the construction phase (Chang et al., 2005; Chen and Zhang, 2004; Zimmerman and Chang, 2005). In yeast cells lacking minus-end binding γ-tubulin complexes, microtubules underwent extensive treadmilling with the assistance of accessory proteins that promote assembly or inhibit disassembly (Anders and Sawin, 2011). Indeed, things can be moved simply through assembly or disassembly, if the timing of these activities is controlled by other components in a cell.

Microtubules in cilia and flagella use neither assembly nor disassembly to produce motility but instead provide tracks for motor proteins. However, the beating mechanism may depends on the ability of tubulin subunits to fluctuate between straight and curved conformations similar to those that drive dynamic instability in cytoplasmic microtubules (see Section 3.15) and also enable the Z-ring, consisting of dynamic FtsZ filaments, to play its role in membrane constriction during division of bacterial cells, chloroplasts, and some mitochondria.

2.4. Membrane shaping and remodeling

There are many kinds of filaments or 2D networks that assemble on to one side of a lipid membrane and produce an asymmetry that causes the membrane to bend; this becomes an active process if the filaments then disassemble catastrophically, leaving the membrane curved, and then reassemble to induce further bending. At the final stage, the membrane may be so curved that disassembly of the filaments promotes scission or fusion of membrane compartments. The dynamin family is able to reach this point in a single step by inducing extreme curvature of the membrane during assembly (Hoppins and Nunnari, 2009; Low and Löwe, 2010; Prinz and Hinshaw, 2009; Schmid and Frolov, 2011). ESCRT (endosomal sorting complex required for transport) filaments, also involved in membrane scission and fusion, are disassembled by an accessory AAA ATPase (Guizetti et al., 2011; Hurley, 2010; Samson et al., 2011). In this review, focusing on members of the tubulin and actin superfamilies, the prokaryotic proteins FtsZ and MreB provide examples of filaments that drive membrane curvature. Eukaryotic actin also remodels membranes, either by myosin-mediated contraction,

as in cytokinesis, or by assembly-mediated pushing, as in filopodia formation or lamellipodia protrusion (Bugyi and Carlier, 2010; Le Clainche and Carlier, 2008; Mattila and Lappalainen, 2008). In the latter case, the site and rate of assembly are determined by accessory proteins such as Arp2/3 and formins.

3. The Tubulin/FtsZ Family

3.1. Evolutionary gap in living organisms

Although it is clear that tubulin and FtsZ share a common ancestor, the evolutionary progression from relatively simple filaments assembled from identical monomeric subunits to closed tubes assembled from stable heterodimers is not obvious. Phylogenetic studies have suggested that cells of the last common eukaryotic ancestor already had a full range of the different dyneins and accessory proteins required to form fully functional "9 + 2" cilia and flagella (Hartman and Smith, 2009; Wickstead and Gull, 2007; Wilkes et al., 2008) and also had all the types of kinesin needed both for driving mitotic or meiotic spindle microtubules and for moving membranous cargos around in the cytoplasm (Wickstead et al., 2010). Since no bacteria or archaea have yet been shown to contain 13-protofilament microtubules or to have any of the eukaryotic motor proteins that move along them, it seems that many intermediate organisms have been lost. Nevertheless, it has been deduced from the relative simplicity of homodimeric cytoplasmic dynein that organisms with cytoplasmic microtubules and motor proteins existed before the development of cilia or flagella.

The genomic FtsZs of eubacteria are all quite closely related and, as discussed later, are well represented in terms of published crystal structures. Most archaea, on the other hand, have several FtsZ genes, and some sequences (referred to as FtsZ3 in Fig. 1.1; Larsen et al., 2007; Makarova and Koonin, 2010; Vaughan et al., 2004) have interesting features in common with the TubZ group of plasmid-encoded proteins (Fig. 1.2). It seems likely that their bacterial hosts acquired these plasmids by horizontal DNA transfer from an archaeon. Studies of TubZ have shown that it assembles into filaments that undergo GTP-driven treadmilling (Larsen et al., 2007), and the structure of TubZ filaments has been solved to near-atomic resolution (Aylett et al., 2010). A comparison of the structures of tubulin, FtsZ type-1 and TubZ, as shown in Figs. 1.2–1.4 and discussed in detail in the following sections, indicates that TubZ shares structural similarities with tubulin that bacterial FtsZ's lack. In particular, a long helix at the C terminus is related to the helical hairpin that constitutes the C-terminal domain of tubulin. However, it seems unlikely that kinesin and dynein could bind to the long straight C-terminal helix of TubZ, whose surface

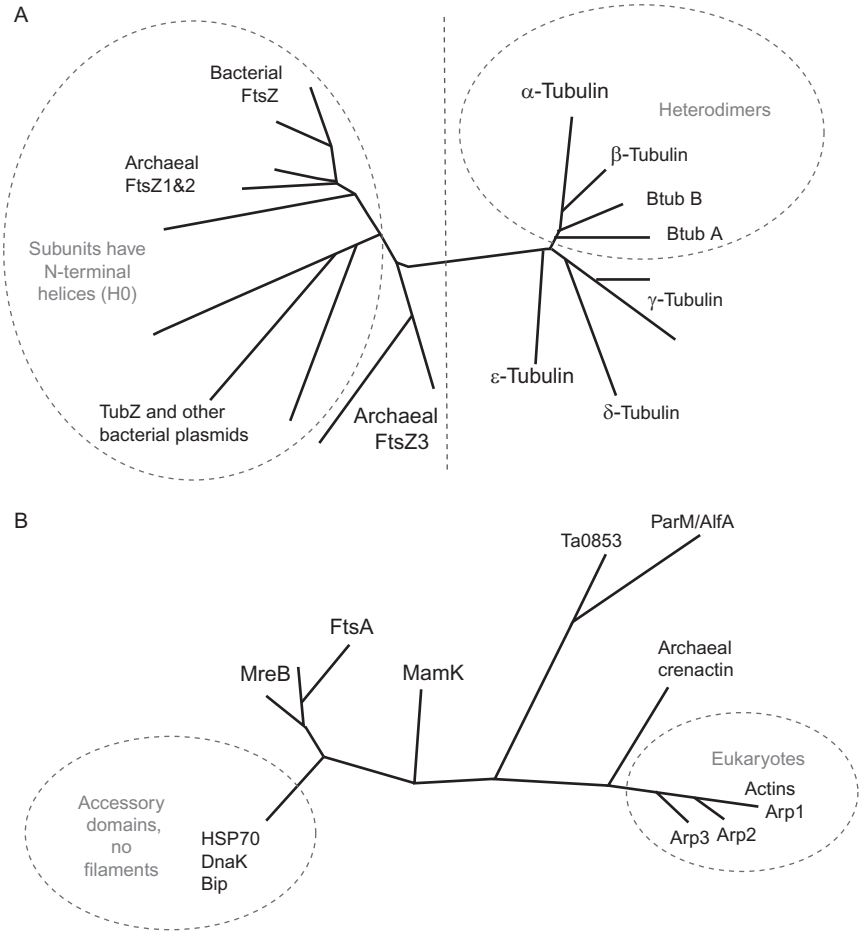

Figure 1.1 Tubulin and actin family trees. (A) The phylogenetic relationships between different subgroups of the tubulin/FtsZ protein superfamily, based on analyses by Vaughan et al. (2004), Larsen et al. (2007), Makarova and Koonin (2010), and Martin-Galiano et al. (2011). Members to the right of the central line all have extended H1-S2 and H2-S3 loops (Inclan and Nogales, 2001; see Figs. 1.2 and 1.3). The Btub dimer is thought to have been horizontally transferred to a bacterium from a now-extinct early eukaryote; TubZ and similar plasmids may have been transferred to bacteria from archaea (see text). (B) Different subgroups of the Hsp70/actin-like/actin protein superfamily; there is not a clear consensus regarding the relationships between different branches (Becker et al., 2006; Bork et al., 1992; Ettema et al., 2011; Itoh et al., 1999; Yutin et al., 2009) but it seems probable that the first proteins to assemble as filaments were similar to MreB.

lacks the groove at the top of the hairpin bend, which provides a significant part of the binding site for these motor proteins in tubulin (Amos and Hirose, 2007; Bodey et al., 2009; Sindelar and Downing, 2010;

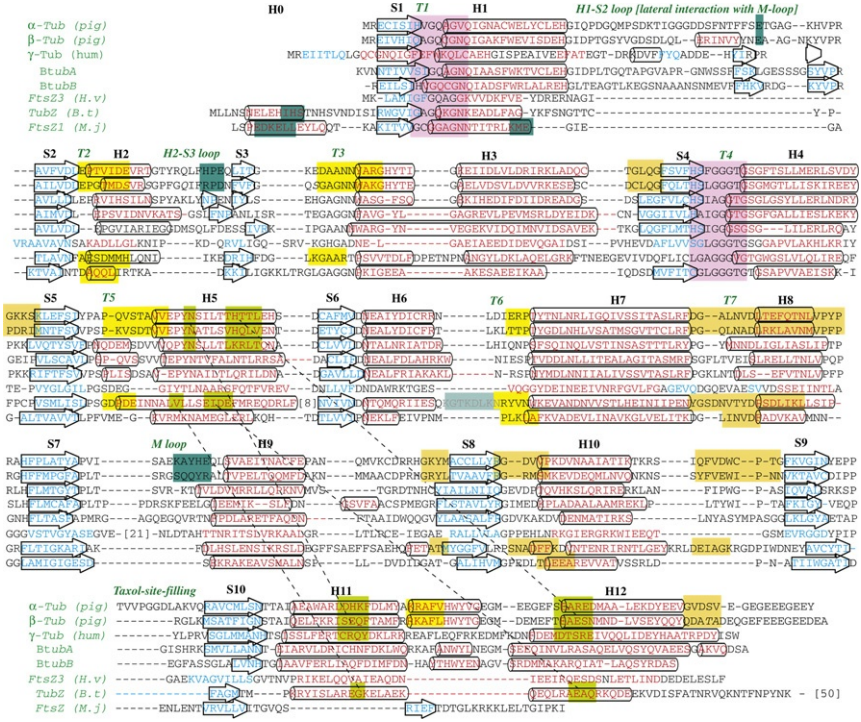

Figure 1.2 Tubulin family amino acid sequences. Structurally aligned sequences of some members of the tubulin family. The secondary structures of eukaryotic α, β, and γ tubulin are based on the crystal structures in PDB files 1JFF (Löwe et al, 2001), 1Z2B (Gigant et al., 2005), 3HKB (Dorléans et al., 2009), and 3CB2 (Rice et al., 2008). The structures of bacterial tubulins BtubA and BtubB from *Prosthecobacter* are from 2BTQ (Schlieper et al., 2005); that of *Bacillus thurigensis* TubZ from 2XKA (Aylett et al., 2010); that of *Methanococcus jannaschii* FtsZ1 from 1FSZ (Löwe and Amos, 1998). Residues identified [by PyMOL] as being in α-helices are in red, those in β-strands are in cyan, loops are in black. The secondary structure predicted [by JPRED] for a typical archaeal FtsZ3 is also shown. Helices H0-H12 and strands S1-S10 are labeled, as are some of the important loops. The conserved signature motifs in T1 and T4 are highlighted in pink. The GTPase domain consists of S1-T6; the activation domain T7-S10. Residues known to contribute to intra-protofilament interactions, including loops T2, T3, T5-T7, are shown with yellow (on GTPase domain) or orange (on activation domain) backgrounds. Residues involved in inter-protofilament contacts have backgrounds in blue-green (lateral contacts in a microtubule; note the much-reduced H1-S2 and H2-S3 loops in all FtsZ sequences) or teal (interstrand contacts in pairs of FtsZ or TubZ filaments—much of T6 is not resolved in the TubZ crystal structure but is presumed to be involved in the contact). Greenish-yellow backgrounds and dashed lines indicate contacts made by the C-terminal helices of tubulins or TubZ with the surface of H5 in the GTPase domains; in the case of TubZ, one of the contacts is with the next subunit in the protofilament. Note that these alignments agree perfectly over the GTPase domain with alignments based only on amino acid sequence (e.g., using CLUSTAL) but diverge substantially where the sequences become less conserved.

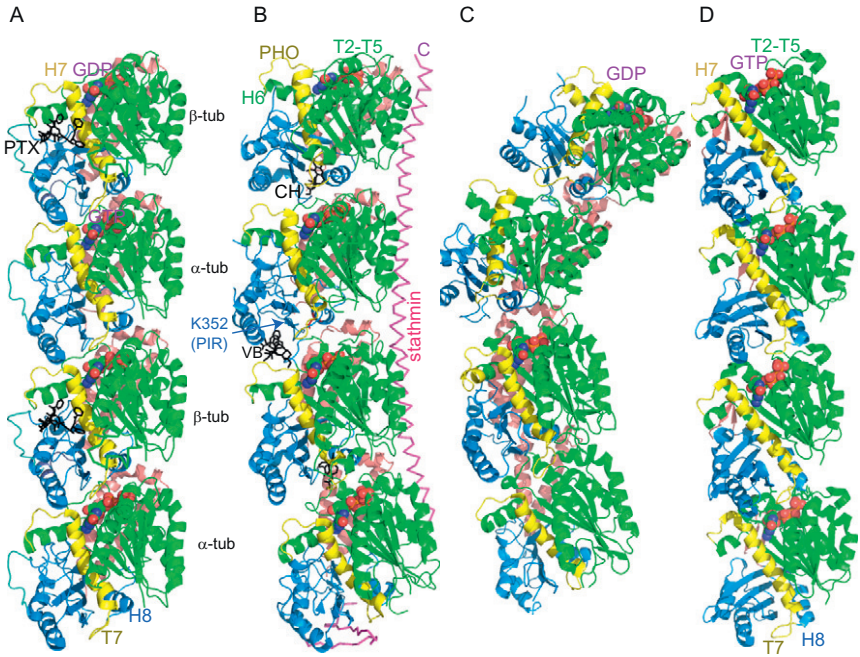

Figure 1.3 Tubulin family structures, inside view. Views of cartoon models of tubulin protofilaments in the straight (A) (1JFF; Löwe et al, 2001) and curved (B) (1Z2B; Gigant et al., 2005) conformations. GTPase domains are colored green, activation domains blue, central helices (H7) yellow, and C-terminal domains pink. A guanosine nucleotide sites between tubulin monomers, always GTP in the non-exchangeable site within each heterodimer and, so far, only GDP has been seen in the exchangeable sites between dimers. RB3/stathmin is shown in magenta. Bound Taxol (TX), Colchicine (CH), and Vinblastine (VB) are shown as stick models in black. The site for Phomopsin (PHO) on β-tubulin, on the loop between H6 and H7, comes from 3DU7 (Cormier et al., 2008). Pironetin (PIR) binds covalently to α-tubulin K352 (Usui et al., 2004). (C) Model of BtubAB protofilament in a curved conformation (2BTQ; Schlieper et al., 2005), with GDP between heterodimers and no nucleotide in the middle of each heterodimer. Both nucleotide sites are fully active. (D) Model of a protofilament of FtsZ that crystallized in the apo-state but was able subsequently to bind GTP (1W5B; Oliva et al., 2004). Subunits form homodimers that are slightly twisted, while adjacent dimers interact even more loosely.

Tan et al., 2008). Clearly, the C-terminal region has been able to change quite substantially during the course of evolution, without affecting the fold of the domains that form the main filament.

Genuine bacterial tubulin sequences, BtubA and BtubB, were discovered in the bacterial genus *Prosthecobacter* (Jenkins et al., 2002), and the proteins were found to be almost identical in structure to eukaryotic tubulin (Schlieper et al., 2005). It seems highly likely that this group of eubacteria

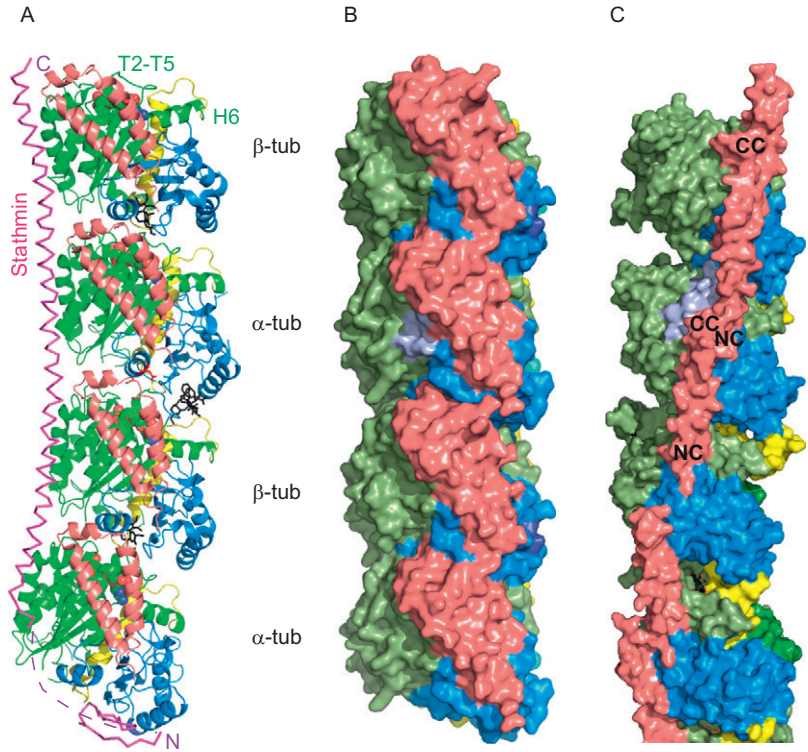

Figure 1.4 Tubulin family structures, outside view. (A). Cartoon model of curved tubulin protofilament (1Z2B) seen as if from outside a microtubule. Domains are colored as in Fig. 1.3. (B) Surface model of a straight tubulin protofilament (1JFF), in similar colors and viewed from a similar direction. Helix H5 of one subunit is highlighted in lilac to show its position relative to the pink C-terminal domain. (C) Surface model of TubZ with GTP bound (2XKA; Aylett et al., 2010). The TubZ protofilament has a gentle twist. The C-terminal helix (pink) interacts with its own subunit first (NC), then with the next subunit (CC).

acquired them by horizontal gene transfer, since they are restricted to so few species. Also, no eubacteria are known to have genomic FtsZ3, the probable intermediate between FtsZ1 and tubulin. Because the two partners in the Btub heterodimer are less distinct from each other (both exchange and hydrolyze GTP) than eukaryotic α and β-tubulin are, they may have been acquired from an extinct ancestor (archaeon or early eukaryote, or some intermediate) in which the gene for a monomeric tubulin had already undergone duplication but the changes needed for a non-exchangeable nucleotide-binding site had not taken place (Martin-Galiano et al., 2011). However, it is not possible to rule out the possibility that they might have reverted to functioning as monomers after being transferred to bacteria.

An adjacent locus encodes a kinesin light chain homologue, including a tetratricopeptide repeat domain, used by kinesin for binding to cargo. All three proteins are cotranscribed under the control of a single promoter (Jenkins et al., 2002). If the operon arrived originally as a plasmid, it might have used Btub assembly to drive its own segregation. It is not known what use is made of the Btubs by the host cells.

3.2. Filaments and tubes

The protofilaments of FtsZ/tubulin homologues are similar in many respects but their superstructures differ. Normal microtubules consist of 13 protofilaments arranged in parallel and with their subunits in a characteristic helical lattice (Amos and Klug, 1974; Erickson, 1974). The lateral interactions that stabilize the lattice are mediated by surface loops that are extended in tubulin compared with FtsZ and TubZ (see Section 3.7.1). The conserved 13-protofilament lattice coevolved with motor proteins and may be needed for their combined activity (Section 3.15); since cytoplasmic microtubules, dynein, and kinesin are all thought to have preceded cilia/flagella, the oscillatory beating of the latter may represent an amplification of a more subtle cooperative activity taking place between cytoplasmic microtubules and motors (Kulic et al., 2008).

Rather less is known about the superstructure of FtsZ. *In vitro*, FtsZ can form sheets, tubes, single, and double filaments (Erickson et al., 2010; Löwe and Amos, 2009). Observation of filaments within bacterial cells at reasonable resolution has only recently become possible. Electron tomograms of FtsZ in frozen cells of *Caulobacter crescentus* have suggested that FtsZ forms either single or double filaments, some of which cluster into small bundles (Li et al., 2007). The exact role of FtsZ remains unclear. While some early models now seem less likely, such as that FtsZ simply provides a ring-shaped scaffold for other proteins to assemble the division septum, it has not been determined whether cycles of GTP hydrolysis directly drive a conformational changes in the filaments to exert force upon the membrane or whether filament depolymerization allows membrane constriction (Mingorance et al., 2010).

The TubZ subfamily of proteins are somewhat divergent, forming protofilaments that twist and writhe along their length, and also show treadmilling behavior by default, rather than dynamic instability (Aylett et al., 2010; Chen and Erickson, 2008; Larsen et al., 2007). How TubZ filaments treadmill to separate plasmid copies is not yet understood. A likely scenario is that antiparallel filaments assemble between a pair of newly replicated DNA molecules, and then each filament continues to grow, possibly at both ends, therefore pushing the daughter plasmids apart. When the concentration of free protein subunits is reduced, the minus end will stop growing and then start to shrink, while the plus end continues

to grow. Each filament will move independently, but most likely in its original direction, separating the two copies of the plasmid. Termination of plasmid movement is likely to occur due to release of the TubR*C* adaptor–centromere complex, possibly through mechanical contact with the cell poles (Aylett et al., 2010; Ni et al., 2010).

3.3. Conformational changes in protofilaments

Conformational changes have mainly been discussed in terms of two protofilament conformations, "straight" and "curved." However, it is becoming clear that this is an oversimplification, and that tubulin-like protofilaments assume more than just two conformations. There must, for example, be two or more straight conformations, since the average longitudinal subunit spacing in microtubules assembled from GMPCPP-tubulin is ~4% greater than for GDP-tubulin (Hyman et al., 1995). As will be discussed, structural data obtained from bacterial homologues may explain this phenomenon and provide clues about possible conformational changes during assembly and disassembly.

3.3.1. Protofilaments curl during disassembly

The process by which microtubules disassemble is relatively well understood. GDP-tubulin protofilaments "peel" outward from the ends of depolymerizing microtubules. This curved form of the protofilament is visible by electron microscopy (Kirschner et al., 1974; Mandelkow et al., 1991; Voter and Erickson, 1979).

FtsZ protofilaments have also been seen in curved configurations (Erickson et al., 1996) that have been proposed to define the GDP-bound state (Lu et al., 2000). However, it has since been reported that the interaction between FtsZ filaments and a liposome is able to induce curvature of the latter even when a non-hydrolysable GTP analogue is added (Osawa and Erickson, 2011; Osawa et al., 2009). Thus, it appears that even GTP-bound protein can flex into a curved conformation. The role of GTP hydrolysis may be to facilitate disassembly, so that the protein can take part in repeated cycles of reassembly and membrane curving, rather than to generate force directly.

3.3.2. Microtubule assembly from sheets or splayed protofilaments

During rapid assembly at the plus end, there is often a narrow sheet of protofilaments that take the lead (Chrétien et al., 1995). Its slight outward curvature may indicate that the initial conformation after assembly differs both from the straight conformation in microtubules and the more highly curved disassembling state. A curved structure of tubulin polymerized with the non-hydrolysable nucleotide analogue GMPCPP and studied by cryo-EM (Wang and Nogales, 2005) has been proposed to resemble the curved

sheets. However, such leading sheets seem to be rare in cells, where growth is efficiently controlled, and instead the ends of growing protofilaments may be funnel-shaped (O'Toole et al., 2003a). Yeast cells treated with a microtubule-depolymerizing drug, which was then washed out, showed simultaneous growth of all of their microtubules; Höög et al. (2011) then used electron tomography to characterize microtubules in bundles of known polarity and found that the vast majority of plus ends had a gently flared structure, distinct from the curled protofilaments typical of disassembling microtubule ends. The flared structure of ends that are actively growing *in vivo* was confirmed by Kukulski et al. (2011). The long sheets extending from growing ends *in vitro* are probably a result of assembly overshoot from the high concentrations of soluble tubulin employed. Although the flared-cone configuration remains to be fully confirmed in species other than in yeast cells, it is likely to be fairly general. An investigation of microtubule ends in mouse embryonic fibroblasts (Koning et al., 2008) did not make a distinction between splaying and curling protofilaments, but it is probably significant that there were at least twice as many "frayed" ends as expected.

3.3.3. Recognizing and measuring a GTP-bound cap

Until recently, it was widely assumed that the exchangeable GTP in a tubulin heterodimer would be hydrolyzed spontaneously once embedded in a lattice, meaning that the GTP-tubulin cap on a growing microtubule end would be only one heterodimer long (Drechsel and Kirschner, 1994). Evidence from a number of sources now suggests that the cap is usually much longer. Monte Carlo simulations of microtubule dynamics with parameters refined to accurately reproduce experimental measurements of the rates of growth and shrinkage, catastrophe and rescue suggested the cap may be several microns long, depending on the concentration of free GTP-tubulin dimers (Piette et al., 2009). Also, high-quality optical trapping data (Schek et al., 2007) indicated that microtubules often undergo extensive shortening excursions during periods of overall net growth; such instantaneous "rescues" would occur readily if a GTP-tubulin cap remained after the loss of many subunits. Further support is provided by measurements of the lengths of "comets" of fluorescent "+TIP" proteins accumulating at the plus ends of growing microtubules (Bieling et al., 2007, 2008; Dixit et al., 2009; Jiang and Akhmanova, 2010; Kukulski et al., 2011).

Vertebrate CLIP-170 was the first microtubule +TIP protein seen to form comets but it has since been shown that CLIP-170 recognizes the tips by binding to the "master" +TIP, EB1, and to the tyrosine-bearing C-terminal tail of tubulin (Dixit et al., 2009). Observations of +TIPs indicate a decoration time of ~8 s, many times greater than the average single-molecule dwell time (~0.05 s). The difference can be explained by rapid on/off exchange of +TIP molecules from a longer-living end region of tubulin lattice that differs from the GDP-tubulin lattice in the body of the

microtubule. The flared ends described in Section 3.3.2 are much shorter (~20 nm) than the length by which microtubules are likely to grow during the 8.5-s period (~300 nm). Thus, protofilaments apparently do not need to be splayed in stretches of microtubule that bind EB proteins tightly. This point is discussed further in Sections 3.10 and 3.11.

3.4. Atomic structures of tubulin family

Atomic structures of several tubulin family members are available. A structural alignment of the sequences of these various proteins (Fig. 1.2) reveals that the secondary structural features have been strongly conserved despite very low sequence conservation between prokaryotic and eukaryotic members of the family; only residues around the nucleotide-binding site exhibit notable similarity.

3.4.1. The domains making up tubulin-like proteins

Despite the lack of amino acid sequence conservation, all tubulin-like proteins have a conserved fold consisting of two globular domains (Löwe and Amos, 1998; Nogales et al., 1998a,b): a near-N-terminal GTPase domain (shown in green in Figs. 1.3 and 1.4) and an activation domain (shown in blue; originally referred to as the "intermediate domain" in tubulin). These can be expressed and purified separately for both FtsZ (Oliva et al., 2004) and TubZ (unpublished result, Aylett and Löwe), and although there is frequently a hydrophobic interface between the domains, it seems likely that they are, or were once, separately folding entities and that the tubulin/FtsZ fold resulted from the fusion of a G protein with its GTPase-activating protein (Oliva et al., 2004). The two globular domains are linked by a long single helix (H7; yellow in Figs. 1.3–1.6) that traverses the length of the protein. The GTPase and activation domains of tubulins have longer loops protruding from them than the prokaryotic proteins; the M-loop on the activation domain of one subunit interacts laterally with the H1-S2 and H2-S3 loops of the GTPase domain of an adjacent subunit (Li et al., 2002; Meurer-Grob et al., 2001; Nogales et al., 1999; Sui and Downing, 2010).

While both N-terminal and C-terminal extensions to the basic fold are common to many groups in the family, they vary considerably in structure. TubZ and most solved FtsZ proteins have an N-terminal helical extension (H0; Fig. 1.2), which is not present in tubulins. At the C terminus, tubulin has a helical hairpin that folds onto the side of the protein core (Fig. 1.4A and B), TubZ has a long continuous helix (Fig. 1.4C), while the C-terminal extensions of most FtsZs appear to be long and flexible. C-termini are typically involved in protein–protein interactions with cognate binding partners. The helical hairpins of tubulins are located on the exterior of the microtubule and contribute to the binding site for kinesin and dynein (Amos and Hirose, 2007; Carter et al., 2008; Mizuno et al., 2004;

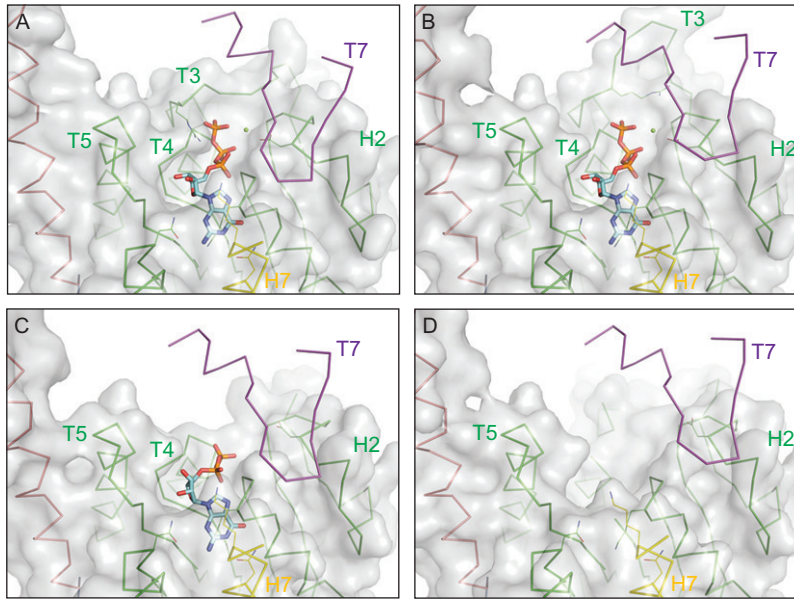

Figure 1.5 Relaxation of loops around the GTP binding site in TubZ. Cα traces of one subunit, a transparent van der Waals surface of the same subunit, and a Cα trace of loop T7 of the adjacent subunit from the structures of TubZ as a protofilament (2XKA and 2XKB; Aylett et al., 2010). Protein domains are colored as in Figs. 1.3 and 1.4. The nucleotides are shown as stick representations. (A,B) Mg-GTPγS-TubZ in the closely bound and loosely bound conformations. In B, T3 is ordered in an extended conformation and T7 is not interacting closely with GTP. (C) GDP-TubZ, loop T3 completely disordered. (D) TubZ without nucleotide, loops T3 and T4 both disordered. All structural representations generated by PyMOL (Schrödinger).

Nogales et al., 1999; Wade, 2009), FtsZ C-terminal peptides bind to actin-like FtsA (Yan et al., 2000) that bridges FtsZ filaments to the cell membrane (Löwe et al., 2004), and the C terminus of TubZ, positioned on the outside of the double filament (Aylett et al., 2010), is believed to recruit the TubR*C* adaptor–centromere complex (Larsen et al., 2007).

The GTPase domain, which provides the binding site for the guanine nucleotide, has a Rossmann fold (Rossmann et al., 1974) and is structurally the most highly conserved region; all known structures of tubulin family members overlay extremely well, with substantial variation only in surface loops located far from the active site. Interestingly, although the tubulin GTPase domain is divergent from other classes performing this function, such as the ras family (Gamblin and Smerdon, 1998; Sprang, 1997), loops that move within the active site occupy similar spaces to switches from small GTPase domains; in particular, the T3 loop was proposed to be the equivalent of the switch II region and to propagate nucleotide-induced conformational changes (Nogales et al., 1999).

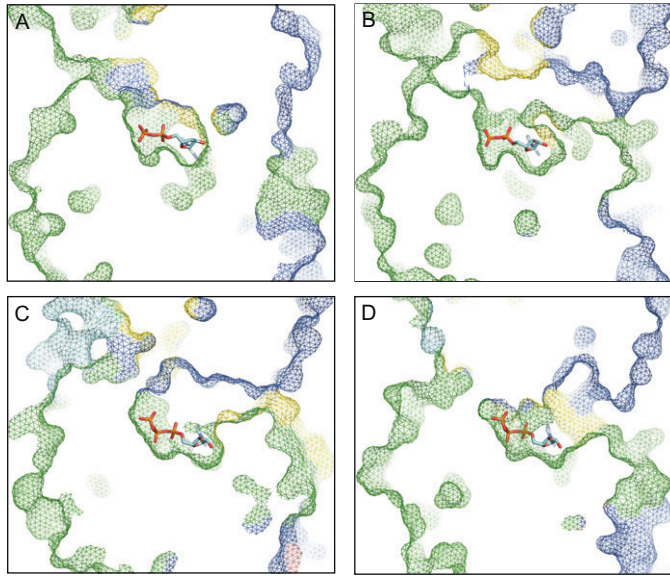

Figure 1.6 Phosphate release from the tubulin fold. Plots illustrating slices through the van der Waals surfaces calculated from crystal structures of the area of the nucleotide-binding pocket. (A) The straight tubulin protofilament—1JFF. (B) The curved tubulin tetramer stabilized by a stathmin homologue—1SAO (Ravelli et al., 2004). (C) The dimeric pseudo-protofilament of FtsZ—1W5A. (D) The twisting protofilament of GTPγS-TubZ—2XKA.

3.4.2. Straight and curved protofilament structures

Since subunits of all members of the family must interact with another subunit to activate their GTPase, structures of assembled complexes are crucial for understanding their activity. The subunits assemble as polar protofilaments, with a nucleotide sandwiched between the GTPase domain of one monomer and the activation domain of the next.

3.4.2.1. Tubulin protofilaments Two high-resolution structures have been adopted as prototypes for the straight and curved forms of the tubulin protofilament. The structure of αβ-tubulin protofilaments in Zn-induced 2D crystals, solved by electron crystallography (Fig. 1.3A), remains the most informative for the tubulin field, as the protofilament is in a near native state, and the polymerization interface is believed to be closest to that in the microtubule (Nogales et al., 1998a,b); the view in Fig. 1.3A is roughly equivalent to that from inside a microtubule. On the other hand, crystal structures of the tubulin–stathmin complex present conformations in which the interfaces are distorted and the two tubulin heterodimers are thought to represent a stable analogue of the curved product of depolymerization

(Gigant et al., 2000). In Fig. 1.3B, stathmin's long helix can be seen binding alongside the row of GTPase domains in the protofilament. The amino-terminal part of stathmin caps the bottom of one α-tubulin, preventing polymerization.

In all these structures, changes within each monomer subunit are small; there is a slight axial displacement of helix H7 in each tubulin monomer plus a slight rotation between the GTPase and activation domains, while contact between GTPase domains is maintained by local movement of helix H8 and loop T5. Contact is also maintained between the C-terminal helical hairpins (Fig. 1.4) so they, combined with their contacts on the activation and GTPase domains, act like a flexible backbone.

Compared with the straight conformation, adjacent subunits are curled sideways, and spaces are opened up between the subunits, allowing microtubule-depolymerizing drug molecules (Section 3.9) to bind and help maintain the curved conformation. The more open nucleotide-binding site, compared with the straight conformation (Fig. 1.5A and B), will facilitate nucleotide exchange. The major change is in the way that interactions between adjacent activation domains via helices H6 and T6 are disrupted and rearranged. Between 1JFFb and 1SA0b, there are big changes in the S5-H6 (T5) and H6-H7 (T6) loops. The importance of the "subpolymer" of activation domains plus H6-T6-H7 is highlighted by the scatter of binding sites throughout this region, for drug molecules that stabilize the association of subunits into protofilaments (Section 3.9).

BtubA and BtubB, found in the bacterial genus *Prosthecobacter* (Jenkins et al., 2002), closely resemble αβ-tubulin and form heterodimers (Schlieper et al., 2005; Sontag et al., 2005, 2009). The protofilament structure seen by crystallography (Schlieper et al., 2005) is highly curved (Fig. 1.3C).

3.4.2.2. Plasmid-encoded protein filaments The TubZ crystal structures recently solved (Aylett et al., 2010; Ni et al., 2010) finally provide a nearly complete set of states for a single tubulin family protein. Besides two monomeric structures, probably both representing an apo-state of the protein due to a locked crystal contact, two protofilament structures provide GTPγS, GDP, and apo-states of the polymerized protein. TubZ is the only tubulin structure available that treadmills in an apparently constitutive manner (Chen and Erickson, 2008; Larsen et al., 2007).

3.4.3. The GTPase sites

3.4.3.1. The pockets between subunits Tubulin/FtsZ homologues bind guanosine nucleotides in conjunction with Mg^{2+} in a cleft on the surface of the GTPase domain (Löwe and Amos, 1998; Löwe et al., 2001; Nogales et al., 1998a). The nucleotide is cradled by loops T1-T6 on the surface of the GTPase domain, exposing the γ-phosphate. Loop T7 and helix H8 of the activation domain of another subunit approach GTP during

protofilament assembly. The latter is believed to promote GTP hydrolysis but, in the case of tubulin heterodimers, this happens only at the exchangeable site (E-site) while GTP trapped in the non-exchangeable N-site within a heterodimer is never hydrolyzed, because β-tubulin has lysine at the end of H8, instead of an acidic residue (like α-tubulin E254). Thus, in contrast to actin-like filaments, the nucleotide itself makes up part of the subunit–subunit interface within a tubulin family protofilament. The interface is extensive and buries the γ-phosphate (Figs. 1.5 and 1.6). Therefore, nucleotide hydrolysis and phosphate release can affect polymer stability directly. The activation domain surface includes the loop T7, which contributes two carboxylic acid residues, to activate water for attack on the exposed γ-phosphate and couple the formation of the straight tubulin protofilament to nucleotide hydrolysis (Löwe et al., 2001; Nogales et al., 1998b). Not surprisingly, nucleotide exchange occurs only in the soluble state in eukaryotic tubulins; it is unclear whether some FtsZs are capable of nucleotide exchange when polymerized (Chen and Erickson, 2009; Tadros et al., 2006).

3.4.3.2. Differences in tubulin with bound GTP versus GDP Subunits bound to GTP-like or GDP.Pi-like nucleotides (such as GMPCPP or GTPγS) are much more stable members of a protofilament than subunits with GDP bound. Unfortunately, no structure at near-atomic resolution shows tubulin with a nucleotide other than GDP in the E-site. However, the structure of α-tubulin with GTP-Mg^{2+} in the N-site is closely superimposable on that of β-tubulin with GDP; apart from the H1-S2 loop, which is disordered in α-tubulin, the N-site and E-site interfaces are essentially identical. The similarity includes equal ∼12° bends at all interfaces in the curved configuration. The small domain movement described in Section 3.4.2.2 between the straight and curved conformations is the same in both monomers.

Furthermore, although the structures of monomeric γ-tubulin and many FtsZs have been solved in all of the available nucleotide states, no significant changes in the conformation of the GTPase domain have been identified (Oliva et al., 2007; Rice et al., 2008). A structural explanation for the reduced affinity between subunits could simply be the destabilizing effect of the reduced binding surface and the charge imbalance in the subunit interface due to the missing phosphate (Díaz et al., 2001).

3.4.3.3. Changes in inter-subunit affinity The presence of the γ-phosphate may reduce the energy required for the subunit–subunit interface to be stable. A charge–charge interaction between loop T7 and the γ-phosphate of GTP is present at the N-site within the tubulin dimer interface and could account for the unusual stability of the heterodimer. However, the presence of the catalytic carboxylic acid residues precludes this mechanism in any

catalytically active tubulin/FtsZ subunit. The increased affinity when GTP is present is proposed to be due to subtle conformational changes in the conformation of loops T3 and T7, in close proximity to the γ-phosphate, as measured *in vitro* and seen in high-resolution crystal structures (Díaz et al., 2001; Dorléans et al., 2009). The ability of proteins such as EB1 to detect nucleotide state when bound to the outside of a protofilament (Section 3.10) suggests that other changes occur, but they may not have any effect on protofilament stability.

3.5. Assembly and the nucleotide hydrolysis cycle

Because the protofilaments in microtubules are straight and microtubules assemble from GTP-bound tubulin, while GDP-bound tubulin forms rings when microtubules disassemble, it was natural to assume that GTP-bound heterodimers have a straight conformation and GDP-bound subunits a curved conformation unless constrained to be straight. It was suggested that the energy produced during GTP hydrolysis was stored in the microtubule lattice by the constraining bonds and released during disassembly. Similarly, hydrolysis of GTP in FtsZ protofilaments might drive membrane remodeling (Lu et al., 2000; Osawa et al., 2009). However, the proposed direct relationship between preferred conformation and nucleotide state has been challenged by structural findings.

3.5.1. Two-state, lattice-constraint model

Oliva et al. (2007) compared FtsZ structures in different crystal forms and nucleotide states, and in the presence or in the absence of regulatory proteins. Finding no conformational change involving domain movement, they suggested that previously designated "straight" and "curved" conformations of FtsZ were due to interspecies differences in domain orientation. It appeared that individual subunits have an essentially fixed conformation, although interfaces between subunits can convert stochastically between straight and curved conformations.

Similarly, all atomic structures of monomeric γ-tubulin were found to resemble αβ-tubulin subunits in one conformation; in particular, the posture of helix H6 and adjacent H6–H7 loop agreed with the αβ-tubulin–stathmin structures. This was the case whether the crystallized protein had GTP, GDP, or no nucleotide bound (Aldaz et al., 2005; Rice et al., 2008). Rice et al. suggested that, regardless of their nucleotide content, protofilaments preferentially assume the curved form, unless constrained to be straight and that the lattice contacts in a microtubule can provide the energy to make the structure stable. According to this view, the nucleotide would influence subunit assembly or disassembly by controlling longitudinal binding affinity but lateral binding would control curvature. The small changes listed in Section 3.4.2.1 between the straight and curved conformations of

αβ-tubulin would be a consequence, rather than the cause, of bending. However, the appearance of straight individual GDP-bound protofilaments stabilized with Taxol (Elie-Caille et al., 2007) suggests that lateral bonds are not essential to hold tubulin protofilaments straight and that the control of conformation is more complex.

3.5.2. An "intermediate" curved GTP-bound conformation

Wang and Nogales (2005) proposed a compromise between the previous two models, a third conformational state that is only possible for GTP-bound subunits, at the start of reassembly. A smoothly curved, GTP-bound conformation was suggested to be intermediate between straight filaments and the open GDP state in stathmin stabilized tubulin. This idea was supported by the observations that tubulin sheets seen extending from the growing ends of microtubules curve gently outward (Chrétien et al., 1995) and that tubulin bound to GMPCPP, a nearly non-hydrolysable analogue of GTP, also forms gently curved protofilaments (Muller-Reichert et al., 1998; Wang and Nogales, 2005; Wang et al., 2005). Similarly, two distinct curved conformations have been proposed for FtsZ protofilaments (Erickson et al., 2010). In the case of tubulin, flexible lateral contacts might be made initially in the lightly curved sheets, might prime closure into a cylinder, and finally straighten the dimers to form the microtubule lattice.

On phosphate release, Wang and Nogales proposed that the contact between T7 and the nucleotide of the adjacent subunit within the E-site interface becomes disrupted, leaving contacts only on the side of the subunit–subunit interface further from the nucleotide, therefore placing it in a fully curved-like state. The effect of nucleotide hydrolysis would therefore be to disrupt the subunit–subunit interface and favor a less stable form of the tubulin protofilament. Loop movements at the N-site mimic those at the E-site, but the dimer is kept intact by the high affinity between β-tubulin's loop T7 and the γ-phosphate of GTP.

3.6. New insights from TubZ filaments

Structures of the divergent TubZ family of plasmid-borne tubulins provide new insights and confirm previous assumptions about states of tubulin for which structural information is missing, including some GTP-bound states (Aylett et al., 2010).

3.6.1. Changed domain angle in TubZ

TubZ demonstrates a significant rotation of the C-terminal domain relative to the same region of the protein in the tubulin and FtsZ subfamilies and this gives the protofilament an invariant twist. Since no changes in the relative orientation of the two domains are seen between the GTPγS, GDP,

and monomeric forms of the protein, it remains likely that changes resulting in the "curved" form occur in the interface, rather than within the core of the protein.

3.6.2. The conserved bipartite active site

The tubulin family GTPase domain binds the guanine nucleotide in the active site, and the activation domain contributes the twin carboxylic acid residues that activate water for its nucleophilic attack on the γ-phosphate and its subsequent release. Guanine nucleotide exchange appears only to be possible either when the GTPase domain is in a monomeric state or is the terminal subunit of a protofilament because the subunit interface buries the nucleotide-binding site (Figs. 1.5A–D and 1.6D). The base of H8, including the two catalytic acidic residues, is placed over the γ-phosphate. The completion of the active site by a domain on a separate subunit ensures that polymerization is coupled to nucleotide hydrolysis. Crystal structures of the TubZ filament (Aylett et al., 2010) and an FtsZ filament (Oliva et al., 2004) both indicate contacts between the subunits similar to those of the αβ-tubulin heterodimer, despite only ∼15% sequence similarity.

3.6.3. Sensing of nucleotide hydrolysis: loop T3 and helix H2

The geometry of the active site limits the regions of the protein that may directly come into contact with the γ-phosphate. Given that no tubulin homologue has shown any conformational changes within the ordered sheet and helices of the GTPase domain, and that such movements within a domain built around a rigid sheet are unlikely, only small regions of the domain are capable of sensing hydrolysis. This point has been discussed for other GTPase families, including the small G proteins making up the Ras family. Only two flexible surface loops of these proteins come into contact with the γ-phosphate, and these undergo conformational changes on hydrolysis, for which they have been named switches I and II. Tubulin family GTPase domains are not structurally or topologically identical to the Ras family, and the regions occupying the same space in the domain are in different conformations and regions of the sequence, consisting of H2 and T3 (Nogales et al., 1999). So far, all such conformational changes identified in the tubulin family have mapped to these regions. Díaz et al. (2001) identified conformational changes in T3 of FtsZ, while the TubZ protofilaments (Aylett et al., 2010) show variability in both H2 and T3 related to guanine nucleotide state.

Loop T3 occupies the space immediately adjacent to the γ-phosphate. It is relatively flexible, and is therefore missing from many tubulin family structures, including all of the γ-tubulin monomers. However, the part of the loop contacting the γ-phosphate is quite conserved both in sequence and structure. In protofilament structures, T3 makes a subunit–subunit contact with T7 and H8 of the adjacent subunit, so it is reasonable to expect

that it will be more ordered due to protofilament formation and less ordered on phosphate release; in TubZ, T3 is disordered in all structures of the apo- and GDP states, as it is in most structures of other members of the tubulin family. Significantly, in the GTPγS state, loop T3 occupies two different conformations, one resting on the surface of the subunit and matching that known in other tubulin family members; the other stretched out to abut the adjacent subunit. Both contact the γ-phosphate of the nucleotide and the base of the GTPase domain of the adjacent subunit. Possibly these changes are indicative of flexibility in T3.

The conformational changes seen in H2 of TubZ appear to depend on sequence differences. The residue (D64) contacting the magnesium in the active site is one helical turn into H2, whereas in both tubulin and FtsZ families, the equivalent residue is contributed by loop T2, preceding H2. Because the relaxed conformation of H2 is rotated slightly away from the nucleotide in TubZ compared to its position seen in structures of tubulin and FtsZ, coordination of the magnesium ion by D64 results in rotation of H2 toward the active site, where it occupies the same conformation as that found in other structures and contacts the T7 loop of the adjacent subunit.

3.6.4. Variations in activation domain and T7 loop structure

Loops T7, H8, and S9 all make important contact with the adjacent subunit, binding the exposed surface presented by H2, T3, and T5 (Fig. 1.5). Though tubulin and FtsZ filaments are almost perfectly straight, TubZ filaments are helical. Because of this, adjacent TubZ subunits are tilted slightly relative to other members of the family, leading to greater contact between loop T7 and the adjacent subunit than in tubulins or FtsZs, and less contact by H8 and S9, principally with T3 and T5. TubZ T7 is extended by two amino acids relative to those of tubulins and FtsZs. This facilitates two changes between the proteins. First, the C-terminal domain of TubZ is rotated relative to that of tubulins and FtsZs, so there is more distance to cover to reach H8. Second, the T7 loop is extended by ~2 Å toward H2, which combines with a small displacement across the surface of the adjacent subunit to allow T7 to make close contact. These differences, coupled to the relatively high B factors of H2 in the available structures of tubulin protofilaments, suggest that the interaction between tubulin T7 and H2 is not as tight as that in TubZ.

The H8-T3 contact is emphasized in the straight filaments of tubulins and FtsZs, and movements of these regions have been identified in both subfamilies. Tubulins have a T3 loop that is several amino acids shorter than in TubZ and is constrained at either end by rigid secondary structures, while H3 is sandwiched by the H11-H12 loop at the C terminus. Thus, T3 movements may have smaller direct effects in tubulins. On the other hand, tubulin's loop T5 is much longer and more flexible than in other homologues; although it is not in direct contact with the γ-phosphate,

it may perhaps change conformation in response to small changes in T3. The top of tubulin's H11-H12 helical hairpin makes contact with both T3 and T5 and could respond to changes in either.

3.6.5. Phosphate channels

While the GDP-Pi nucleotide state is believed to allow the subunit–subunit interface, and thus the protofilament, to remain stable, when the γ-phosphate is released the subunit–subunit interface is left in a GDP state. The available structures of subunit–subunit interfaces in eukaryotic tubulins show no clear path by which the γ-phosphate can leave after hydrolysis. The binding surface over the nucleotide covers everything. However, the structures of TubZ contain a channel of sufficient size to allow release. It stretches from the gap between T5 and H7 up to the γ-phosphate itself (Fig. 1.6D). Phosphate release in the TubZ subfamily occurs much more rapidly than in tubulin or FtsZ (Chen and Erickson, 2008). The equivalent path in the straight tubulin protofilament (Fig. 1.6A) is blocked by the elongated loop T5, and is well below the required size for the release of Pi. In tubulins, it seems that the most likely path for release lies at the juncture of T7 and H2, where the aqueous milieu comes closest to the γ-phosphate (Fig. 1.6B). In a microtubule, such a path would require opening of the subunit interface, which could possibly occur thermally without any bending of the protofilament, or might be controlled by the large H1-S2 loop, which would block release when the conformation is seen at the interface within the αβ-tubulin heterodimer. Flagellar microtubules appear to be stabilized by acetylation of a lysine (residue 40 of *Chlamydomonas* α-tubulin; LeDizet and Piperno, 1987), which may affect the conformation of the entire loop (Perdiz et al., 2011). This loop is also involved in the formation of lateral contacts (Section 3.7.1 and Fig. 1.9A) so the stability of lateral interactions could also be linked to Pi release from the active site in tubulin. The same loop may also contribute to the mechanism that signals nucleotide state to accessory proteins such as EB1 (Sections 3.10 and 3.11).

3.6.6. Protofilament flexibility

The protofilament structure of TubZ shows considerable variability in the subunit–subunit interface, presumably in response to forces due to crystal contacts, and indicates that this region is flexible. Subunits are capable of relative rotation against the adjacent GTPase domain in a notionally "inward and outward" direction; the picture is not as simple as GTPγS favoring a straighter form. Tightly interacting (D64-Mg^{2+}) subunits (Fig. 1.5A) show the base of the T7 loop close to the γ-phosphate, whereas those lacking a close interaction of T7 with H2 were more varied, with some adjacent subunits tilted toward the C-terminal domain and others tilted away. Movements in other tubulin family members may be more restricted. In tubulin, the T7-H2 interaction is weaker but the longitudinal

connection is supplemented by nucleotide-independent interactions between loops H11 and H12. These connections between adjacent tubulin subunits are maintained in the curved conformation, as are T4 and T5 interactions with H8 and H10-S9 of the adjacent subunit. The contacts stabilizing a straight microtubule protofilament on the "inner" side are those of H7 with the adjacent H10, and T7 with nucleotide. Accordingly, the H7-H10 interaction was also closely packed in TubZ protofilaments when T7 contacted H2.

3.6.7. Interaction between subunits during polymerization

The variations seen in TubZ in the GTPγS state provide new insight into the process of protofilament assembly. The new structures can also be compared with a crystal structure showing a semi-continuous FtsZ protofilament with GTP bound to all the active sites (Oliva et al., 2004); it was crystallized in the apo-state and then soaked in nucleotide. The result (Fig. 1.3D) shows a protofilament made up of homodimers, within which T7 is shifted slightly away from the nucleotide, including a relative rotation of the subunits by ~2.5°. Different dimers are more loosely associated but line up to make a straight protofilament. The inter-subunit spacing is 4.32 nm within a "close" GTP-dimer and 4.64 nm between the dimers, whereas it is 4.26 nm in GDP-bound protofilaments (Löwe and Amos, 1999).

The structures available suggest that several loops (T3, T5, T6, and the H11-H12 hairpin of tubulins) may all protrude flexibly around the binding site when GTP is there (Figs. 1.5 and 1.7). A subunit in solution is likely to add to the (+)-end of a protofilament by making initial contact with these protruding loops, which will initially inhibit loop T7 of the new subunit making contact with the GTP. This makes sense, since it would not be useful to trigger nucleotide hydrolysis during the initial process of assembly and immediately destabilize the contact. It is likely that thermal flexing of the T3, T5, and T6 loops eventually allows T7 to approach and trigger hydrolysis. A collapse of these loops, moving tubulin subunits closer together, would explain the observed reduction (Hyman et al., 1995) in average longitudinal periodicity in a microtubule from ~4.2 to 4 nm (Assuming there is no change in the spacing between the monomers within a heterodimer, after its chaperone-assisted formation, to account for the average change, the inter-subunit spacing between assembled tubulin heterodimers may initially be ~4.4 nm, before GTP hydrolysis and Pi release at the E-site).

In the case of TubZ at least, H2 is also involved in the binding mechanism. H2 lies further from the active site in TubZ than in other tubulin homologues, but moves inward toward the active site in the presence of T7 and Mg^{2+}. This conformational change stabilizes both H2 and T7, holding the adjacent subunits close to one another with increased rigidity. It seems

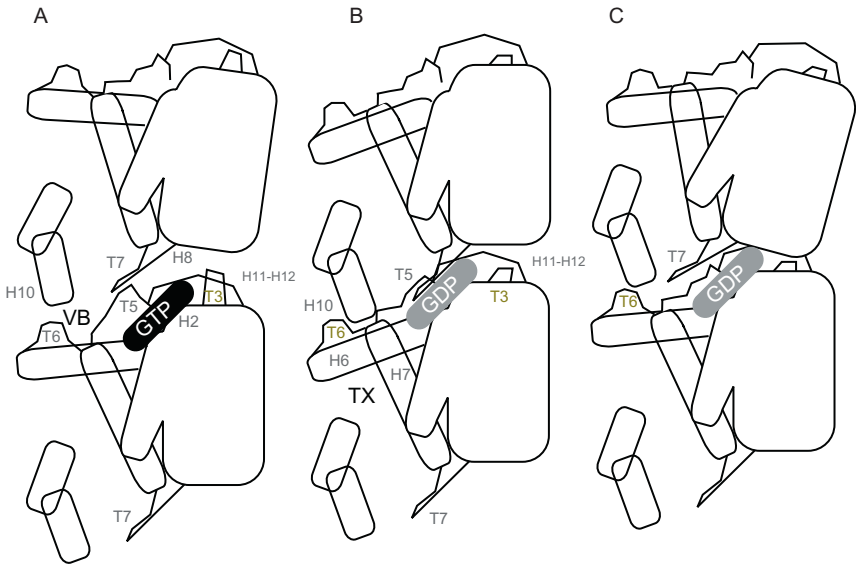

Figure 1.7 Proposed changes at the intra-protofilament interface between subunits in the tubulin/FtsZ family. (A) An early stage in assembly when loops T3, T5, T6, and, in the case of TubZ at least, helix H2 protrude around the bound GTP; the loops bond to another subunit but inhibit its catalytic loop T7 from triggering hydrolysis of the GTP. Thermal fluctuation will eventually bring T7 close enough for this but filaments assembled with non-hydrolysable nucleotides, such as GMPCPP, will remain in this extended state even after lateral bonds formed between different protofilaments have caused them to straighten. There may be an earlier stage in assembly when the protofilament is slightly twisted, as well as curved, and the GTP is even more protected from T7. This would explain why binding of Vinblastine to tubulin, in the pocket labeled VB, causes assembly of strongly helical protofilaments and inhibits GTP hydrolysis; it may also account for the non-interacting splayed protofilaments at the end of a growing microtubule (see text). (B) A straight protofilament with GDP bound. The flexible loops are collapsed and the subunits closer together; straightening has fixed helix H6 and loop T6 in a slightly rotated position. Binding of Taxol (TX) in the pocket next to helices H8 and H7 can stabilize the straight conformation in tubulin protofilaments, even in the absence of lateral bonding. (C) A curved protofilament with GDP bound. The protofilaments of depolymerizing microtubules assume this conformation at the microtubule ends, where it is possible to break the lateral bonds.

likely that Mg^{2+} release is linked to hydrolysis of the γ-phosphate, removing one of its ligands, and that this is then telegraphed into destabilization of the subunit–subunit interface through relaxation.

3.7. Lateral interactions in the tubulin family

While the nucleotide-dependent subunit–subunit interaction is highly conserved between the subfamilies of tubulins, the inter-protofilament interaction is less defined.

3.7.1. Microtubule lattice

Evidence for two similar lateral interactions between adjacent tubulin protofilaments first came from studies of flagellar doublet microtubules (Amos and Klug, 1974): an A-lattice where β-tubulin of one protofilament interacts with α-tubulin in the neighboring one, and a B-lattice where β-tubulin interacts with another β-tubulin in the adjacent protofilaments. 13-Protofilament cytoplasmic microtubules appear to have mainly B-lattice in the body but have a "seam" with A-lattice connections (McIntosh et al., 2009; Song and Mandelkow, 1993). In either case, the "rise" between monomer subunits in adjacent protofilaments is ~9.2 Å, so that the distance traveled up the axis by a helix running through 13 subunits is ~120 Å, or exactly the distance occupied by three monomers in the GDP-tubulin lattice (Fig. 1.8A).

Pure αβ-tubulin assembles into microtubules with a wide range of protofilament numbers. The helical surface lattice is conserved because the protofilaments in microtubules with fewer or more than 13 protofilaments take up slightly helical configurations rather than running straight (Chrétien and Wade, 1991).

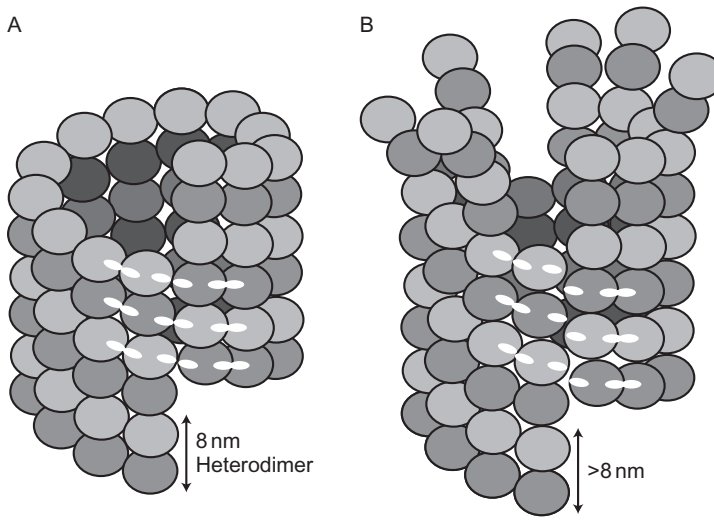

Figure 1.8 Microtubule lattice. (A) A segment in the main body of a GDP-bound microtubule. Here, the 4-nm spacing of monomer subunits in the protofilaments and the 0.9-nm shift between monomers in adjacent protofilaments allow the subunits at the closing seam to match perfectly (white dashes). (B) The increased longitudinal spacing of the GTP-bound lattice is due to extended loops between subunits in the protofilaments, while the angle needed to make a lateral interaction does not change. Hence, connections cannot be made simultaneously between all 13 GTP protofilaments and there must be a glitch in the lattice. Ends of growing protofilaments, presumed to be GTP bound, are shown splayed.

Compared with FtsZ and TubZ, the loops between S7 and H9 (known as the M-loop) and between H1 and S2 are extended (Figs. 1.2, 1.3, and 1.9). Sui and Downing (2010) obtained high-resolution 3D images with a resolution of better than 0.8 nm, from electron microscopy images of frozen microtubules, which resolved the secondary structural features involved in inter-subunit contacts; their images of microtubules with 11–16 protofilaments revealed that hinges, formed by M-loops interacting with H1-S2 and H2-S3 loops at the inner radius of each tube (Fig. 1.9A), are flexible enough to allow variations in tube curvature and lattice twisting. This facility is necessary if the main body of a microtubule is free to bend and twist, as in a flagellum. However, since the lattices of microtubules with fewer or more than 13 protofilaments twist in order to preserve the unit cell parameters (Chrétien and Wade, 1991), the lateral bonds must be resistant to longitudinal shear.

γ-Tubulin subunits make lateral interactions similar to those in the main body of a microtubule but at exactly the angle needed to form a 13-protofilament microtubule (Kollman et al., 2010). The M-loop of γ-tubulin is short, only ~2 amino acids longer than in FtsZ, while the H1-S2 loop is more structured than those of α or β and presumably less flexible. *In vivo*, microtubule structure is also influenced by accessory proteins such as EB1 or doublecortin binding, which bind to sites on the outer surface, between protofilaments (Fig. 1.9), and restrain the lateral curvature to that of 13 protofilament microtubules (des Georges et al., 2008; Fourniol et al., 2010; Vitre et al., 2008).

Another important conclusion from the work of Sui and Downing (2010) was that interactions at a microtubule "seam" (α−β and β−α) appear structurally indistinguishable from those in the B-lattice arrangement (α−α and β−β) between other pairs of protofilaments. This makes it unlikely that the seam represents a line of weakness in the GDP-bound microtubule, in need of external stabilization by EB1.

3.7.2. Doublet and triplet microtubules

Flagellar and ciliary axonemes have doublet microtubules consisting of a closed 13-protofilament "A-tubule" and a 10-protofilament curved sheet attached by both edges to the outside surface of the A-tubule and known as the B-tubule. In basal bodies and centrioles, a second sheet is attached to the B-tubule, to give the C-tubule of a triplet microtubule. Although associated proteins are needed to attach one edge of a sheet, the edge on which M-loops are exposed can attach unaided. This is apparent since pure tubulin assembled *in vitro* has been observed to form microtubules with attached sheets (Mandelkow and Mandelkow, 1979). The fairly non-specific stickiness of M-loops is also apparent from their involvement in the formation of flat sheets of protofilaments, when tubulin is assembled in the presence of zinc salts (Nogales et al., 1998a,b); here, the way in which an M-loop

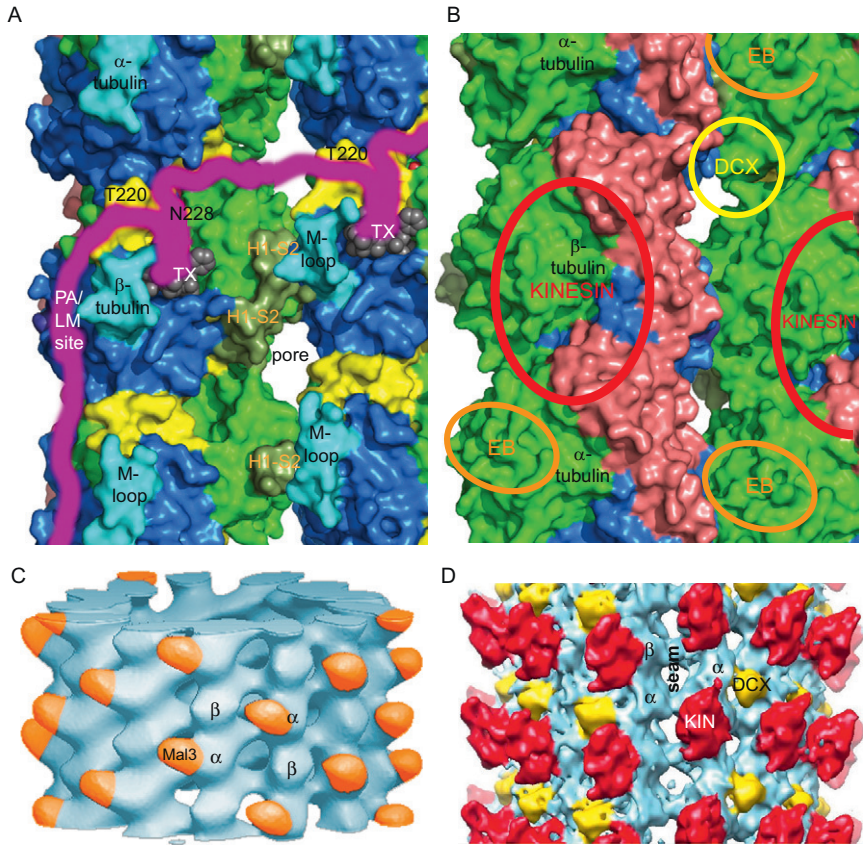

Figure 1.9 Binding sites on tubulin. (A,B) Inside and outside surfaces of a microtubule, with the main domains colored as in Figs. 1.3 and 1.4. (A) Drugs that stabilize assembly (such as Taxol—TX—shown as gray spheres, Peloruside A—PA, Laulimide—LM) bind to a variety of sites on the activation domain of β-tubulin (see text). They may map out the extended binding site for MAPs like tau (purple). Cyclostreptin binds either to N228, in the Taxol pocket, or to T220, near a pore. Tubulin H1-S2 loops (pea-green) interact laterally with the M-loops (cyan) of adjacent subunits. The H1-S2 loop of β-tubulin also interacts longitudinally with the α-tubulin of the same heterodimer but the H1-S2 loop of α-tubulin is partially disordered, at least when next to GDP-bound β-tubulin. (B) Outside surface, labeled to show the locations of binding sites for kinesin motor domains (each of which binds across a tubulin heterodimer), a DCX domain of doublecortin and CH domains of Mal3 (EB). (C) Reconstructed image (des Georges et al., 2008) of an A-lattice microtubule decorated with CH domains of Mal3 (yeast homologue of EB1—orange) binding mainly to one subunit of a heterodimer. (D) Reconstructed image (Fourniol et al., 2010) of a B-lattice microtubule decorated with kinesin motor domains (KIN, red) and doublecortin domains (DCX, yellow). The latter binds only to B-lattice interfaces, leaving an empty "seam" (middle).

interacts with another protofilament produces an antiparallel arrangement, with a totally different lattice from that in any microtubule.

Diffraction patterns and filtered images obtained from doublet microtubules suggested that A-tubules have a helically symmetrical A-lattice while B-tubules have a B-lattice (Amos and Klug, 1974). It is possible that axonemal A-tubules differ from cytoplasmic microtubules because they do not assemble from a γ-tubulin-defined template. Instead, δ-, ε-, ζ-, and η-tubulins play roles in basal body assembly, and a basal body is needed in turn for axonemal assembly (Dutcher, 2001). On the other hand, homologues of EB1 play a role in assembly at the microtubule tips (Pedersen et al., 2003) and may encourage A-lattice assembly. Recent studies on doublet microtubule structure (Downing and Sui, 2007) have not reached sufficiently high resolutions to define details of the tubulin lattice.

3.7.3. TubZ double and tetrameric filaments

Two types of TubZ filaments have been identified by electron microscopy, double filaments featuring simple closed twofold rotational symmetry and quadruple filaments composed of two double filaments winding around one another, having exchanged their twist for increased writhe (Aylett et al., 2010). Docking of crystal structures of TubZ protofilaments into the reconstructed densities of TubZ double filaments allowed the generation of a pseudo-atomic model of the double filament. The N-terminal extension, including H0 (Fig. 1.2), of TubZ appears to form the main interprotofilament contact. Significantly, this orientation is the same, with respect to the notional "inside" and "outside," as that of tubulin in eukaryotic microtubules. Reconstructed images of the quadruple filaments seen *in vitro* have also been analyzed but the resolution is currently insufficient to show whether they consist of double filaments in parallel or antiparallel.

Electron cryotomography of bacterial cells overexpressing TubZ revealed large, well-ordered bundles of filaments in the cytoplasm (Aylett et al., 2010). Individual filaments were similar in morphology to those observed *in vitro* for dimeric protofilaments. Signs of thin crossbridges between them raised the possibility that the C-terminal tail of TubZ mediates bundling but again it could not be determined whether filaments had uniform or mixed polarity.

3.7.4. FtsZ double filaments and sheets

Protofilament sheets formed *in vitro* after addition of Ca^{2+} to purified bacterial FtsZ (Löwe and Amos, 1999) consisted of paired protofilaments, which were straight, instead of twisting around each other like those of TubZ. The structure was modeled to near-atomic resolution by docking the monomeric crystal structure into a density map obtained by electron crystallography and protofilaments appeared to make contact in a very similar manner to TubZ, and therefore also conserve the orientation relative

to tubulin. The parallel, back-to-back arrangement observed would inhibit protofilament bending and may explain the formation of stable flat sheets *in vitro*. Double filaments of FtsZ proteins have been observed by electron microscopy of FtsZs from other species in the absence of calcium (Oliva et al., 2003; Olson et al., 2010; White et al., 2000) but they may be unstable except at pHs below 7 (Chen et al., 2007); it is not known whether the two protofilaments are parallel or antiparallel in these cases. The parallel double filaments seen in large sheets may not occur *in vivo* but, if two filaments were to make contact in a similar manner but antiparallel, they would both be able to bend in the same direction and might support each other during membrane constriction. However, the structures involved in this activity *in vivo* remain unclear; those reported range from short individual protofilaments to substantial bundles (Fu et al., 2010; Li et al., 2007).

3.8. Roles of the C-termini

The C-terminal extension of tubulin acts as a binding site for kinesins and other motor proteins, and is located on the exterior of the microtubule. Similarly, the C terminus of FtsZ performs recruitment functions and may be located on the outside of FtsZ double protofilaments. Finally, the C terminus of TubZ, believed to recruit the TubR adaptor protein (Larsen et al., 2007; Ni et al., 2010), is positioned on the outside of the filament interface.

In eukaryotic tubulins, the loop of the C-terminal helical hairpin also helps in cementing an interaction within the protofilament. The contact is preserved in the curved protofilament structure. No similar interaction has been observed for FtsZs. However, in the case of TubZ, the C-terminal helical tail makes an interaction with the adjacent subunit in the same protofilament, featuring a hydrophobic contact with helix H5. In tubulin, hairpin helices H11 and H12 each make hydrophobic contacts with H5 of their own subunit (Fig. 1.4). It is possible that these are compensatory adjustments, the folding of the tubulin C-terminal tail back upon itself during evolution allows the formation of this contact within a single subunit.

Another possible role for the C-terminal domains of TubZ and β-tubulin might be in sensing the state of the nucleotide-binding site, through contact with loops T3 and T5, and using this information to modulate its interaction with other complexes. For example, a recent report that a kinesin motor domain binds approximately three times more tightly to GMPCPP microtubules than to GDP microtubules (Nakata et al., 2011) suggested that kinesin's loop 8 was involved. This part of kinesin binds to H11-H12 of β-tubulin.

3.9. Tubulin-binding drugs

Compounds that bind to tubulin and affect its conformation show a surprising variety of structures and modes of action. However, it is likely that they all bind to tubulin conformations that occur naturally and their presence may select particular conformations that might not otherwise be strongly favored. The best understood compounds are Taxol, which stabilizes the assembled state, and Colchicine and Vinblastine, which both interfere with microtubule assembly. Their differential effects on GTPase activity was a puzzle for many years; while GTPase activity is unaffected by Taxol, it is increased by Colchicine binding and inhibited by Vinblastine (Rai and Wolff, 1996). Assembly-stabilizing compounds most likely take advantage of sites adapted for binding natural assembly controllers such as MAPs (Kar et al., 2003a,b) but poison tubulin activity by binding so tightly that assembly is virtually irreversible. Assembly destabilizers bind in one or other of the two kinds of intra-protofilament interfaces and prevent the formation of straight heterodimers and protofilaments.

3.9.1. Binding to the luminal pocket

Both Paclitaxel (Taxol) and Epothilone have been imaged bound to tubulin (Nettles et al., 2004; Snyder et al., 2001) in a pocket in β-tubulin between the central helix and the M-loop (Fig. 1.9A); the equivalent space on α-tubulin is filled by an extended loop between S9 and S10 (residues T361-VVPGGD-L368; see Fig. 1.2). The site occupied by Taxol, behind the M-loop and below loop T6, is present in all eukaryotic tubulins, although it does not always bind Taxol; interestingly, prokaryotic proteins seem to have an equivalent pocket, suggesting it could be a conserved site for binding accessory molecules. It lies on the inside surface of a microtubule but would be more accessible on a prokaryotic filament.

Direct structural information is limited to Paclitaxel and Epothilone bound to two-dimensional sheets of tubulin (Nettles et al., 2004; Nogales et al., 1998a). Even in these cases, the resolution is insufficient to show the precise conformations of the bound drugs and their interactions with protein residues. Though the conformation of bound Paclitaxel in 1TUB and 1JFF is most likely incorrect (Snyder et al., 2001), there is no consensus on the choice between the "T" or "REDOR" conformations (Sun et al., 2010; Yang et al., 2009). Discodermolide (Canales et al., 2008) displaces tau more efficiently than Taxol because of its higher affinity for the luminal pocket but tubulin with Discodermolide bound has not yet been imaged.

Cyclostreptin also competes with Paclitaxel in the luminal pocket (Edler et al., 2005). Though it binds covalently only to residue Thr-220 of β-tubulin in unpolymerized protein, it links also to residue Asn-228 in the luminal pocket of assembled microtubules (Bai et al., 2008). Unexpectedly, the first

site is externally accessible and distinct from the luminal pocket. It was proposed to provide an intermediate binding position for Paclitaxel, en route to the luminal site (Canales et al., 2008), but it is not clear why tubulin would have evolved a binding site here unless it is part of a series of sites that bind to an extended accessory protein such as a MAP (Fig. 1.9A).

3.9.2. Binding to the side pocket

Some natural compounds that promote cold-stable microtubules do not compete with Taxol but act in synergy (Clark et al., 2006; Hamel et al., 2006; Pryor et al., 2002). They are proposed to bind to β-tubulin at a site accessible from the outside of a microtubule, distinct from the external site to which Cyclostreptin binds (Fig. 1.9A). This proposed binding site for Peloruside A (Huzil et al., 2008) and Laulimalide (Bennett et al., 2010; Nguyen et al., 2010) may stabilize the entire activation domain, and thereby keep the heterodimer in the straight conformation, as well as stabilizing the M-loop in lateral bonding; the effects of these drugs will not be clear until the role of the whole activation domain is better understood—see next section.

3.9.3. How is assembly stabilized?

It seems unlikely that Taxol stabilizes assembly by directly supporting the M-loop, given that it can induce straight individual GDP-bound protofilaments (Elie-Caille et al., 2007). Also, the M-loops of Taxol-stabilized MTs are flexible and able to adjust to varying curvatures (Sui and Downing, 2010). Direct conformational effects on the active site on the GTPase domain are also difficult to imagine. However, an interaction with the flexible H7-H10 interface lying next to the pocket may stabilize the entire activation domain and support the interaction between H6/H7 and the next subunit. When this interaction is present, there is a continuous subfilament of activation domains, whose presence as a stable entity may tend to keep the protofilament straight.

3.9.4. Stabilizing drugs versus endogenous assembly promoters

Structural MAPs stabilize microtubules against disassembly. MAPs like tau can bind dynamically to just the outer surface of a pre-assembled tube, where they have an inhibitory effect on kinesin's processive run length (Dixit et al., 2008), although tau is reported to have no effect on axonal transport *in vivo* (Yuan et al., 2008). However, tau binds more stably when copolymerized with tubulin, when each of the 3 or 4 repeat motifs is proposed to bind to the luminal pocket of a β-tubulin subunit (Kar et al., 2003a,b) and binding in this manner may even improve gliding motility *in vitro* (Peck et al., 2011). Besides the repeat motifs, other sections of a tau molecule bind to tubulin and contribute to microtubule stability. Experiments with Discodermolide (Kar et al., 2003b) suggest that although there is one level of saturation when a 4R-tau molecule binds 4 tubulin dimers,

a stronger binding constant is reached when each tau molecule is bound to ~6 tubulin molecules. This stronger binding probably includes contributions from the "proline-rich domain" docked into the side pockets of additional dimers, as speculated in Fig. 1.9A. We propose that stabilization of the activation domain by both the repeat motifs in the luminal pocket and the proline-rich domain in the side pocket helps to keep each protofilament in a microtubule in a straight conformation.

3.9.5. Destabilizing agents that bind within curved heterodimers

Many drugs inhibit tubulin assembly by favoring the curved protofilaments so they cannot associate laterally to form microtubules. Some work at substoichiometric concentrations by poisoning just the ends of filaments, others need to be present in stoichiometric amounts. They may induce disassembly into small oligomers, such as rings, or transform protofilaments into long helices or spirals. A major group binds in between the two monomers of a heterodimer. Colchicine and Podophyllotoxin have both been shown in crystal structures [PDB structures 1SA0, 1SA1, 1Z2B] to bind to β-tubulin in a pocket close to the non-exchangeable GTP (Dorléans et al., 2009; Ravelli et al., 2004). Binding here while the heterodimer is curved seems to fix the conformation so that it cannot straighten (Barbier et al., 2010). Substoichiometric levels of these drugs may bind to subunits at microtubule ends and block dynamic activity. Important compounds that probably bind in similar sites include Benomyl (Clement et al., 2008), Rotenone (Srivastava and Panda, 2007), and Nocodazole (Xu and Luduena, 2002) but their binding conformations remain to be investigated.

3.9.6. Agents that stabilize curly protofilaments

Compounds such as Vinblastine, that prevent microtubule assembly by binding to the longitudinal interface between heterodimers, are of great interest from a structural point of view. Vinblastine-induced helices remain poorly characterized but may be single or double in paracrystals (Amos et al., 1984; Nogales et al., 1995). Although these helical protofilaments are associated with microtubule disassembly, the inhibition of GTPase activity (Lin and Hamel, 1981) indicates they are profoundly different from normal depolymerization products. Vinblastine/Phomopsin binding sites are known from crystal structures (PDB 1Z2B, 3DU7) containing tubulin dimers in complex with stathmin (Cormier et al., 2010; Gigant et al., 2005; Ravelli et al., 2004). Vinblastine binds in the interface between heterodimers, while Phomopsin A binds to a similar site on the β-tubulin subunit at the top end of the tubulin tetramer. Phomosin A's interaction with α-tubulin has not been visualized, presumably because it is too big to fit into the space between heterodimers with GDP rather than GTP in the exchangeable site. It is possible to imagine that the presence of either compound in the interface between heterodimers with GTP in the

nucleotide pocket would prevent formation of the conformation needed for hydrolysis. A molecular dynamics analysis (Rendine et al., 2010) indicated that binding of Vinblastine between heterodimers would move T7 and H8 of α-tubulin away from GTP bound to β-tubulin and the insertion of solvent molecules would account for the decrease in the rate of hydrolysis.

Pironetin is interesting because it competes with Vinblastine in the interface between heterodimers but, instead of binding primarily to β-tubulin, it binds covalently to lysine K352 of α-tubulin (Usui et al., 2004). Colchicine was found to bind more readily to the intra-dimer site if either Vinblastine or Pironetin was bound to the inter-dimer interface, supporting the idea that an allosteric change effects curvature.

Cryptophycin-1-bound tubulin forms small (24 nm diameter) rings (Watts et al., 2002); whereas stathmin binding leads to protofilament curvature that would produce rings with 13–15° bends between all monomers, electron micrographs of tubulin with Cryptophycin-1 showed rings consisting of eight dimers and clearly distinct heterodimers, with 32° inter-dimer bends. Although the drug binds primarily to the β-subunit, it protects both monomers against proteolysis, suggesting conformational changes in both.

3.10. EB proteins

As mentioned in Section 3.3.3, an important role of the master +TIP, EB1 (and homologues such as Mal3 and Bim1C, in yeasts), at the growing tip of a microtubule is to recruit other molecules needed there. Unexpectedly, it has emerged that microtubule growth rate, catastrophe frequency, and shrinkage rate at the end are all independent of the concentration of the master +TIP itself (Katsuki et al., 2009). These workers found that Mal3 weakly stabilizes the main body of a microtubule; molecules bound sparsely to mainly GDP-tubulin lattice can halt disassembly and promote rescues, supplementing the effects of a sprinkling of γ-tubulin (Bouissou et al., 2009) and GTP-β-tubulin subunits (Dimitrov et al., 2008).

The globular "calponin homology" (CH) domain of the protein binds near the groove between protofilaments (Fig. 1.9C), making an extensive contact with one tubulin subunit (des Georges et al., 2008). This site is consistent with metal-shadowed EM images (Sandblad et al., 2006) and with the results of an alanine scanning study of *Saccharomyces cerevisiae* α-tubulin, interacting with the EB homologue Bim1C (Richards et al., 2000). The basic peptide on the C terminus of the CH domain, having three successive arginines, may interact with the acidic C-terminal "E-hook" of a neighboring tubulin subunit and stabilize the microtubule lattice (des Georges et al., 2008). Zanic et al. (2009) found that the binding of EB1 to the microtubule lattice assembled from tubulin lacking E-hooks ("S-tubulin," produced by proteolysis with Subtilisin; Sackett and Wolff, 1986) was reduced.

The C-termini of both EBs and tubulins appear to be unstructured when free (Honnappa et al., 2006) but must interact with each other in a stereospecific way. For example, the observation that EBs stabilize only 13-protofilament microtubules indicates that the crossbridging interaction needs two protofilaments set at a particular angle to each other. Also, Mal3, the fission yeast EB, has been shown to preferentially bind to the A-lattice seam of a B-lattice microtubule (Sandblad et al., 2006) and promote the formation of a high level of A-lattice if co-assembled with tubulin (des Georges et al., 2008). This suggests that the C-terminal extension of the CH domain binds more strongly to the nearest E-hook in an A-lattice than in a B-lattice. Since a microtubule growing out of a γ-tubulin ring complex (γTuRC) has a B-lattice and single A-lattice seam, it seems unlikely that EB proteins promote A-lattice assembly in cells. Possibly EBs have evolved to prefer A-lattice so that they preferentially stabilize complete tubes, with the presence of a seam being a sign of a fully closed lattice (Fig. 1.8A).

Binding in high concentration to the tips of growing microtubules indicates a strong preferential interaction with the cap of tubulin dimers containing GTP in the exchangeable sites. There is much interest in the structural difference that EB proteins recognize. The conclusion that end dynamics are independent of EB1 concentration (Katsuki et al., 2009) is consistent with the GTP-bound cap not being in need of external stabilization; here, therefore, a CH domain may bind strongly to just one subunit of GTP-tubulin, instead of cross-linking the lattice. However, the fact that EB1 does not bind to soluble tubulin heterodimers suggests that binding depends on features present after assembly, at least into a protofilament, but the alanine scanning study mentioned above found important residues on part of the GTPase domain that one would expect to be masked by full lattice assembly. To account for all of these observations, it is likely that parts of EB1, including the basic extension from the CH domain, interact with the intraluminal surface, such as the GTP-stabilized H1-S2 loop (Section 3.3.3; Fig. 1.9); this requires that the end structure with GTP in the exchangeable site has a conformation that exposes these residues.

Studies of EB interaction with tubulin assembled with GMPCPP suggest that GMPCPP not a very good analogue of GTP. EB interaction was enhanced compared with GDP-bound lattice (Zanic et al., 2009) but was still fairly weak (Maurer et al., 2011). GMPCPP-tubulin polymers (Section 3.5.2) may mimic an intermediate state, such as with GDP-Pi in the exchangeable site. In contrast, the study by Maurer et al. showed that GTPγS-assembled microtubules bound EB1 strongly all along the tube. These authors suggested that GTPγS tubulin might be in a slightly curved conformation even when constrained in the microtubule lattice, as a possible explanation for EB1's ability to recognize the nucleotide state. Alternatively, we suggest that the lattice is unstable because of a mismatch in spacings (Fig. 1.8B; Section 3.11.5) and that there may be (temporary)

openings all along a GTPγS or GMPCPP microtubule. It seems unlikely that EB1 senses the change in nucleotide state in the same way as kinesin may (Section 3.8), when their binding sites are so different (Fig. 1.9).

3.11. So, what is the initial state of GTP-bound protofilaments?

As already mentioned, it is becoming clear that tubulin and its homologues assume several subtly different conformations that are influenced, though not rigidly determined, by the nucleotide bound (Fig. 1.7). The least understood state, with GTP bound to the E-site, is gradually coming into focus from a range of different observations. These have been mentioned already but are summarized in the following list. The overall conclusion is that there is an important conformational change during assembly, at the GTP-bound interface between tubulin heterodimers or between monomers of the prokaryotic proteins.

3.11.1. Increased longitudinal spacing

Heterodimers certainly assume at least one other conformation than those seen in tubulin crystal structures, since the average longitudinal subunit spacing in protofilaments assembled from GMPCPP-tubulin is greater than for GDP-tubulin (Section 3.6.7). TubZ protofilaments crystallized with either bound GDP or non-hydrolysable GTPγS have revealed two forms of longitudinal interaction (Fig. 1.5A and B). In all interactions where GDP is bound and in some with GTPγS, T7 is close to the nucleotide, as in all available tubulin structures. However, in the remaining cases, T7 is poised further away from the nucleotide, apparently held away by loops T2-T5 surrounding the nucleotide. A similar movement would explain the change in longitudinal subunit spacing in tubulin protofilaments. The two conformations seen for TubZ suggest that the loops around the nucleotide are springy. The greater flexibility of newly polymerized microtubules (Janson and Dogterom, 2004; Section 3.15) is in accord with longer springier loops making the longitudinal connections between tubulin dimers when GTP is bound.

3.11.2. Vinblastine inhibits GTP hydrolysis

A variety of poisonous compounds form cross-links between tubulin heterodimers and apparently fix the interface in an extended curved, and possibly twisted, conformation to produce helical protofilaments, as observed for Vinblastine (Lin and Hamel, 1981) or Maytansine (Gupta and Bhattacharyya, 2003), or even closed rings, as observed for Cryptophycins (Watts et al., 2002) or Dolastatin (Moores and Milligan, 2008). As suggested in Section 3.9.5, the presence of these drugs could inhibit

the straightening and compression required for GTP hydrolysis and may also prevent nucleotide exchange.

3.11.3. Twisted conformation of FtsZ dimer

The only high-resolution structure of a polymer-like complex with exchangeable GTP bound is a dimer of FtsZ (Fig. 1.3D; Oliva et al., 2004). Compared with a straight protofilament, loop T7 of the upper subunit is twisted up and away from the GTP on the subunit below (Section 3.6.7). It is possible that this represents the initial interaction between FtsZ subunits during protofilament assembly, since subunits must join together firmly before hydrolysis is triggered. We envisage stages when thermal flexing allows newly assembled protofilaments to straighten, and then T3 and other loops change conformation and allow T7 to approach and hydrolyze GTP.

In the case of tubulin, the intra-dimer interface presumably reaches a closely bound state in the soluble heterodimer, with the help of chaperones (Grynberg et al., 2003; Tian et al., 1999); the loops around GTP on α-tubulin are clearly compressed, though the approach of the β T7 loop cannot promote hydrolysis.

3.11.4. Splayed ends of growing microtubules

As mentioned in Section 3.3.2, 3D electron-tomographic images of growing microtubule ends show funnel shapes made up of splayed protofilaments, different in appearance from the curled protofilaments at depolymerizing ends. Splaying would provide access to parts of the protofilament that would be blocked in a closed tube. It could be a consequence of twisting, which would inhibit protofilaments from making lateral interactions.

3.11.5. EB proteins specifically recognize growing ends

EB proteins, which bind more avidly to growing tips than to the GDP-bound lattice, presumably recognize and strongly associate with a specific conformation of assembled GTP-bound tubulin (Section 3.10). The splayed protofilament ends obviously allow access to regions on α-tubulin that may be important for strong binding but do not explain the full size of the comets (Section 3.3.3). However, it may be significant that EB proteins bind well all along microtubules assembled with non-hydrolysable GTP analogues and that these have longer longitudinal spacings than GDP-bound lattice (Section 3.6.7). This could mean that 13 protofilaments are inhibited from associating into a closed tube; there will be a mismatch at the final seam between the 120 Å helical rise along 13 subunits associated laterally (Fig. 1.8B; Section 3.7.1) and the longer distance along three subunits in a protofilament. Thus, it is possible that polymers assembled in GTPγS are not closed microtubules but have an open seam, of which only one edge

may provide strong binding sites for EB proteins. GMPCPP microtubules, which bind EB proteins less avidly than GTPγS lattice, may close and reopen in an unstable fashion and allow occasional binding. The apparently closed tubes next to the splayed end of a growing microtubule may, therefore, have open seams or unstable connections that allow EB proteins to bind strongly for short intervals, until the E-site GTP is hydrolyzed and the γPi finally released. The C-shapes sometimes seen in cross-sections through cells would be explained in this way. It is also possible that some part of an EB molecule has access to a luminal sites through pores in the microtubule wall (Fig. 1.9).

3.12. Control of microtubule dynamics by accessory proteins

There are some particularly interesting examples of proteins that control microtubule dynamics by interacting with plus or minus ends. To promote tubulin assembly or disassembly, accessory proteins mostly bind in some way that affects protofilament stability. MAPs that become an integral part of a stably assembled microtubule have been discussed briefly in Section 3.9.3. Doublecortin (Fig. 1.9D), a neuronal protein that binds in the groove between protofilaments (Fourniol et al., 2010), also seems to remain bound in order to stabilize assembled microtubules. But other proteins that affect assembly and disassembly act more transiently and interact mainly with assembling or disassembling filament ends.

3.12.1. Kinesins

Kinesin motor domains bind across both monomers of a heterodimer and even those involved in motility to produce a slightly curved dimer conformation (Hirose et al., 1999, 2006). Depolymerizing kinesins (kinesin-13s and kinesin-8s) have an extended L2 loop at the minus end of the molecule (Shipley et al., 2004) and they induce strongly curved protofilaments (Moores and Milligan, 2008; Moores et al., 2006). It is assumed that driving protofilaments into a curved conformation promotes microtubule disassembly and this will occur most readily at a microtubule end.

3.12.2. Proteins with TOG domains

Besides the CH domain-containing EB family, another group of proteins is able to specifically recognize the growing ends of microtubules and these contain globular TOG (tumor-overexpressed gene) domains (Ohkura et al., 2001; Slep, 2010). Proteins such as yeast STU2, Xenopus XMAP215, or plant MAP200 contain a series of 2–5 ~200-residue TOG domains (Al-Bassam et al., 2007). Unstructured linkers between the globular domains include an important basic region (Widlund et al., 2011) that may serve a similar role to the basic peptide that follows the CH domain of an EB protein (Section 3.10). Like the EB proteins, TOG-domain proteins bind

weakly to the fully assembled microtubule lattice but more tightly near the ends. XMAP215 molecules appear to diffuse along a microtubule until they encounter a growing end and may then remain the end for many rounds of tubulin subunit addition. Since, unlike EB1, XMAP215 binds to free tubulin heterodimers, as well as to assembled protofilaments, it is proposed to act as a processive microtubule polymerase (Brouhard et al., 2008). It may assist assembly by binding to multiple dimers, increasing their opportunity to associate with each other. The combined effect of Taxol and MAP200 (Hamada et al., 2009) is interesting; MAP200-tubulin mixtures treated with Taxol formed long coiled filaments that were rare when MAP200 was allowed to interact with pre-assembled, prestabilized microtubules. Again, this suggests that a full interaction requires access to a region of tubulin that is masked by lattice closure. For TOG-domain proteins, the relevant region is unlikely to feature the proposed hydrolysis-sensing H1-S2 loop of α-tubulin that may be important to target EB1, since XMAP215 binds also to unstable GDP-tubulin ends and strongly promotes catastrophes. Until more structural information becomes available, we can only speculate that MAP215 has its dual activity, as both a polymerase and a depolymerase, by favoring separated protofilaments and not a closed lattice.

3.13. γ-Tubulin complexes

γ-Tubulin, apparently present in all eukaryotes (Dutcher and Trabuco, 1998), is essential for the initiation of microtubule assembly (Luders and Stearns, 2007). At centrosomes, it is in ring-shaped complexes, γ-TuRCs, which also include several associated proteins. At other organizing sites, smaller complexes are sufficient to initiate microtubule assembly. Besides being at initiation sites, γ-tubulin has also been localized all along microtubules, where its positions matched sites of pause or rescue in microtubule dynamics (Bouissou et al., 2009).

The interactions between subunits in the crystals of γ-tubulin monomers, mentioned in Section 3.5.1, resemble the lateral contacts between protofilaments in a microtubule (Aldaz et al., 2005). Kollman et al. (2010) discovered that a simple complex of γ-tubulin with only two accessory proteins, Spc97 and Spc98, self-assembles into a helical filament that may provide a template for microtubule nucleation. It seems likely that the accessory proteins impose the correct curvature between adjacent tubulin subunits. Reconstructed images showed that Spc97 and Spc98 form a two-pronged fork with a γ-tubulin monomer on the end of each prong. Most importantly, these small fork complexes can associate further into a helical structure in which the γ-tubulin monomers define the pitch and radius of the 3-start helical family of a 13-protofilament microtubule (Fig. 1.8). The large γTuRCs that have been isolated from cells (Moritz and Agard,

2001) include several other accessory proteins (Guillet et al., 2011), whose roles must include limiting the extent of assembly to a single turn of the helix.

3.14. Less well-known tubulin family members

Several conserved eukaryotic tubulins have specialized roles in basal bodies/centrioles (Section 3.7.2). They include ε-tubulin, η-tubulin, and ζ-tubulin, which cluster into individual phylogenetic groups (Dutcher et al., 2002) but are found in widely differing eukaryotic genomes. Extant eukaryotic organisms lacking motile axonemes, triplet microtubule basal bodies, or centrioles all seem to have evolved from organisms that did possess these organelles but subsequently lost the genetic information needed to assemble them. It is likely δ-tubulin was lost at the same time (Dutcher, 2003).

3.14.1. δ-Tubulin

The little that is known about this member of the family includes some intriguing observations that suggest it would be interesting to investigate the structures formed. Sequences from a wide range of species agree well with other superfamily members in the GTPase domain, including the tubulin signature motif GGTGSG in the T4 loop (Inclan and Nogales, 2001), but the T7 loops lack the motif involved in longitudinal interactions (GXXNXD), which is well conserved among other superfamily members, even γ-tubulin (Fig. 1.2). Other parts of the activation domain contain insertions and deletions that make longitudinal interactions with other tubulins unlikely (Inclan and Nogales, 2001). Thus, δ-tubulin may interact with other tubulins only via its plus-end surface or through lateral interactions. Deletion of δ-tubulin in *Chlamydomonas reinhardtii* produced cells lacking one or both flagella (Dutcher and Trabuco, 1998). Examination of the mutant basal bodies using dual-axis tomography subsequently revealed that most of the the basal body contained only doublet rather than triplet microtubules except at its distal end, where the C-tubules were present (O'Toole et al., 2003b). Recent tomographic studies (Sam Li, personal communication) suggest that δ-tubulin forms a special protofilament on one edge of the C-tubule, where it joins to the B-tubule. It is unclear why it is needed there but not at the similar junction between B- and A-tubules.

However, the catalytic residue E254 in H8, essential in α-tubulin for GTP hydrolysis, has been preserved in some δ-tubulins, suggesting that they might form active protofilaments. The role of δ-tubulin is most interesting in mammalian cells. Although it is present in centrosomes during mitosis, in the manchette of mouse sperm cells, it is also present in the perinuclear ring (Smrzka et al., 2000). Both large and small rings were seen in mouse testis (Kato et al., 2004); small rings appeared to function as temporary intercellular bridges, while large perinuclear rings were observed during spermatid development, when the nucleus is highly compacted. The formation of

these rings suggests a role that may resemble that of FtsZ in bacteria, though possibly reinvented, since δ-tubulin is somewhat less similar to FtsZ than αβ-tubulin is.

3.14.2. Misato

Misato protein has clear homology to tubulin, but has quite long inserts. It is conserved from yeast to humans and is localized to mitochondria (Kimura and Okano, 2007) but is distinct from the FtsZs found in endosymbiotic organelles, including some mitochondria (Löwe et al., 2004), since the sequences include features found in tubulin but not in FtsZs. After silencing of misato, mitochondria became fragmented, suggesting it plays some kind of structural or membrane-remodeling role but, currently, it is not known whether the protein even forms protofilaments.

3.15. Microtubules are flexible in spite of being stiff

If microtubules behaved according to classical polymer theory, any bending would be due to elastic distortion from the straight conformation and a restoring force proportional to the amount of distortion would prevent high curvature. Measurements of microtubule persistence length, the length over which a filament behaves as a uniform elastic rod, suggest that this model may be appropriate for long microtubules undergoing small amounts of bending but microtubule behavior shows many deviations from an "ideal polymer" (van den Heuvel et al., 2008).

The complex bending behavior of microtubules is less surprising if one regards them as bundles of FtsZ-like filaments rather than uniformly elastic tubes. There appear to be multiple stable states for intact microtubules, well away from the straight conformation; for example, *in vitro*, microtubules have been observed in gliding assays to go into fixed helical or circular shapes (e.g., Amos and Amos, 1991 saw 0.5-μm radius circles floating in solution). *In vivo*, mitotic spindles may include many curved microtubules without tending to spring apart. To explain such behavior, a lattice of conformationally bistable heterodimers has been modeled (Mohrbach et al., 2010). The heterodimers are viewed as fluctuating between curved and straight states, even after assembly into a tube, in analogy to the bistable flagellin model (Calladine, 1982) that was developed to explain the switching helical modes of bacterial flagella (Maki-Yonekura et al., 2010). The assembled curved state was proposed to resemble that in the tubulin–stathmin complex but a possible alternative is that in a microtubule, a continuous subpolymer of activation domains (Section 3.9) assists the backbone of C-terminal domains (Section 3.8) in providing a scaffold, while the GTPase-domain loops around GDP switch between tight and loose binding conformations, similar to the alternative states seen in TubZ filaments (Fig. 1.5). Either way, bistable GDP-bound dimer subunits with fairly

elastic lattice connections would allow microtubules to bend and twist as observed (Mohrbach et al., 2010).

The alternative conformations available during bending may vary slightly, depending on the nucleotide in the exchangeable site between dimers, as described in Section 3.6.7 for TubZ filaments. Variation of this nature apparently led to conflicting measurements *in vitro* of microtubule stiffness (Janson and Dogterom, 2004; Kurachi et al., 1995). Short microtubules were found to be more flexible than longer ones, quickly growing ones less stiff than slowly growing ones; finally, sections at the growing ends were seen to be more flexible than the central region. Similarly, microtubules growing in cells may run through the cytoplasm as long straight tracks but then bend dramatically near the periphery of the cell (e.g., Brangwynne et al., 2007; Drummond and Cross, 2000).

4. The Actin Family

The actin family of ATPases (Fig. 1.1B) is structurally related to the ATPase domains of a number of multidomain proteins, including the 70-kDa heat-shock protein family (Hsp70), and a variety of metabolic pathway kinases including hexokinase (Bork et al., 1992; Kabsch and Holmes, 1995). The ATPase domain by itself evolved the ability to assemble into cytomotive filaments in prokaryotes, where it is not universally necessary, but became an indispensable component of eukaryotic life. The actin family proteins found in a prokaryotic group known as the crenarchaea are most similar to eukaryotic actins (Ettema et al., 2011), which is consistent with the impression that a branch of archaeal FtsZs are the prokaryotic homologues most similar to tubulin.

Eukaryotic cell migration and morphogenesis, including cytokinesis, are driven by protrusive or contractile processes requiring actin filaments. Lamellipodial and filopodial actin filament arrays provide the force for membrane protrusions through actin filament assembly (Carlier and Pantaloni, 2010; Le Clainche and Carlier, 2008; Pollard and Borisy, 2003). A contractile ring of actomyosin filaments is largely responsible for the constriction of a cell during its division into two daughter cells. Stress fibers, straight contractile bundles, are important in cell crawling, retracting the tail of the cell by pulling against adhesion sites (Cai and Sheetz, 2009; Pellegrin and Mellor, 2007; Tojkander et al., 2011); in multicellular organisms, similar bundles play a role in morphogenesis and help support cells against tension (Millan et al., 2010; Prasain and Stevens, 2009).

Several different classes of actin family filaments are found in prokaryotes, including ParM, MreB, FtsA, and MamK (Carballido-Lopez, 2006; Michie and Löwe, 2006). The reasons for the substantial structural variation

in the assembled filaments remain poorly understood (Jockusch and Graumann, 2011). However, the diversity in prokaryotes compensates for a lack of the many accessory proteins found in eukaryotes, and that each protein may have been tailored toward an evolutionarily optimal structure to fulfill certain functional constraints. In this way, each individual prokaryotic genome can remain small.

ParM, for example, appears to have the single role of segregating plasmid copies, by polymerizing filaments between them (Salje et al., 2010). MamK is found only in bacteria that can sense the earth's magnetic field, and the filaments formed seem to be responsible for aligning magnetic-nanocrystal-filled compartments (magnetosomes) along the cell axis (Komeili et al., 2006; Pradel et al., 2006). MreB is the most common bacterial actin homologue, being present in most non-spherical cells and essential for maintaining their shapes. FtsA is also widespread and is needed to recruit the Z-ring to the cell membrane, to which FtsA binds through a C-terminal amphipathic helix (Löwe et al., 2004; Pichoff and Lutkenhaus, 2005; Yan et al., 2000).

4.1. Actin family filament complexes

As in the case of the tubulin family, all actin family structures are made up of longitudinal protofilaments. An alignment of the amino acid sequences based on our current understanding of these structures (Fig. 1.10) is in full agreement with results obtained by comparing all known sequences (Yutin et al., 2009). Thus, despite there being very low sequence conservation between eukaryotic actin and its prokaryotic homologues (<15%), the structurally conserved interactions between neighboring subunits in a protofilament (Fig. 1.11) suggest that there have been complementary changes in these sites during evolution.

4.2. Atomic structures of the actin family

4.2.1. 4-Domain actin subunits

The actin family subunit is an ATPase characterized by two domains that may have been produced by gene duplication. The structure is usually discussed in terms of four subdomains (Ia, Ib, IIa, and IIb; Figs. 1.10–1.12) forming a rectangular box with approximate dimensions 55 × 55 × 35 Å (Kabsch et al., 1990). Subdomains Ia and IIa, which comprise the most conserved region of the superfamily, have almost identical topology. Three different arrangements of domains I and II have been observed in high-resolution structures: open and twisted, closed and twisted, and closed and untwisted (Oda and Maeda, 2010). The contact between subdomains Ia and IIa remains unchanged by these relative movements (Fujii et al., 2010). In the closed conformations, the cleft between domains I and II embraces

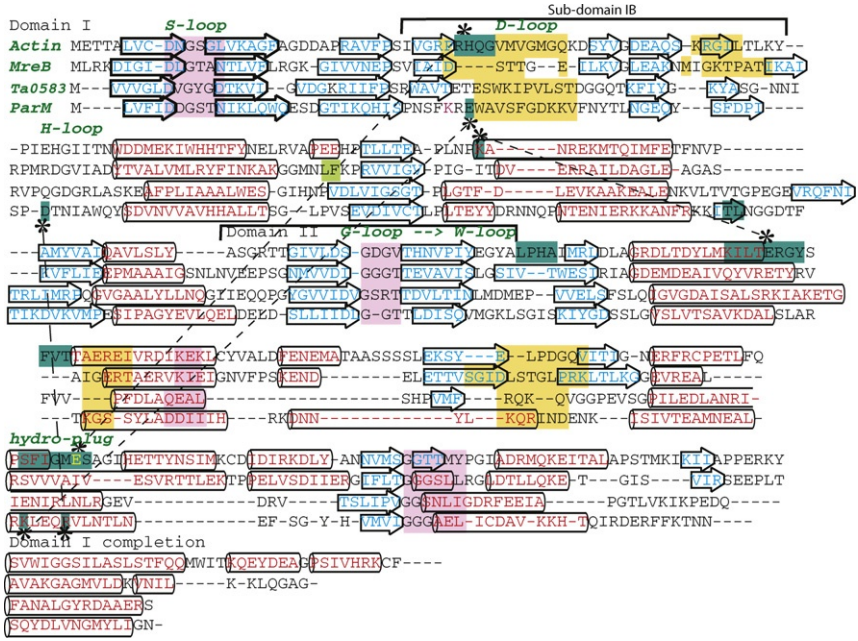

Figure 1.10 Actin family amino acid sequences. Structurally aligned sequences of some members of the actin family. The segments forming domains I and II are indicated. The secondary structures are based on the crystal structures in PDB files 2ZWH (Oda et al., 2009), 3G37 (Murakami et al., 2010), 3MFP (Fujii et al., 2010), 1JCE (van den Ent et al., 2001), 2FSJ (Roeben et al., 2006), 1MWM (van den Ent et al., 2002), and 2ZHC (Popp et al., 2008). This structural alignment is essentially identical to one based on multiple sequence comparison (Yutin et al., 2009). Residues identified as being in α-helices are in red, those in β-strands are in cyan, loops are in black. Conserved nucleotide-binding pocket motifs are highlighted in pink. Residues that contribute to intra-protofilament interactions, including the W, D, and DNase-1 binding loops, are shown with yellow (barbed end) or orange (pointed end) backgrounds; subdomain IB and the part of domain II that it contacts are both bracketed. Residues thought to be involved in lateral, inter-protofilament, contacts have backgrounds in blue-green and dashed lines indicate some interactions made. The lateral contact in actin involves a loop known as the "hydrophobic plug." The equivalent peptide in MreB is equally hydrophobic but its function is unknown. A hydrophobic dipeptide (highlighted in green), on the opposite side of this species of MreB subunit, is known to interact with membranes (Salje et al., 2011).

the nucleotide and Mg^{2+}. The phosphates are buried within the structure, while the base sits upon the surface of the protein.

As expected, residues that interact with the nucleotide are well conserved. A difference from the tubulin family is that the nucleotide in actin family filaments does not directly contact the adjacent subunit (Kabsch et al., 1990) but there is only a short β-sheet between the ATP site and the main interaction point (Figs. 1.10 and 1.11). This sheet forms one side of a second

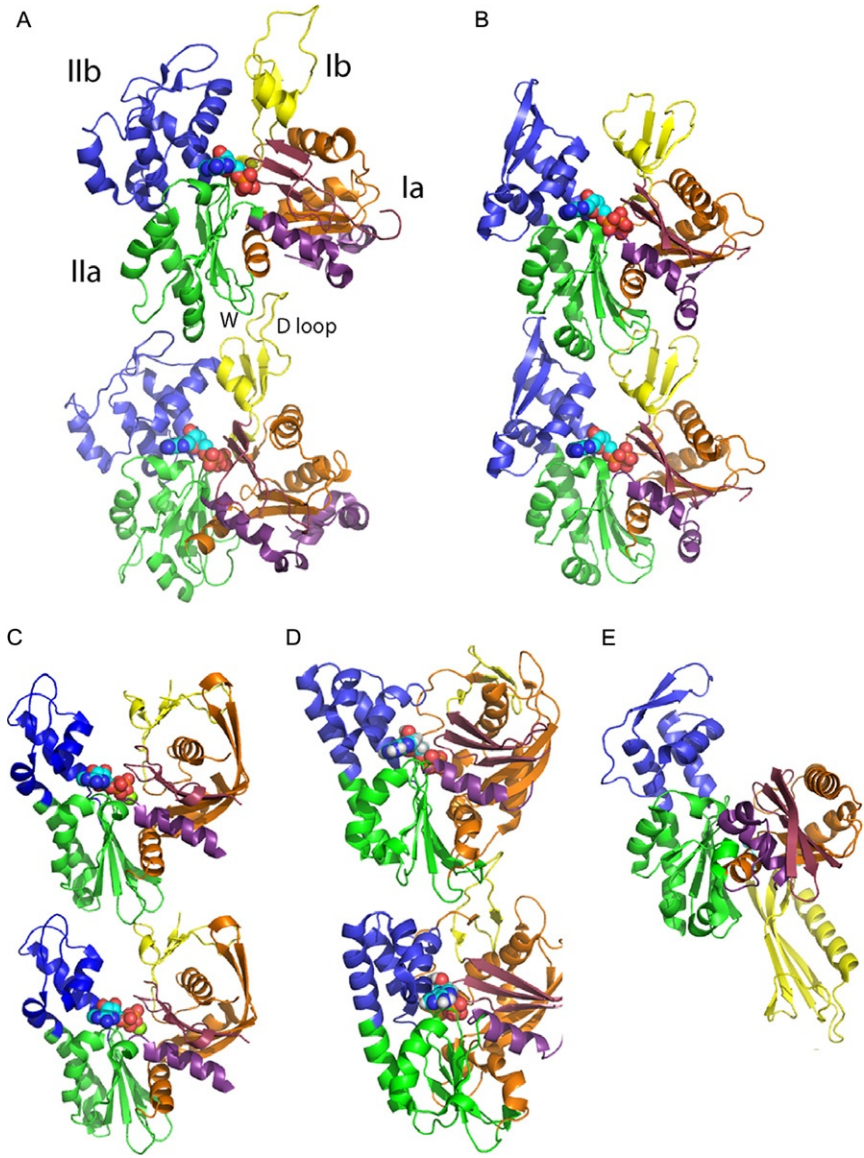

Figure 1.11 Actin family protofilament interactions. (A–D) Ribbon diagrams of some actin family dimers as seen in near-atomic structures of protofilaments. Domain I of each monomer is colored red and orange, with subdomain Ib, that loops out between the red and orange segments, colored yellow; the C-terminal contribution to subdomain Ia is purple. Domain II is in green and blue. The F-actin structure (A) is based on PDB files 2ZWH (Oda et al., 2009), 3G37 (Murakami et al., 2010), and 3MFP (Fujii et al., 2010). The MreB structure (B) is from 1JCG (van den Ent et al., 2001), the Ta0583 structure (C) is from 2FSN (Roeben et al., 2006), and the ParM structure

cleft that can open up between subdomains Ia and IIa, named the "target-binding cleft" because actin-binding proteins and small molecules that affect filament stability tend to bind there; in the case of proteins, the interaction typically involves the insertion of an α-helix (Dominguez and Holmes, 2011). The whole region is structurally well conserved between prokaryotic and eukaryotic family members but not known whether it universally provides binding sites for associated proteins.

4.2.2. Filament structures at near-atomic resolution: MreB, Ta0583, and F-actin

Two crystal structures of actin-like filaments have been solved; the eubacterial protein, MreB, (van den Ent et al., 2001) and an archaeal protein, Ta0583, (Roeben et al., 2006) both form linear polymers *in vivo* and within the crystals. The monomers in the crystals have flattened structures, subdomains I and II being collinear rather than being twisted like the actin monomers seen in crystal structures. Thus, the MreB protofilaments were the first actin-like filaments shown to differ significantly from pseudo-atomic models based on fitting high-resolution eukaryotic actin monomer structures into filament density maps derived from fiber diffraction and electron microscopy (Holmes et al., 1990, 1993; Lorenz et al., 1993). However, it now seems likely that the filamentous conformation F-actin is also flattened. This was discovered when exceptional resolution was achieved from a highly oriented liquid-crystalline sol of actin filaments, revealing the Cα backbone of the protein (Oda et al., 2009), and was confirmed by direct visualization when density maps of the F-actin structure at 6.6 Å resolution, achieved by advances in electron cryomicroscopy, resolved all the secondary structures (Fujii et al., 2010; Murakami et al., 2010).

Although actin protofilaments twist around each other while MreB forms approximately straight filaments, the new models of F-actin show an assembled conformation remarkably similar to that of MreB. Lateral interactions occurring between subdomain IIa of one subunit and Ib and IIb of an adjacent subunit require the flattened conformation in order to

(D) from 2ZHC (Popp et al., 2008). The inter-subunit interactions are very similar, especially in F-actin and MreB. The D-loop interaction with a pair of domain II loops, each one strand away from the G-loop (see Fig. 1.10), is also seen in ParM. The conformation of actin's W-loop seems to vary subtly depending on the nucleotide bound (Kudryashov et al., 2010), suggesting that the strength of its interaction with the neighboring D-loop is nucleotide sensitive. (E) The crystal structure of an FtsA monomer (PDB file 1E4F; van den Ent and Löwe, 2000) shows that subdomain Ib has been replaced by subdomain Ic (yellow) that loops out from a different point in domain I and occupies a position equivalent to Ib of another subunit in an actin or MreB protofilament, so that in FtsA, it contacts the W-loop within the same monomer instead of sensing the state of another monomer (see text).

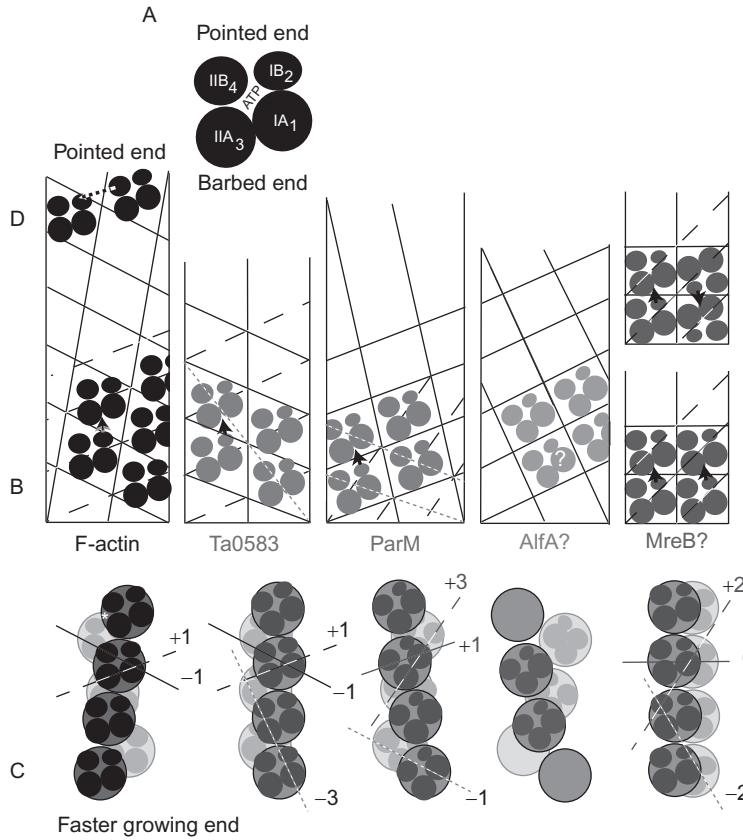

Figure 1.12 The helical lattices of actin family filaments. (A) The protein domains in each subunit and the two naming schemes in use. Regions of the polypeptide that correspond to the four subdomains are indicated in Figs. 1.10 and 1.11. (B) Opened-out helical surface lattices and (C) families of helices in the various 2-protofilament complexes: F-actin, ParM, and AlfA (Polka et al., 2009) double protofilaments are staggered and helical—right handed in F-actin, left handed in the plasmid-encoded filaments. Ta0583 filaments are straight. MreB protofilaments are straight and subunits line up unstaggered. F-actin, Ta0583, ParM, and AlfA filaments are thought to be polar. However, it is not yet known whether MreB protofilaments associate *in vivo* in a polar or a bipolar fashion. All the filament lattices can be regarded as quasi-equivalent; interactions within the protofilaments are conserved (black arrowheads), as is the orientation of outside versus inside surfaces. If pairs of protofilaments are held together by multiple weak electrostatic interactions, it is possible to envisage a straight double filament morphing into a helical filament with either a right handed or a left handed twist. (D) The pointed end of F-actin is less active than the barbed end because the final subunit interacts in a special way with the end subunit of the partner protofilament (Narita et al., 2011).

form the interfaces between protofilaments. The modeled change to the actin fold places a key catalytic glutamine residue and accompanying water molecule in position for nucleotide hydrolysis, explaining the vastly increased rate of hydrolysis in the filamentous state. The γ-phosphate is at the juncture of the two domains, and approximately on the axis of rotation, implying a mechanism for its involvement in the stabilization of one conformation over another. Thus, a twisted-to-flat conformational change between the domains of an actin monomer may serve a similar role to the proposed untwisting conformational change between interacting tubulin subunits during assembly (Section 3.11).

4.2.3. Conformational change during assembly of prokaryotic subunits

There is currently no evidence that prokaryotic actin family subunits ever go into a twisted conformation. Monomeric forms of MreB or Ta0583 have not been crystallized but ParM monomers are flat and have only been seen to change in opening or closing the cleft (van den Ent et al., 2002); the nucleotide-dependent movement of a mutated ParM has been utilized as a sensor of ADP concentration (Kunzelmann and Webb, 2010). It is possible that assembly of most actin-like proteins takes place simply after the cleft has closed on ATP.

In FtsA, subdomain Ib is replaced with another domain (Ic) on the opposite side of the protein, in a position corresponding to domain IIb of another subunit in a standard protofilament of this family. It is thus possible that FtsA also assembles filaments that mimic the standard protofilament (van den Ent and Löwe, 2000), though the different arrangement may indicate that assembly is not dynamic (see below).

4.3. Nucleotide hydrolysis

The nucleotide is buried within the actin monomer fold (Kabsch et al., 1990), raising questions about why hydrolysis of ATP is poor in monomeric protein but good in assembled filaments and how ADP is released by filament disassembly. The conformations of most crystal structures have so far resembled the actin state originally solved, where the nucleotide is stable in the active site. The main difference has been an inward or outward rotation "closing" or "opening" the Ib and IIb domains over the active site. A structure of actin bound to profilin, a protein that accelerates ATP exchange, is particularly "open" suggesting a role for this conformational change in nucleotide exchange (Chik et al., 1996; Kabsch et al., 1990; Otterbein et al., 2001; Rould et al., 2006; Schutt et al., 1993; van den Ent et al., 2002). As described above, the new EM structures have provided information on the steps in nucleotide hydrolysis that take place in the filaments.

4.3.1. Effect of ATP hydrolysis in filaments

After assembly, ATP hydrolysis takes place and leaves the filament in a more unstable state. It has been proposed (Kudryashov et al., 2010) that hydrolysis promotes a small conformational change in the W-loop that contributes to the longitudinal contact with another subunit (Fig. 1.11). A second loop on the other side of the G-loop (Fig. 1.10) may also contribute. In F-actin, changes in this region can directly affect subdomain Ib of the next monomer, and indeed, nucleotide state-related changes have been detected in the DNase I-binding loop (D-loop; Dominguez and Holmes, 2011). Transfer of information from the nucleotide, via the β-sheet in the target-binding cleft, seems likely to be part of a conserved mechanism in the actin family. In the case of FtsA, however, the interaction between loops W and D within the same subunit may make any interaction with another subunit insensitive to nucleotide state. Indeed, FtsA may not qualify as a member of the cytomotive-filament class, its function being to act as the link between the cell membrane and the dynamic ring of FtsZ filaments.

4.3.2. Phosphate channel

Since phosphate (Pi) release is slow after ATP hydrolysis, newly polymerized F-actin consists of ADP-Pi actin but this state is hard to investigate at the atomic level. Actin has not been crystallized in a filamentous state, for investigation by X-ray crystallography. However, cryo-EM work has reached 5–8 Å resolution and thereby rotation of subdomains, rearrangement of α helices and loops, and relocations of magnesium ions and phosphates have been visualized (Murakami et al., 2010). According to an atomic model fitting into this structure, the outer subdomains rotate by ~16 °, greatly increasing the inter-molecular interface and thus stabilizing polymerization. A cylindrical cavity, on the surface that interacts with another protofilament, opens up during polymerization and may allow γ-phosphate to escape. Locations of water molecules obtained by crystallography suggested a mechanism for how the polymerization induces breakage of a hydrogen bond, moves a nucleophilic water, and opens the back door to enable the ATP hydrolysis.

4.4. Lateral interactions in actin filaments

Geometrically, the actin filament may be considered either as two protofilaments twisted around each other or as a single 13/6 helix with a rise and rotation of 27 Å and 166° per monomer (Hanson and Lowy, 1964). But structurally, there are strong grounds for thinking of actin as two separate protofilaments, with the subunit repeats staggered against one another. The new models of F-actin (Fujii et al., 2010; Murakami et al., 2010; Narita et al., 2011; Oda et al., 2009) reveal relatively tight axial interactions but

markedly loose, hydrophilic, inter-protofilament interactions. It is well known that the protofilament twist is variable (Egelman et al., 1982), while the longitudinal spacing of the subunits is constant. However, lateral contacts are certainly involved in F-actin polymerization, when the longitudinal protofilaments take turns to add a new monomer, and may thus be important in controlling ATPase activity, the opening and closing of the cleft in which the nucleotide sits. The position where the assembly-stabilizing drug phalloidin binds, between long-pitch strands of F-actin (Pfaendtner et al., 2010), may account for its inhibition of phosphate release and this might contribute to the stabilization.

4.4.1. The pointed end of F-actin

The pointed end of an actin filament has a much slower polymerization and depolymerization rate than the barbed end, and this difference may account for subunit treadmilling by purified actin under constant protein and ATP concentration. The slower rate of subunit addition at the (−)-end would allow hydrolysis of ATP to occur before an additional subunit can be added, whereas the greater speed of exchange at the (+)-end would allow subunits to be "locked" into the filament by polymerization before hydrolysis could occur. The structure of the pointed end has recently been resolved using a single particle analysis of cryo-electron micrographs (Narita et al., 2011) and shows that the terminal subunit is tilted toward the penultimate subunit, compared with the structure of the main bulk of the filament. This explains why the pointed end is less dynamic. Additional contacts between the two end subunits inhibit dissociation of the end subunit, on the longer protofilament. The contact with the penultimate subunit, on the shorter protofilament, is on the D-loop, which appears to be held in a conformation that would inhibit the docking of a new subunit on to this protofilament.

Although the dynamics of actin in eukaryotic cells are regulated heavily by accessory proteins, and therefore the propensity of actin to treadmill is unlikely to have any great effect alone *in vivo*, it seems likely that the natural dynamics have exerted a significant effect on the evolution of the actin cytoskeleton. Actin polymerizing proteins utilize the natural (+)-end for growth, whereas "assisted" treadmilling through actin depolymerizing factor (ADF) depolymerization at the (−)-end appears likely to occur *in vivo*. Of greater biological significance is the fact that although the different lateral contacts in prokaryotic actin homologues will specify different behavior at the filament tips, the reduced number of modifying proteins affecting the bacterial systems will mean that such dynamics gain greater significance, and the first steps toward revealing such mechanisms can now be undertaken.

4.4.2. Subunit associations in prokaryotic filaments

The superstructures formed by ParM, T0583, and MreB have different topologies from F-actin (Fig. 1.11), with MreB complexes possibly being most different. The structure of straight MreB protofilaments is known in atomic detail, as described above, but the way in which they interact is less well understood. *In vitro*, they have been seen forming bundles, which were straight or curved, and also flat sheets, in which the protofilaments appeared to alternate in orientation, though the precise relationship within a pair of protofilaments was unclear (van den Ent et al., 2001). Recent observations of MreBs overexpressed in cells, as described below, support the idea that pairs of protofilaments (Fig. 1.12) are the functional unit.

Ta0583, a protein expressed in the thermophilic archaeon *Thermoplasma acidophilum*, also forms sheets of straight protofilaments *in vitro* (Roeben et al., 2006). The crystal structure shows straight filaments paired back-to-back, with the monomers staggered just as in F-actin. It may, therefore, be related to a straight ancestor of F-actin, though the fold of the monomer seems to have diverged from that common to MreB and actin, and is very like ParM (Fig. 1.11). Roeben et al. pointed out that the conformation of the nucleotide differs from that in actin but resembles that in ParM. They suggested that Ta0583 derives from a ParM-like actin homologue, once encoded by a plasmid, that was transferred into *Thermoplasma*. Alternatively, ParM may, like TubZ, have been transferred into eubacteria from an archaeon. ParM can assemble as single protofilaments *in vitro* under certain conditions (Popp et al., 2009) but usually it forms polar double filaments. These have staggered subunits, with an overall twist and rise very similar to actin (van den Ent et al., 2002); however, they are left handed (Orlova et al., 2007; Popp et al., 2008), instead of right handed like F-actin. Some reconstructed images from electron micrographs gave the impression that the interactions between subunits were substantially different from those of F-actin (Orlova et al., 2007) but more recent cryo-EM images (Popp et al., 2008 and the Namba group, personal communication) show a ParM protofilament structure that is fully consistent with F-actin, MreB, and Ta0583 protofilaments. The same side of the protofilament is always involved in inter-protofilament interactions, and some of the residues making contacts are positioned in regions that correspond to actin's hydrophobic plug (Fig. 1.10).

4.4.3. Single protofilaments of Giardia actin

The protozoan parasite *Giardia intestinalis* possesses a minimalist actin system (Paredez et al., 2011), lacking myosin, formin, and other cytoplasmic actin-binding proteins. Nevertheless, its absence produced defects suggesting roles in cytokinesis, nuclear positioning, and defining cell polarity.

Its organization was shown to be controlled by Rac, as in other eukaryotes and also in some prokaryotes (see Section 4.5.4). The observation of individual 3.5-nm protofilaments in addition to 7-nm double filaments is particularly interesting. Clearly, the structural relationship between this protein and prokaryotic members of the actin family requires more detailed investigation.

4.5. Filament dynamics in the actin family

Different members of the actin family vary as much in their activities as do members of the tubulin family, ranging from treadmilling and dynamic instability to membrane modeling and more structural roles.

4.5.1. The effects of cofilin and other factors on F-actin

Purified actin filaments are not very active and treadmill only slowly. However, while studying treadmilling in individual actin filaments, Fujiwara et al. (2002) saw occasional fast length excursions or catastrophes, and it is becoming clear that this behavior is an important part of the repertoire of actin. This is apparent in cells, where actin appears to be ~100 times more active than *in vitro* (Bugyi and Carlier, 2010).

The greater activity of actin *in vivo* is ascribed to the effect of actin-associated proteins (Dominguez and Holmes, 2011). One of the most important is ADF/cofilin, which preferentially binds ADP-actin and may help couple ATP hydrolysis to filament turnover. Since cofilin severs filaments, it has been argued that simply increasing the number of shrinking filament ends accelerates turnover (Andrianantoandro and Pollard, 2006). However, some *in vitro* research had suggested that cofilin assists treadmilling by directly accelerating subunit dissociation from filament pointed ends (Carlier et al., 1997). In a study where cofilin was mixed with two additional co-factors, Aip1 and Coronin, Kueh et al. (2008) found that filaments depolymerized in bursts, abruptly losing hundreds of subunits each time. These bursts of disassembly could be initiated from either end of a filament and, just occasionally, from within. A short filament could depolymerize completely in a single burst. These results support imaging studies of single actin filaments in cells (Diez et al., 2005; Staiger et al., 2009, 2010); at the cell cortex, filaments were seen to grow smoothly from their ends, consistent with barbed end elongation, but depolymerized in a series of jumps.

Listeria actin comet tails provide a convenient experimental system. By modeling filament turnover in the tails, Kueh et al. (2010) concluded that severing alone would not give disassembly curves with simple exponential loss of polymer mass, as measured experimentally. Instead of a mechanism whereby cofilin accelerates turnover by simply increasing the number of shrinking filament ends, the analysis favored the acceleration of

depolymerization by increasing the rate of catastrophes. Based on structural investigations, Orlova et al. (2004) had earlier suggested that cofilin may intensify an intrinsic mode of F-actin instability to disrupt actin filaments; it was suggested to do this by inserting in the interface between the two protofilaments (Kudryashov et al., 2006). Thus, the unstable state may correspond to partial separation of the two strands of the actin filament, cooperatively unwinding and destabilizing the filament so that it may dissociate stochastically. Cofilin binding may increase the time spent in an unwound, unstable state and thus make dissociation more likely. Kueh et al. also observed that adding cytochalasin D or capping protein (CapZ) to their mix of proteins inhibited bursts of disassembly at both the barbed and pointed ends of a filament. These capping agents are believed to specifically bind to barbed ends and inhibit subunit addition, but by binding there, they may also inhibit a coordinated change to the unstable state all along a filament.

4.5.2. Associated proteins on actin filament ends

Proteins and protein complexes that control the activity of the two ends of F-actin have been studied in detail (Bugyi and Carlier, 2010; Pollard, 2007). The Arp2/3 complex is actin's equivalent of the γ-tubulin complex, nucleating the assembly of a double protofilament from the pointed end. It is able to promote assembly of the actin network at the advancing edge of a motile cell by attaching to the side of an existing filament and initiating a branch. Growth at the free end then assists the protrusion of the membrane. Crystal structures and reconstructed images from electron micrographs have helped to provide details of the steps in this process.

Formins, in contrast, bind to the fast-growing ends of filaments, protecting them from capping and also supporting processive elongation by binding alternately to the two protofilament ends. Treadmilling may be prevented by having capping proteins bound at the pointed end, in which case, the barbed end can continue to grow. As for the Arp2/3 complex, the structure of the formin complex is known in atomic detail. However, disagreement about the effect on this process of profilin (Pollard, 2007; Romero et al., 2007), a protein that binds to and blocks the barbed end surface of a monomer (Schutt et al., 1993), indicates that the mechanism is not fully understood.

4.5.3. Dynamic instability of ParM and other plasmid filaments

The ParMRC plasmid partitioning apparatus is one of the best-characterized systems for bacterial DNA segregation (Salje et al., 2010). Bundles of filaments push plasmids to opposite poles of the cell. The system comprises three components: an actin-like protein, ParM, a DNA-binding adaptor protein, ParR, and a centromere-like region, *parC*. The dynamic ParM filaments have been proposed to search the cell space for plasmids and then

move ParR–*parC*-bound DNA molecules apart. ParM filaments with uncapped ends exhibit ATP-driven dynamic instability, an activity that had previously only been observed in microtubules (Garner et al., 2004). ParM has been reported to show equal activity at both tips, allowing a single filament to push two plasmids apart *in vitro* (Garner et al., 2007). However, the latter observation has been challenged (Popp et al., 2007) and, indeed, it is easier to envisage a mechanism in which the active machinery consists of more than one filament. Certainly, ParM filaments assemble *in vivo* into small bundles, as shown by cellular cryo-EM (Salje et al., 2009), and similar bundles were seen in the presence of crowding reagents *in vitro*. Bundles may be composed of filaments arranged in a mixed antiparallel arrangement. Unlike actin filament bundles, ParM filament bundles are tightly packed and do not require cross-linking proteins; the 12 subunits per longitudinal repeat, compared with ~13 subunits in F-actin, will allow filaments to pack easily into either hexagonal or square arrays.

In vitro analysis of plasmid-encoded actin-like protein, AlfA, revealed bundles of parallel (or antiparallel) filaments that were much more twisted than ParM or actin filaments (Becker et al., 2006; Polka et al., 2009). Both studies found no evidence of dynamic instability *in vitro*, though the AlfA monomers polymerized more readily than either ParM or actin. AlfA filaments may begin to assemble preferentially between a pair of plasmids and there is no need for growing and shrinking filament ends to search for plasmids. Another actin-like, plasmid-encoded protein, Alp7A, assembles into dynamic filaments that are required for segregation of plasmid LS20 in *Bacillus subtilis* (Drew and Pogliano, 2011). Fluorescently labeled Alp7A showed cycles of rapid growth and shrinkage like ParM. It was also shown, using photobleaching, that seemingly static filaments already fully extended, from pole to pole in a cell, exhibited unidirectional growth, suggesting a treadmilling motion similar to that of TubZ.

4.5.4. Interaction of MreB filaments with the cell membrane

MreB is present in almost all rod-shaped bacteria and is important for maintenance of cell width and cell viability. However, a null mutant of *B. subtilis* could grow with almost normal morphology in the presence of high concentrations of magnesium and an osmoprotectant such as sucrose (Formstone and Errington, 2005). In the absence of magnesium and sucrose, the mutant cells progressively increased in width and finally lysed. Salje et al. (2011) found that MreB functionality depended on the protein binding to cell membranes, which was shown to be a direct interaction, either through an amphipathic helix (*Escherichia coli* MreB) or a membrane insertion loop (*Thermotoga maritima* MreB). Electron tomography revealed that MreB assembles into double filaments that lie directly on the surface of a lipid membrane, with their protofilaments probably back-to-back in an antiparallel alignment. If the protein was overexpressed in cells or assembled

in vitro at high concentration on to purified vesicles, it formed sheets of protofilaments, resembling the sheets seen in the absence of membrane (Section 4.4.2), and could induce negative curvature in the lipid bilayers. This effect on membrane was nucleotide independent, which is reminiscent of recent findings for the membrane-curving activity of FtsZ (Section 3.3.1). The roles of the two types of filament differ in that MreB is not required to progressively constrict the membrane completely.

Nevertheless, like FtsZ filaments, MreB filaments are dynamic structures *in vivo*, as revealed by time-lapse imaging (Defeu Soufo and Graumann, 2005; Kim et al., 2006), and presumably hydrolyzes nucleotide during these movements. The next section describes how some bacterial cells may also use MreB for cell motility involving adhesion sites similar to the focal adhesion sites of crawling eukaryotic cells. A bacterium makes contact with a surface via its outer wall, so the ability to crawl depends on periplasmic structures that transmit the movements of active complexes associated the inner membrane to adhesion complexes on the outer wall. Most bacterial species possessing MreB seem to lack this ability. *B. subtilis* MreB, for example, may simply be involved in shape determination and in setting the orientation of cell-wall synthesis (Dominguez-Escobar et al., 2011; Garner et al., 2011).

MreB is the first known example of a membrane-binding actin filament. However, the role of associating with the cytoplasmic surface of the cell membrane and stabilizing its shape appears to have been conserved in eukaryotic cells. Thus, a cortical layer of actin filaments covers and protects eukaryotic cell membranes, using associated proteins such as spectrin to mediate the interaction with lipids.

4.5.5. Cell crawling

New insight into whole-cell movement driven by cytoplasmic filaments may come from comparisons between eukaryotic and prokaryotic mechanisms. *Myxococcus xanthus*, a Gram-negative bacterium, uses an interesting gliding activity, known as A-motility (for adventurous journeys). AglZ (one of a fairly large group of proteins needed for A-motility) is localized in clusters at regular intervals along the cell membrane, apparently arranged on MreB filament bundles on the cytoplasmic surface of the cell membrane (Mauriello et al., 2010). The clusters remain fixed relative to the substratum while the bulk of the cell advances. Disruption of the filaments abolished the motility. There is a clear parallel here with the crawling activity of animal cells, which appears to depend on traction forces exerted on extracellular adhesion complexes by actin or actomyosin filaments inside the cells (Bereiter-Hahn, 2005). Motility is controlled using small GTPases in bacteria, as well as in eukaryotic cells (Charest and Firtel, 2007). The bacterial movement is stopped by inhibitors of PMF generation, and the AglRQS complex has been identified as the relevant PMF-driven motor (Sun et al., 2011). The requirement of MreB filaments promotes a vision of myosin-like

heads rotating on this membrane-bound motor complex and processively driving the filaments. Future studies may soon reveal molecular details of the gliding mechanism and may also help uncover features of the still-obscure mechanism of eukaryotic cell crawling.

5. Concluding Remarks and Future Directions

The conserved linear protofilaments of members of the tubulin and actin superfamilies are fundamental to their structures and to their varied cytomotive activities, whether in producing directed movement or in shaping lipid membranes. For each family, a picture is emerging of the conformational changes that accompany assembly and disassembly and their relationship to nucleotide hydrolysis.

5.1. Conformational changes associated with nucleotide hydrolysis cycles

During assembly of actin family subunits into protofilaments, a cleft between the two halves of each monomer closes up and this may also require straightening of a twist in the subunit; ATP hydrolysis is facilitated by this change in conformation. The completion of hydrolysis is apparently communicated along strands in a β sheet that connects the nucleotide-binding cleft to the interface with the next subunit in the protofilament, in order to weaken the filament bonds. For the mechanism to be understood in detail, high-resolution structures of filaments in a complete set of different nucleotide states would be helpful. This may be possible by means of X-ray crystallography, for some of the prokaryotic members of the family. The flexible helical structure of eukaryotic F-actin probably means that filaments will never crystallize and that progress will continue to depend on advances in electron microscopy.

In the case of the tubulin family, GTP hydrolysis occurs after the interfaces between different subunits in a protofilament move closer and may need a twist between the subunits to be straightened. As the primary sensor of successful GTP hydrolysis in the tubulin family, loop T3 appears to be the equivalent of switch II in classical G proteins, while tubulin's loop T5 appears to play an important accessory role. The same loops are directly involved in subunit–subunit association and so the loss of phosphate and related changes in the protein loops directly weaken the filament bonds. As for actin, detailed questions may be answered by new structural data from the varied family members. In the case of αβ-tubulin, it would be particularly informative to visualize the structure of Vinblastine-bound filaments, with GTP in the exchangeable nucleotide-binding site. Unfortunately, crystals of tubulin in complex with Vinblastine have been poorly ordered,

except in the presence of stathmin, which holds the tubulin in a disassembly-related conformation. The best hope, therefore, is that the problem can be solved by electron microscopy.

5.2. Subunit conformations at filament ends

The last subunits at the pointed end of an actin filament have been shown to make a unique lateral interaction that accounts for the reduced activity at this end and confirms the importance of having flexibility in the actin D-loop to favor assembly. During the process of subunit addition at the barbed end, the D-loop of the new subunit will be free to flex and fit into its binding site on the end of a protofilament.

The ends of microtubule protofilaments undergoing growth *in vivo* have been seen splayed out; this means that only one new interaction is needed for a free subunit to bind on to a filament end. We predict that MAPs which enhance the dynamic activity of microtubules may do so by helping to maintain the ends in a favourable configuration, that is, with splayed-out protofilaments. It would be very interesting to reconstruct high-resolution images of splayed protofilament ends, using the EM techniques applied to actin filament ends. It might even be possible to visualize MAP molecules bound there, including EB1 in the tightly-bound conformation.

Crystal structures of prokaryotic tubulin family filaments have shown that the loops around GTP bound on a plus end are extended and may provide a flexible interface on to which the new subunit can bind. It is currently unclear why addition to the minus end is less dynamic.

For filaments in both the actin and tubulin families, the primary step in assembly probably involves making a bond between only two subunits, the new addition and the subunit on the end of a protofilament. Lateral bonds may be added later, in time to compensate for the weakening effect of nucleotide hydrolysis on the lateral bonds.

5.3. Cooperativity

For filamentous nucleotide-controlled proteins, we need a better understanding of the longitudinal cooperation between subunits, as seems to occur in catastrophic disassembly of actin filaments or microtubules, or in cooperative bending or twisting of filaments undergoing motility. It seems likely that EM tomography on cilia and flagella (Heuser et al., 2009; Movassagh et al., 2010; Sui and Downing, 2006) will continue to provide ever higher-resolution structural information, so the behavior of active tubulin filaments should become clearer. Eventually, it may be possible to detect allosteric changes within protofilaments that seem to facilitate binding of multiple kinesin motor domains (Muto et al., 2005). The straightening of actin protofilaments in tense muscle has been seen already

(Taylor et al., 1989), and modern tomographic techniques are likely to provide more detail of such changes during activity.

5.4. Relationships between family members help trace the course of evolution

The atomic structure of the plasmid protein TubZ suggests that it occupies an intermediate position between eubacterial FtsZs and eukaryotic tubulins. Because it is unique in eubacteria and because extant archaeal genomes contain protein sequences closely related to TubZ, it is very likely that TubZ was introduced into eubacteria by horizontal gene transfer from some type of archaeon. This suggests that eukaryotes and archaea had a common ancestor that was not shared with eubacteria. BtubAB heterodimers seem likely to have appeared much later, in an organism somewhere between archaea and early eukaryotes. The relationships between members of the actin family indicate that eukaryotes share a common ancestor with at least one branch of the archaea. Eukaryotes also have a system of ESCRT proteins required for processes involving membrane fusion or fission (Hurley, 2010), that are homologous to proteins used, in place of FtsZ, for cytokinesis in crenarchaea (Lindas et al., 2008; Samson et al., 2008). It is possible that an ancestral organism possessed FtsZ/tubulin, crenactin, and ESCRT homologues but the descents that diverged to form new archaeal branches each lost one or two of the three kinds of protein because of their need to maintain a small genome. In prokaryotes, DNA replication and cell division are closely coordinated, by mechanisms that are not yet understood (Berlatzky et al., 2008; Shebelut et al., 2010; Toro and Shapiro, 2010). The organism that founded the eukaryotes, in which genome size seems to be less important, may have freed some evolutionary constraints by developing check-point-controlled mechanisms, whereby chromosome separation takes place independently, after replication. The size of the genome may be crucial only if these two activities are closely coupled. A change in the way that one or more of the cytomotive filaments are employed could perhaps have triggered the transition. Further investigation of filaments in archaea may provide insight into both motility mechanisms and their evolution.

ACKNOWLEDGMENTS

We thank our colleagues for sharing information and engaging in stimulating discussions. These colleagues include Drs Fusinita van den Ent, Jeanne Salje, Marian Oliva, Julia Höng, Gayathri Pananghat, Kate Michie, Iain Duggin, Piotr Szwedziak, Qing Wang, Keiko Hirose, Amedée des Georges, Rob Cross and many others.

REFERENCES

Al-Bassam, J., Larsen, N.A., Hyman, A.A., Harrison, S.C., 2007. Crystal structure of a TOG domain: conserved features of XMAP215/Dis1-family TOG domains and implications for tubulin binding. Structure 15, 355–362.

Aldaz, H., Rice, L.M., Stearns, T., Agard, D.A., 2005. Insights into microtubule nucleation from the crystal structure of human gamma-tubulin. Nature 435, 523–527.

Amos, L.A., Amos, W.B., 1991. The bending of sliding microtubules imaged by confocal light microscopy and negative stain electron microscopy. J. Cell Sci. Suppl. 14, 95–101.

Amos, L.A., Hirose, K., 2007. A cool look at the structural changes in kinesin motor domains. J. Cell Sci. 120, 3919–3927.

Amos, L.A., Klug, A., 1974. Arrangement of subunits in flagellar microtubules. J. Cell Sci. 14, 523–549.

Amos, L.A., Jubb, J.S., Henderson, R., Vigers, G., 1984. Arrangement of protofilaments in two forms of tubulin crystal induced by vinblastine. J. Mol. Biol. 178, 711–729.

Anders, A., Sawin, K.E., 2011. Microtubule stabilization *in vivo* by nucleation-incompetent gamma-tubulin complex. J. Cell Sci. 124, 1207–1213.

Andrianantoandro, E., Pollard, T.D., 2006. Mechanism of actin filament turnover by severing and nucleation at different concentrations of ADF/cofilin. Mol. Cell 24, 13–23.

Aylett, C.H.S., Wang, Q., Michie, K.A., Amos, L.A., Löwe, J., 2010. Filament structure of bacterial tubulin homologue TubZ. Proc. Natl. Acad. Sci. USA 107, 19766–19771.

Bai, R., Vanderwal, C.D., Diaz, J.F., Hamel, E., 2008. Interaction of a cyclostreptin analogue with the microtubule taxoid site: the covalent reaction rapidly follows binding. J. Nat. Prod. 71, 370–374.

Barbier, P., Dorleans, A., Devred, F., Sanz, L., Allegro, D., Alfonso, C., et al., 2010. Stathmin and interfacial microtubule inhibitors recognize a naturally curved conformation of tubulin dimers. J. Biol. Chem. 285, 31672–31681.

Becker, E., Herrera, N.C., Gunderson, F.Q., Derman, A.I., Dance, A.L., Sims, J., et al., 2006. DNA segregation by the bacterial actin AlfA during *Bacillus subtilis* growth and development. EMBO J. 25, 5919–5931.

Bennett, M.J., Barakat, K., Huzil, J.T., Tuszynski, J., Schriemer, D.C., 2010. Discovery and characterization of the laulimalide-microtubule binding mode by mass shift perturbation mapping. Chem. Biol. 17, 725–734.

Bereiter-Hahn, J., 2005. Mechanics of crawling cells. Med. Eng. Phys. 27, 743–753.

Berlatzky, I.A., Rouvinski, A., Ben-Yehuda, S., 2008. Spatial organization of a replicating bacterial chromosome. Proc. Natl. Acad. Sci. USA 105, 14136–14140.

Bieling, P., Laan, L., Schek, H., Munteanu, E.L., Sandblad, L., Dogterom, M., et al., 2007. Reconstitution of a microtubule plus-end tracking system *in vitro*. Nature 450, 1100–1105.

Bieling, P., Kandels-Lewis, S., Telley, I.A., van Dijk, J., Janke, C., Surrey, T., 2008. CLIP-170 tracks growing microtubule ends by dynamically recognizing composite EB1/tubulin-binding sites. J. Cell Biol. 183, 1223–1233.

Bodey, A.J., Kikkawa, M., Moores, C.A., 2009. 9-Angstrom structure of a microtubule-bound mitotic motor. J. Mol. Biol. 388, 218–224.

Bork, P., Sander, C., Valencia, A., 1992. An ATPase domain common to prokaryotic cell cycle proteins, sugar kinases, actin, and hsp70 heat shock proteins. Proc. Natl. Acad. Sci. USA 89, 7290–7294.

Bouissou, A., Verollet, C., Sousa, A., Sampaio, P., Wright, M., Sunkel, C.E., et al., 2009. {gamma}-Tubulin ring complexes regulate microtubule plus end dynamics. J. Cell Biol. 187, 327–334.

Brangwynne, C.P., MacKintosh, F.C., Weitz, D.A., 2007. Force fluctuations and polymerization dynamics of intracellular microtubules. Proc. Natl. Acad. Sci. USA 104, 16128–16133.

Brouhard, G.J., Stear, J.H., Noetzel, T.L., Al-Bassam, J., Kinoshita, K., Harrison, S.C., et al., 2008. XMAP215 is a processive microtubule polymerase. Cell 132, 79–88.

Bugyi, B., Carlier, M.F., 2010. Control of actin filament treadmilling in cell motility. Annu. Rev. Biophys. 39, 449–470.

Cai, Y., Sheetz, M.P., 2009. Force propagation across cells: mechanical coherence of dynamic cytoskeletons. Curr. Opin. Cell Biol. 21, 47–50.

Calladine, C.R., 1982. Construction of bacterial flagellar filaments, and aspects of their conversion to different helical forms. Symp. Soc. Exp. Biol. 35, 33–51.

Canales, A., Matesanz, R., Gardner, N.M., Andreu, J.M., Paterson, I., Diaz, J.F., et al., 2008. The bound conformation of microtubule-stabilizing agents: NMR insights into the bioactive 3D structure of discodermolide and dictyostatin. Chemistry 14, 7557–7569.

Carballido-Lopez, R., 2006. The bacterial actin-like cytoskeleton. Microbiol. Mol. Biol. Rev. 70, 888–909.

Carlier, M.-F., Pantaloni, D., 2010. From molecules to movement: *in vitro* reconstitution of self-organized actin-based motile processes. In: Carlier, M.-F. (Ed.), Actin-based Motility. Springer, Dordrecht Heidelberg London New York, pp. 237–254.

Carlier, M.F., Laurent, V., Santolini, J., Melki, R., Didry, D., Xia, G.X., et al., 1997. Actin depolymerizing factor (ADF/cofilin) enhances the rate of filament turnover: implication in actin-based motility. J. Cell Biol. 136, 1307–1322.

Carter, A.P., Garbarino, J.E., Wilson-Kubalek, E.M., Shipley, W.E., Cho, C., Milligan, R. A., et al., 2008. Structure and functional role of dynein's microtubule-binding domain. Science 322, 1691–1695.

Chang, H.Y., Smertenko, A.P., Igarashi, H., Dixon, D.P., Hussey, P.J., 2005. Dynamic interaction of NtMAP65-1a with microtubules *in vivo*. J. Cell Sci. 118, 3195–3201.

Charest, P.G., Firtel, R.A., 2007. Big roles for small GTPases in the control of directed cell movement. Biochem. J. 401, 377–390.

Chen, Y., Erickson, H.P., 2008. *In vitro* assembly studies of FtsZ/tubulin-like proteins (TubZ) from *Bacillus* plasmids: evidence for a capping mechanism. J. Biol. Chem. 283, 8102–8109.

Chen, Y., Erickson, H.P., 2009. FtsZ filament dynamics at steady state: subunit exchange with and without nucleotide hydrolysis. Biochemistry 48, 6664–6673.

Chen, W., Zhang, D., 2004. Kinetochore fibre dynamics outside the context of the spindle during anaphase. Nat. Cell Biol. 6, 227–231.

Chen, Y., Anderson, D.E., Rajagopalan, M., Erickson, H.P., 2007. Assembly dynamics of *Mycobacterium tuberculosis* FtsZ. J. Biol. Chem. 282, 27736–27743.

Chik, J.K., Lindberg, U., Schutt, C.E., 1996. The structure of an open state of beta-actin at 2.65 A resolution. J. Mol. Biol. 263, 607–623.

Chrétien, D., Wade, R.H., 1991. New data on the microtubule surface lattice. Biol. Cell 71, 161–174.

Chrétien, D., Fuller, S.D., Karsenti, E., 1995. Structure of growing microtubule ends: two-dimensional sheets close into tubes at variable rates. J. Cell Biol. 129, 1311–1328.

Clark, E.A., Hills, P.M., Davidson, B.S., Wender, P.A., Mooberry, S.L., 2006. Laulimalide and synthetic laulimalide analogues are synergistic with paclitaxel and 2-methoxyestradiol. Mol. Pharm. 3, 457–467.

Clement, M.J., Rathinasamy, K., Adjadj, E., Toma, F., Curmi, P.A., Panda, D., 2008. Benomyl and colchicine synergistically inhibit cell proliferation and mitosis: evidence of distinct binding sites for these agents in tubulin. Biochemistry 47, 13016–13025.

Cormier, A., Marchand, M., Ravelli, R.B., Knossow, M., Gigant, B., 2008. Structural insight into the inhibition of tubulin by vinca domain peptide ligands. EMBO Rep. 9, 1101–1106.

Cormier, A., Knossow, M., Wang, C., Gigant, B., 2010. The binding of vinca domain agents to tubulin: structural and biochemical studies. Methods Cell Biol. 95, 373–390.

Defeu Soufo, H.J., Graumann, P.L., 2005. *Bacillus subtilis* actin-like protein MreB influences the positioning of the replication machinery and requires membrane proteins MreC/D and other actin-like proteins for proper localization. BMC Cell Biol. 6, 10.

des Georges, A., Katsuki, M., Drummond, D.R., Osei, M., Cross, R.A., Cross, R.A., et al., 2008. Mal3, the Schizosaccharomyces pombe homolog of EB1, changes the microtubule lattice. Nat. Struct. Mol. Biol. 15, 1102–1108.

Díaz, J.F., Kralicek, A., Mingorance, J., Palacios, J.M., Vicente, M., Andreu, J.M., 2001. Activation of cell division protein FtsZ. Control of switch loop T3 conformation by the nucleotide gamma-phosphate. J. Biol. Chem. 276, 17307–17315.

Diez, S., Gerisch, G., Anderson, K., Muller-Taubenberger, A., Bretschneider, T., 2005. Subsecond reorganization of the actin network in cell motility and chemotaxis. Proc. Natl. Acad. Sci. USA 102, 7601–7606.

Dimitrov, A., Quesnoit, M., Moutel, S., Cantaloube, I., Pous, C., Perez, F., 2008. Detection of GTP-tubulin conformation *in vivo* reveals a role for GTP remnants in microtubule rescues. Science 322, 1353–1356.

Dixit, R., Ross, J.L., Goldman, Y.E., Holzbaur, E.L., 2008. Differential regulation of dynein and kinesin motor proteins by tau. Science 319, 1086–1089.

Dixit, R., Barnett, B., Lazarus, J.E., Tokito, M., Goldman, Y.E., Holzbaur, E.L., 2009. Microtubule plus-end tracking by CLIP-170 requires EB1. Proc. Natl. Acad. Sci. USA 106, 492–497.

Dominguez, R., Holmes, K.C., 2011. Actin structure and function. Annu. Rev. Biophys. 40, 169–186.

Dominguez-Escobar, J., Chastanet, A., Crevenna, A.H., Fromion, V., Wedlich-Soldner, R., Carballido-Lopez, R., 2011. Processive movement of MreB-associated cell wall biosynthetic complexes in bacteria. Science 333, 225–228.

Dorléans, A., Gigant, B., Ravelli, R.B., Mailliet, P., Mikol, V., Knossow, M., 2009. Variations in the colchicine-binding domain provide insight into the structural switch of tubulin. Proc. Natl. Acad. Sci. USA 106, 13775–13779.

Downing, K.H., Sui, H., 2007. Structural insights into microtubule doublet interactions in axonemes. Curr. Opin. Struct. Biol. 17, 253–259.

Drechsel, D.N., Kirschner, M.W., 1994. The minimum GTP cap required to stabilize microtubules. Curr. Biol. 4, 1053–1061.

Drew, K.R., Pogliano, J., 2011. Dynamic instability-driven centering/segregating mechanism in bacteria. Proc. Natl. Acad. Sci. USA 108, 11075–11080.

Drummond, D.R., Cross, R.A., 2000. Dynamics of interphase microtubules in *Schizosaccharomyces pombe*. Curr. Biol. 10, 766–775.

Dutcher, S.K., 2001. The tubulin fraternity: alpha to eta. Curr. Opin. Cell Biol. 13, 49–54.

Dutcher, S.K., 2003. Long-lost relatives reappear: identification of new members of the tubulin superfamily. Curr. Opin. Microbiol. 6, 634–640.

Dutcher, S.K., Trabuco, E.C., 1998. The UNI3 gene is required for assembly of basal bodies of *Chlamydomonas* and encodes delta-tubulin, a new member of the tubulin superfamily. Mol. Biol. Cell 9, 1293–1308.

Dutcher, S.K., Morrissette, N.S., Preble, A.M., Rackley, C., Stanga, J., 2002. Epsilon-tubulin is an essential component of the centriole. Mol. Biol. Cell 13, 3859–3869.

Edler, M.C., Buey, R.M., Gussio, R., Marcus, A.I., Vanderwal, C.D., Sorensen, E.J., et al., 2005. Cyclostreptin (FR182877), an antitumor tubulin-polymerizing agent deficient in enhancing tubulin assembly despite its high affinity for the taxoid site. Biochemistry 44, 11525–11538.

Egelman, E.H., Francis, N., DeRosier, D.J., 1982. F-actin is a helix with a random variable twist. Nature 298, 131–135.

Elie-Caille, C., Severin, F., Helenius, J., Howard, J., Muller, D.J., Hyman, A.A., 2007. Straight GDP-tubulin protofilaments form in the presence of taxol. Curr. Biol. 17, 1765–1770.

Erickson, H.P., 1974. Microtubule surface lattice and subunit structure and observations on reassembly. J. Cell Biol. 60, 153–167.

Erickson, H.P., 2007. Evolution of the cytoskeleton. Bioessays 29, 668–677.

Erickson, H.P., Taylor, D.W., Taylor, K.A., Bramhill, D., 1996. Bacterial cell division protein FtsZ assembles into protofilament sheets and minirings, structural homologs of tubulin polymers. Proc. Natl. Acad. Sci. USA 93, 519–523.

Erickson, H.P., Anderson, D.E., Osawa, M., 2010. FtsZ in bacterial cytokinesis: cytoskeleton and force generator all in one. Microbiol. Mol. Biol. Rev. 74, 504–528.

Ettema, T.J., Lindas, A.C., Bernander, R., 2011. An actin-based cytoskeleton in archaea. Mol. Microbiol. 80, 1052–1061.

Formstone, A., Errington, J., 2005. A magnesium-dependent mreB null mutant: implications for the role of mreB in Bacillus subtilis. Mol. Microbiol. 55, 1646–1657.

Fourniol, F.J., Sindelar, C.V., Amigues, B., Clare, D.K., Thomas, G., Perderiset, M., et al., 2010. Template-free 13-protofilament microtubule-MAP assembly visualized at 8 A resolution. J. Cell Biol. 191, 463–470.

Fu, G., Huang, T., Buss, J., Coltharp, C., Hensel, Z., Xiao, J., 2010. *In vivo* structure of the *E. coli* FtsZ-ring revealed by photoactivated localization microscopy (PALM). PLoS One e12682.

Fujii, T., Iwane, A.H., Yanagida, T., Namba, K., 2010. Direct visualization of secondary structures of F-actin by electron cryomicroscopy. Nature 467, 724–728.

Fujiwara, I., Takahashi, S., Tadakuma, H., Funatsu, T., Ishiwata, S., 2002. Microscopic analysis of polymerization dynamics with individual actin filaments. Nat. Cell Biol. 4, 666–673.

Gamblin, S.J., Smerdon, S.J., 1998. GTPase-activating proteins and their complexes. Curr. Opin. Struct. Biol. 8, 195–201.

Garner, E.C., Campbell, C.S., Mullins, R.D., 2004. Dynamic instability in a DNA-segregating prokaryotic actin homolog. Science 306, 1021–1025.

Garner, E.C., Campbell, C.S., Weibel, D.B., Mullins, R.D., 2007. Reconstitution of DNA segregation driven by assembly of a prokaryotic actin homolog. Science 315, 1270–1274.

Garner, E.C., Bernard, R., Wang, W., Zhuang, X., Rudner, D.Z., Mitchison, T., 2011. Coupled, circumferential motions of the cell wall synthesis machinery and MreB filaments in *B. subtilis*. Science 333, 222–225.

Gerdes, K., Howard, M., Szardenings, F., 2010. Pushing and pulling in prokaryotic DNA segregation. Cell 141, 927–942.

Gigant, B., Curmi, P.A., Martin-Barbey, C., Charbaut, E., Lachkar, S., Lebeau, L., et al., 2000. The 4 A X-ray structure of a tubulin:stathmin-like domain complex. Cell 102, 809–816.

Gigant, B., Wang, C., Ravelli, R.B., Roussi, F., Steinmetz, M.O., Curmi, P.A., et al., 2005. Structural basis for the regulation of tubulin by vinblastine. Nature 435, 519–522.

Grynberg, M., Jaroszewski, L., Godzik, A., 2003. Domain analysis of the tubulin cofactor system: a model for tubulin folding and dimerization. BMC Bioinformatics 4, 46.

Guillet, V., Knibiehler, M., Gregory-Pauron, L., Remy, M.H., Chemin, C., Raynaud-Messina, B., et al., 2011. Crystal structure of gamma-tubulin complex protein GCP4 provides insight into microtubule nucleation. Nat. Struct. Mol. Biol. 18, 915–919.

Guizetti, J., Schermelleh, L., Mantler, J., Maar, S., Poser, I., Leonhardt, H., et al., 2011. Cortical constriction during abscission involves helices of ESCRT-III-dependent filaments. Science 331, 1616–1620.

Gupta, S., Bhattacharyya, B., 2003. Antimicrotubular drugs binding to vinca domain of tubulin. Mol. Cell. Biochem. 253, 41–47.

Hamada, T., Itoh, T.J., Hashimoto, T., Shimmen, T., Sonobe, S., 2009. GTP is required for the microtubule catastrophe-inducing activity of MAP200, a tobacco homolog of XMAP215. Plant Physiol. 151, 1823–1830.

Hamel, E., Day, B.W., Miller, J.H., Jung, M.K., Northcote, P.T., Ghosh, A.K., et al., 2006. Synergistic effects of peloruside A and laulimalide with taxoid site drugs, but not with each other, on tubulin assembly. Mol. Pharmacol. 70, 1555–1564.

Hanson, J., Lowy, J., 1964. The structure of actin filaments and the origin of the axial periodicity in the I-substance of vertebrate striated muscle. Proc. R. Soc. Lond. B Biol. Sci. 160, 449–460.

Hartman, H., Smith, T.F., 2009. The evolution of the cilium and the eukaryotic cell. Cell Motil. Cytoskeleton 66, 215–219.

Heuser, T., Raytchev, M., Krell, J., Porter, M.E., Nicastro, D., 2009. The dynein regulatory complex is the nexin link and a major regulatory node in cilia and flagella. J. Cell Biol. 187, 921–933.

Hirose, K., Löwe, J., Alonso, M., Cross, R.A., Amos, L.A., 1999. 3D electron microscopy of the interaction of kinesin with tubulin. Cell Struct. Funct. 24, 277–284.

Hirose, K., Akimaru, E., Akiba, T., Endow, S.A., Amos, L.A., 2006. Large conformational changes in a kinesin motor catalyzed by interaction with microtubules. Mol. Cell 23, 913–923.

Holmes, K.C., Popp, D., Gebhard, W., Kabsch, W., 1990. Atomic model of the actin filament. Nature 347, 44–49.

Holmes, K.C., Tirion, M., Popp, D., Lorenz, M., Kabsch, W., Milligan, R.A., 1993. A comparison of the atomic model of F-actin with cryo-electron micrographs of actin and decorated actin. Adv. Exp. Med. Biol. 332, 15–22, discussion 22–24.

Honnappa, S., Okhrimenko, O., Jaussi, R., Jawhari, H., Jelesarov, I., Winkler, F.K., et al., 2006. Key interaction modes of dynamic +TIP networks. Mol. Cell 23, 663–671.

Höög, J.L., Huisman, S.M., Sebo-Lemke, Z., Sandblad, L., McIntosh, J.R., Antony, C., et al., 2011. Electron tomography reveals a flared morphology on growing microtubule ends. J. Cell Sci. 124, 693–698.

Hoppins, S., Nunnari, J., 2009. The molecular mechanism of mitochondrial fusion. Biochim. Biophys. Acta 1793, 20–26.

Howard, J., Hyman, A.A., 2003. Dynamics and mechanics of the microtubule plus end. Nature 422, 753–758.

Hurley, J.H., 2010. The ESCRT complexes. Crit. Rev. Biochem. Mol. Biol. 45, 463–487.

Huzil, J.T., Chik, J.K., Slysz, G.W., Freedman, H., Tuszynski, J., Taylor, R.E., et al., 2008. A unique mode of microtubule stabilization induced by peloruside A. J. Mol. Biol. 378, 1016–1030.

Hyman, A.A., Chrétien, D., Arnal, I., Wade, R.H., 1995. Structural changes accompanying GTP hydrolysis in microtubules: information from a slowly hydrolyzable analogue guanylyl-(alpha, beta)-methylene-diphosphonate. J. Cell Biol. 128, 117–125.

Inclan, Y.F., Nogales, E., 2001. Structural models for the self-assembly and microtubule interactions of gamma-, delta- and epsilon-tubulin. J. Cell Sci. 114, 413–422.

Itoh, T., Matsuda, H., Mori, H., 1999. Phylogenetic analysis of the third hsp70 homolog in *Escherichia coli*; a novel member of the Hsc66 subfamily and its possible co-chaperone. DNA Res. 6, 299–305.

Janson, M.E., Dogterom, M., 2004. A bending mode analysis for growing microtubules: evidence for a velocity-dependent rigidity. Biophys. J. 87, 2723–2736.

Jenkins, C., Samudrala, R., Anderson, I., Hedlund, B.P., Petroni, G., Michailova, N., et al., 2002. Genes for the cytoskeletal protein tubulin in the bacterial genus *Prosthecobacter*. Proc. Natl. Acad. Sci. USA 99, 17049–17054.

Jiang, K., Akhmanova, A., 2010. Microtubule tip-interacting proteins: a view from both ends. Curr. Opin. Cell Biol. 23, 94–101.

Jockusch, B.M., Graumann, P.L., 2011. The long journey: actin on the road to pro- and eukaryotic cells. Rev. Physiol. Biochem. Pharmacol. in press.
Kabsch, W., Holmes, K.C., 1995. The actin fold. FASEB J. 9, 167–174.
Kabsch, W., Mannherz, H.G., Suck, D., Pai, E.F., Holmes, K.C., 1990. Atomic structure of the actin:DNase I complex. Nature 347, 37–44.
Kar, S., Fan, J., Smith, M.J., Goedert, M., Amos, L.A., 2003a. Repeat motifs of tau bind to the insides of microtubules in the absence of taxol. EMBO J. 22, 70–77.
Kar, S., Florence, G.J., Paterson, I., Amos, L.A., 2003b. Discodermolide interferes with the binding of tau protein to microtubules. FEBS Lett. 539, 34–36.
Kato, A., Nagata, Y., Todokoro, K., 2004. Delta-tubulin is a component of intercellular bridges and both the early and mature perinuclear rings during spermatogenesis. Dev. Biol. 269, 196–205.
Katsuki, M., Drummond, D.R., Osei, M., Cross, R.A., 2009. Mal3 masks catastrophe events in *Schizosaccharomyces pombe* microtubules by inhibiting shrinkage and promoting rescue. J. Biol. Chem. 284, 29246–29250.
Kim, S.Y., Gitai, Z., Kinkhabwala, A., Shapiro, L., Moerner, W.E., 2006. Single molecules of the bacterial actin MreB undergo directed treadmilling motion in *Caulobacter crescentus*. Proc. Natl. Acad. Sci. USA 103, 10929–10934.
Kimura, M., Okano, Y., 2007. Human Misato regulates mitochondrial distribution and morphology. Exp. Cell Res. 313, 1393–1404.
Kirschner, M.W., Williams, R.C., Weingarten, M., Gerhart, J.C., 1974. Microtubules from mammalian brain: some properties of their depolymerization products and a proposed mechanism of assembly and disassembly. Proc. Natl. Acad. Sci. USA 71, 1159–1163.
Kollman, J.M., Polka, J.K., Zelter, A., Davis, T.N., Agard, D.A., 2010. Microtubule nucleating gamma-TuSC assembles structures with 13-fold microtubule-like symmetry. Nature 466, 879–882.
Komeili, A., Li, Z., Newman, D.K., Jensen, G.J., 2006. Magnetosomes are cell membrane invaginations organized by the actin-like protein MamK. Science 311, 242–245.
Koning, R.I., Zovko, S., Barcena, M., Oostergetel, G.T., Koerten, H.K., Galjart, N., et al., 2008. Cryo electron tomography of vitrified fibroblasts: microtubule plus ends *in situ*. J. Struct. Biol. 161, 459–468.
Kovar, D.R., Pollard, T.D., 2004. Progressing actin: formin as a processive elongation machine. Nat. Cell Biol. 6, 1158–1159.
Kudryashov, D.S., Galkin, V.E., Orlova, A., Phan, M., Egelman, E.H., Reisler, E., 2006. Cofilin cross-bridges adjacent actin protomers and replaces part of the longitudinal F-actin interface. J. Mol. Biol. 358, 785–797.
Kudryashov, D.S., Grintsevich, E.E., Rubenstein, P.A., Reisler, E., 2010. A nucleotide state-sensing region on actin. J. Biol. Chem. 285, 25591–25601.
Kueh, H.Y., Charras, G.T., Mitchison, T.J., Brieher, W.M., 2008. Actin disassembly by cofilin, coronin, and Aip1 occurs in bursts and is inhibited by barbed-end cappers. J. Cell Biol. 182, 341–353.
Kueh, H.Y., Brieher, W.M., Mitchison, T.J., 2010. Quantitative analysis of actin turnover in *listeria* comet tails: evidence for catastrophic filament turnover. Biophys. J. 99, 2153–2162.
Kukulski, W., Schorb, M., Welsch, S., Picco, A., Kaksonen, M., Briggs, J.A., 2011. Correlated fluorescence and 3D electron microscopy with high sensitivity and spatial precision. J. Cell Biol. 192, 111–119.
Kulic, I.M., Brown, A.E., Kim, H., Kural, C., Blehm, B., Selvin, P.R., Nelson, P.C., Gelfand, V.I., 2008. The role of microtubule movement in bidirectional organelle transport. Proc. Natl. Acad. Sci. USA 105, 10011–10016.
Kunzelmann, S., Webb, M.R., 2010. A fluorescent, reagentless biosensor for ADP based on tetramethylrhodamine-labeled ParM. ACS Chem. Biol. 5, 415–425.

Kurachi, M., Hoshi, M., Tashiro, H., 1995. Buckling of a single microtubule by optical trapping forces: direct measurement of microtubule rigidity. Cell Motil. Cytoskeleton 30, 221–228.

Larsen, R.A., Cusumano, C., Fujioka, A., Lim-Fong, G., Patterson, P., Pogliano, J., 2007. Treadmilling of a prokaryotic tubulin-like protein, TubZ, required for plasmid stability in *Bacillus thuringiensis*. Genes Dev. 21, 1340–1352.

Le Clainche, C., Carlier, M.F., 2008. Regulation of actin assembly associated with protrusion and adhesion in cell migration. Physiol. Rev. 88, 489–513.

LeDizet, M., Piperno, G., 1987. Identification of an acetylation site of *Chlamydomonas* alpha-tubulin. Proc. Natl. Acad. Sci. USA 84, 5720–5724.

Li, H., DeRosier, D.J., Nicholson, W.V., Nogales, E., Downing, K.H., 2002. Microtubule structure at 8 A resolution. Structure 10, 1317–1328.

Li, Z., Trimble, M.J., Brun, Y.V., Jensen, G.J., 2007. The structure of FtsZ filaments *in vivo* suggests a force-generating role in cell division. EMBO J. 26, 4694–4708.

Lin, C.M., Hamel, E., 1981. Effects of inhibitors of tubulin polymerization on GTP hydrolysis. J. Biol. Chem. 256, 9242–9245.

Lindas, A.C., Karlsson, E.A., Lindgren, M.T., Ettema, T.J., Bernander, R., 2008. A unique cell division machinery in the Archaea. Proc. Natl. Acad. Sci. USA 105, 18942–18946.

Lorenz, M., Popp, D., Holmes, K.C., 1993. Refinement of the F-actin model against X-ray fiber diffraction data by the use of a directed mutation algorithm. J. Mol. Biol. 234, 826–836.

Low, H.H., Löwe, J., 2010. Dynamin architecture—from monomer to polymer. Curr. Opin. Struct. Biol. 20, 791–798.

Löwe, J., Amos, L.A., 1998. Crystal structure of the bacterial cell-division protein FtsZ. Nature 391, 203–206.

Löwe, J., Amos, L.A., 1999. Tubulin-like protofilaments in Ca^{2+}-induced FtsZ sheets. EMBO J. 18, 2364–2371.

Löwe, J., Amos, L.A., 2009. Evolution of cytomotive filaments: the cytoskeleton from prokaryotes to eukaryotes. Int. J. Biochem. Cell Biol. 41, 323–329.

Löwe, J., Li, H., Downing, K.H., Nogales, E., 2001. Refined structure of alpha beta-tubulin at 3.5 A resolution. J. Mol. Biol. 313, 1045–1057.

Löwe, J., van den Ent, F., Amos, L.A., 2004. Molecules of the bacterial cytoskeleton. Annu. Rev. Biophys. Biomol. Struct. 33, 177–198.

Lu, C., Reedy, M., Erickson, H.P., 2000. Straight and curved conformations of FtsZ are regulated by GTP hydrolysis. J. Bacteriol. 182, 164–170.

Luders, J., Stearns, T., 2007. Microtubule-organizing centres: a re-evaluation. Nat. Rev. Mol. Cell Biol. 8, 161–167.

Makarova, K.S., Koonin, E.V., 2010. Two new families of the FtsZ-tubulin protein superfamily implicated in membrane remodeling in diverse bacteria and archaea. Biol. Direct 5, 33.

Maki-Yonekura, S., Yonekura, K., Namba, K., 2010. Conformational change of flagellin for polymorphic supercoiling of the flagellar filament. Nat. Struct. Mol. Biol. 17, 417–422.

Mandelkow, E.M., Mandelkow, E., 1979. Junctions between microtubule walls. J. Mol. Biol. 129, 135–148.

Mandelkow, E.M., Mandelkow, E., Milligan, R.A., 1991. Microtubule dynamics and microtubule caps: a time-resolved cryo-electron microscopy study. J. Cell Biol. 114, 977–991.

Martin-Galiano, A.J., Oliva, M.A., Sanz, L., Bhattacharyya, A., Serna, M., Yebenes, H., et al., 2011. Bacterial tubulin distinct loop sequences and primitive assembly properties support its origin from a eukaryotic tubulin ancestor. J. Biol. Chem. 286, 19789–19803.

Mattila, P.K., Lappalainen, P., 2008. Filopodia: molecular architecture and cellular functions. Nat. Rev. Mol. Cell Biol. 9, 446–454.

Maurer, S.P., Bieling, P., Cope, J., Hoenger, A., Surrey, T., 2011. GTP{gamma}S microtubules mimic the growing microtubule end structure recognized by end-binding proteins (EBs). Proc. Natl. Acad. Sci. USA 108, 3988–3993.

Mauriello, E.M., Mouhamar, F., Nan, B., Ducret, A., Dai, D., Zusman, D.R., et al., 2010. Bacterial motility complexes require the actin-like protein, MreB and the Ras homologue, MglA. EMBO J. 29, 315–326.

McIntosh, J.R., Morphew, M.K., Grissom, P.M., Gilbert, S.P., Hoenger, A., 2009. Lattice structure of cytoplasmic microtubules in a cultured mammalian cell. J. Mol. Biol. 394, 177–182.

McIntosh, J.R., Volkov, V., Ataullakhanov, F.I., Grishchuk, E.L., 2010. Tubulin depolymerization may be an ancient biological motor. J. Cell Sci. 123, 3425–3434.

Meurer-Grob, P., Kasparian, J., Wade, R.H., 2001. Microtubule structure at improved resolution. Biochemistry 40, 8000–8008.

Michie, K.A., Löwe, J., 2006. Dynamic filaments of the bacterial cytoskeleton. Annu. Rev. Biochem. 75, 467–492.

Millan, J., Cain, R.J., Reglero-Real, N., Bigarella, C., Marcos-Ramiro, B., Fernandez-Martin, L., et al., 2010. Adherens junctions connect stress fibres between adjacent endothelial cells. BMC Biol. 8, 11.

Mingorance, J., Rivas, G., Velez, M., Gomez-Puertas, P., Vicente, M., 2010. Strong FtsZ is with the force: mechanisms to constrict bacteria. Trends Microbiol. 18, 348–356.

Mitchison, T., Kirschner, M., 1984. Dynamic instability of microtubule growth. Nature 312, 237–242.

Mizuno, N., Toba, S., Edamatsu, M., Watai-Nishii, J., Hirokawa, N., Toyoshima, Y.Y., et al., 2004. Dynein and kinesin share an overlapping microtubule-binding site. EMBO J. 23, 2459–2467.

Mohrbach, H., Johner, A., Kulic, I.M., 2010. Tubulin bistability and polymorphic dynamics of microtubules. Phys. Rev. Lett. 105, 268102.

Moores, C.A., Milligan, R.A., 2008. Visualisation of a kinesin-13 motor on microtubule end mimics. J. Mol. Biol. 377, 647–654.

Moores, C.A., Cooper, J., Wagenbach, M., Ovechkina, Y., Wordeman, L., Milligan, R.A., 2006. The role of the kinesin-13 neck in microtubule depolymerization. Cell Cycle 5, 1812–1815.

Moritz, M., Agard, D.A., 2001. Gamma-tubulin complexes and microtubule nucleation. Curr. Opin. Struct. Biol. 11, 174–181.

Movassagh, T., Bui, K.H., Sakakibara, H., Oiwa, K., Ishikawa, T., 2010. Nucleotide-induced global conformational changes of flagellar dynein arms revealed by *in situ* analysis. Nat. Struct. Mol. Biol. 17, 761–767.

Muller-Reichert, T., Chretien, D., Severin, F., Hyman, A.A., 1998. Structural changes at microtubule ends accompanying GTP hydrolysis: information from a slowly hydrolyzable analogue of GTP, guanylyl (alpha, beta)methylenediphosphonate. Proc. Natl. Acad. Sci. USA 95, 3661–3666.

Murakami, K., Yasunaga, T., Noguchi, T.Q., Gomibuchi, Y., Ngo, K.X., Uyeda, T.Q., et al., 2010. Structural basis for actin assembly, activation of ATP hydrolysis, and delayed phosphate release. Cell 143, 275–287.

Muto, E., Sakai, H., Kaseda, K., 2005. Long-range cooperative binding of kinesin to a microtubule in the presence of ATP. J. Cell Biol. 168, 691–696.

Nakata, T., Niwa, S., Okada, Y., Perez, F., Hirokawa, N., 2011. Preferential binding of a kinesin-1 motor to GTP-tubulin-rich microtubules underlies polarized vesicle transport. J. Cell Biol. 194, 245–255.

Narita, A., Oda, T., Maeda, Y., 2011. Structural basis for the slow dynamics of the actin filament pointed end. EMBO J. 30, 1230–1237.

Nettles, J.H., Li, H., Cornett, B., Krahn, J.M., Snyder, J.P., Downing, K.H., 2004. The binding mode of epothilone A on alpha, beta-tubulin by electron crystallography. Science 305, 866–869.

Nguyen, T.L., Xu, X., Gussio, R., Ghosh, A.K., Hamel, E., 2010. The assembly-inducing laulimalide/peloruside A binding site on tubulin: molecular modeling and biochemical studies with [^{3}H]peloruside A. J. Chem. Inf. Model. 50, 2019–2028.

Ni, L., Xu, W., Kumaraswami, M., Schumacher, M.A., 2010. Plasmid protein TubR uses a distinct mode of HTH-DNA binding and recruits the prokaryotic tubulin homolog TubZ to effect DNA partition. Proc. Natl. Acad. Sci. USA 107, 11763–11768.

Nogales, E., Medrano, F.J., Diakun, G.P., Mant, G.R., Towns-Andrews, E., Bordas, J., 1995. The effect of temperature on the structure of vinblastine-induced polymers of purified tubulin: detection of a reversible conformational change. J. Mol. Biol. 254, 416–430.

Nogales, E., Wolf, S.G., Downing, K.H., 1998a. Structure of the alpha beta tubulin dimer by electron crystallography. Nature 391, 199–203.

Nogales, E., Downing, K.H., Amos, L.A., Löwe, J., 1998b. Tubulin and FtsZ form a distinct family of GTPases. Nat. Struct. Biol. 5, 451–458.

Nogales, E., Whittaker, M., Milligan, R.A., Downing, K.H., 1999. High-resolution model of the microtubule. Cell 96, 79–88.

Oda, T., Maeda, Y., 2010. Multiple conformations of F-actin. Structure 18, 761–767.

Oda, T., Iwasa, M., Aihara, T., Maeda, Y., Narita, A., 2009. The nature of the globular- to fibrous-actin transition. Nature 457, 441–445.

Ohkura, H., Garcia, M.A., Toda, T., 2001. Dis1/TOG universal microtubule adaptors—one MAP for all? J. Cell Sci. 114, 3805–3812.

Oliva, M.A., Huecas, S., Palacios, J.M., Martin-Benito, J., Valpuesta, J.M., Andreu, J.M., 2003. Assembly of archaeal cell division protein FtsZ and a GTPase-inactive mutant into double-stranded filaments. J. Biol. Chem. 278, 33562–33570.

Oliva, M.A., Cordell, S.C., Löwe, J., 2004. Structural insights into FtsZ protofilament formation. Nat. Struct. Mol. Biol. 11, 1243–1250.

Oliva, M.A., Trambaiolo, D., Löwe, J., 2007. Structural insights into the conformational variability of FtsZ. J. Mol. Biol. 373, 1229–1242.

Olson, B.J., Wang, Q., Osteryoung, K.W., 2010. GTP-dependent heteropolymer formation and bundling of chloroplast FtsZ1 and FtsZ2. J. Biol. Chem. 285, 20634–20643.

Orlova, A., Shvetsov, A., Galkin, V.E., Kudryashov, D.S., Rubenstein, P.A., Egelman, E. H., et al., 2004. Actin-destabilizing factors disrupt filaments by means of a time reversal of polymerization. Proc. Natl. Acad. Sci. USA 101, 17664–17668.

Orlova, A., Garner, E.C., Galkin, V.E., Heuser, J., Mullins, R.D., Egelman, E.H., 2007. The structure of bacterial ParM filaments. Nat. Struct. Mol. Biol. 14, 921–926.

Osawa, M., Erickson, H.P., 2011. Inside-out Z rings—constriction with and without GTP hydrolysis. Mol. Microbiol. 81, 571–579.

Osawa, M., Anderson, D.E., Erickson, H.P., 2009. Curved FtsZ protofilaments generate bending forces on liposome membranes. EMBO J. 28, 3476–3484.

O'Toole, E.T., McDonald, K.L., Mantler, J., McIntosh, J.R., Hyman, A.A., Muller-Reichert, T., 2003a. Morphologically distinct microtubule ends in the mitotic centrosome of *Caenorhabditis elegans*. J. Cell Biol. 163, 451–456.

O'Toole, E.T., Giddings, T.H., McIntosh, J.R., Dutcher, S.K., 2003b. Three-dimensional organization of basal bodies from wild-type and delta-tubulin deletion strains of *Chlamydomonas reinhardtii*. Mol. Biol. Cell 14, 2999–3012.

Otterbein, L.R., Graceffa, P., Dominguez, R., 2001. The crystal structure of uncomplexed actin in the ADP state. Science 293, 708–711.

Paredez, A.R., Assaf, Z.J., Sept, D., Timofejeva, L., Dawson, S.C., Wang, C.J., et al., 2011. An actin cytoskeleton with evolutionarily conserved functions in the absence of canonical actin-binding proteins. Proc. Natl. Acad. Sci. USA 108, 6151–6156.

Peck, A., Sargin, M.E., LaPointe, N.E., Rose, K., Manjunath, B.S., Feinstein, S.C., et al., 2011. Tau isoform-specific modulation of kinesin-driven microtubule gliding rates and trajectories as determined with tau-stabilized microtubules. Cytoskeleton 68, 44–55.

Pedersen, L.B., Geimer, S., Sloboda, R.D., Rosenbaum, J.L., 2003. The microtubule plus end-tracking protein EB1 is localized to the flagellar tip and basal bodies in *Chlamydomonas reinhardtii*. Curr. Biol. 13, 1969–1974.

Pellegrin, S., Mellor, H., 2007. Actin stress fibres. J. Cell Sci. 120, 3491–3499.

Perdiz, D., Mackeh, R., Pous, C., Baillet, A., 2011. The ins and outs of tubulin acetylation: more than just a post-translational modification? Cell. Signal. 23, 763–771.

Pfaendtner, J., Lyman, E., Pollard, T.D., Voth, G.A., 2010. Structure and dynamics of the actin filament. J. Mol. Biol. 396, 252–263.

Pichoff, S., Lutkenhaus, J., 2005. Tethering the Z ring to the membrane through a conserved membrane targeting sequence in FtsA. Mol. Microbiol. 55, 1722–1734.

Piette, B.M., Liu, J., Peeters, K., Smertenko, A., Hawkins, T., Deeks, M., et al., 2009. A thermodynamic model of microtubule assembly and disassembly. PLoS One 4, e6378.

Polka, J.K., Kollman, J.M., Agard, D.A., Mullins, R.D., 2009. The structure and assembly dynamics of plasmid actin AlfA imply a novel mechanism of DNA segregation. J. Bacteriol. 191, 6219–6230.

Pollard, T.D., 2007. Regulation of actin filament assembly by Arp2/3 complex and formins. Annu. Rev. Biophys. Biomol. Struct. 36, 451–477.

Pollard, T.D., Borisy, G.G., 2003. Cellular motility driven by assembly and disassembly of actin filaments. Cell 112, 453–465.

Popp, D., Yamamoto, A., Iwasa, M., Narita, A., Maeda, K., Maeda, Y., 2007. Concerning the dynamic instability of actin homolog ParM. Biochem. Biophys. Res. Commun. 353, 109–114.

Popp, D., Narita, A., Oda, T., Fujisawa, T., Matsuo, H., Nitanai, Y., et al., 2008. Molecular structure of the ParM polymer and the mechanism leading to its nucleotide-driven dynamic instability. EMBO J. 27, 570–579.

Popp, D., Iwasa, M., Maeda, K., Narita, A., Oda, T., Maeda, Y., 2009. Protofilament formation of ParM mutants. J. Mol. Biol. 388, 209–217.

Pradel, N., Santini, C.L., Bernadac, A., Fukumori, Y., Wu, L.F., 2006. Biogenesis of actin-like bacterial cytoskeletal filaments destined for positioning prokaryotic magnetic organelles. Proc. Natl. Acad. Sci. USA 103, 17485–17489.

Prasain, N., Stevens, T., 2009. The actin cytoskeleton in endothelial cell phenotypes. Microvasc. Res. 77, 53–63.

Prinz, W.A., Hinshaw, J.E., 2009. Membrane-bending proteins. Crit. Rev. Biochem. Mol. Biol. 44, 278–291.

Pryor, D.E., O'Brate, A., Bilcer, G., Diaz, J.F., Wang, Y., Wang, Y., et al., 2002. The microtubule stabilizing agent laulimalide does not bind in the taxoid site, kills cells resistant to paclitaxel and epothilones, and may not require its epoxide moiety for activity. Biochemistry 41, 9109–9115.

Rai, S.S., Wolff, J., 1996. Localization of the vinblastine-binding site on beta-tubulin. J. Biol. Chem. 271, 14707–14711.

Ravelli, R.B., Gigant, B., Curmi, P.A., Jourdain, I., Lachkar, S., Sobel, A., et al., 2004. Insight into tubulin regulation from a complex with colchicine and a stathmin-like domain. Nature 428, 198–202.

Rendine, S., Pieraccini, S., Sironi, M., 2010. Vinblastine perturbation of tubulin protofilament structure: a computational insight. Phys. Chem. Chem. Phys. 12, 15530–15536.

Rice, L.M., Montabana, E.A., Agard, D.A., 2008. The lattice as allosteric effector: structural studies of alphabeta- and gamma-tubulin clarify the role of GTP in microtubule assembly. Proc. Natl. Acad. Sci. USA 105, 5378–5383.

Richards, K.L., Anders, K.R., Nogales, E., Schwartz, K., Downing, K.H., Botstein, D., 2000. Structure-function relationships in yeast tubulins. Mol. Biol. Cell 11, 1887–1903.
Roeben, A., Kofler, C., Nagy, I., Nickell, S., Hartl, F.U., Bracher, A., 2006. Crystal structure of an archaeal actin homolog. J. Mol. Biol. 358, 145–156.
Romero, S., Didry, D., Larquet, E., Boisset, N., Pantaloni, D., Carlier, M.F., 2007. How ATP hydrolysis controls filament assembly from profilin-actin: implication for formin processivity. J. Biol. Chem. 282, 8435–8445.
Rossmann, M.G., Moras, D., Olsen, K.W., 1974. Chemical and biological evolution of nucleotide-binding protein. Nature 250, 194–199.
Rould, M.A., Wan, Q., Joel, P.B., Lowey, S., Trybus, K.M., 2006. Crystal structures of expressed non-polymerizable monomeric actin in the ADP and ATP states. J. Biol. Chem. 281, 31909–31919.
Sackett, D.L., Wolff, J., 1986. Proteolysis of tubulin and the substructure of the tubulin dimer. J. Biol. Chem. 261, 9070–9076.
Salje, J., Zuber, B., Löwe, J., 2009. Electron cryomicroscopy of *E. coli* reveals filament bundles involved in plasmid DNA segregation. Science 323, 509–512.
Salje, J., Gayathri, P., Löwe, J., 2010. The ParMRC system: molecular mechanisms of plasmid segregation by actin-like filaments. Nat. Rev. Microbiol. 8, 683–692.
Salje, J., van den Ent, F., de Boer, P., Lowe, J., 2011. Direct membrane binding by bacterial actin MreB. Mol. Cell 43, 478–487.
Samson, R.Y., Obita, T., Freund, S.M., Williams, R.L., Bell, S.D., 2008. A role for the ESCRT system in cell division in archaea. Science 322, 1710–1713.
Samson, R.Y., Obita, T., Hodgson, B., Shaw, M.K., Chong, P.L., Williams, R.L., et al., 2011. Molecular and structural basis of ESCRT-III recruitment to membranes during archaeal cell division. Mol. Cell 41, 186–196.
Sandblad, L., Busch, K.E., Tittmann, P., Gross, H., Brunner, D., Hoenger, A., 2006. The *Schizosaccharomyces pombe* EB1 homolog Mal3p binds and stabilizes the microtubule lattice seam. Cell 127, 1415–1424.
Schek, H.T., Gardner, M.K., Cheng, J., Odde, D.J., Hunt, A.J., 2007. Microtubule assembly dynamics at the nanoscale. Curr. Biol. 17, 1445–1455.
Schlieper, D., Oliva, M.A., Andreu, J.M., Löwe, J., 2005. Structure of bacterial tubulin BtubA/B: evidence for horizontal gene transfer. Proc. Natl. Acad. Sci. USA 102, 9170–9175.
Schmid, S.L., Frolov, V.A., 2011. Dynamin: functional design of a membrane fission catalyst. Annu. Rev. Cell Dev. Biol. in press.
Schutt, C.E., Myslik, J.C., Rozycki, M.D., Goonesekere, N.C., Lindberg, U., 1993. The structure of crystalline profilin-beta-actin. Nature 365, 810–816.
Shebelut, C.W., Guberman, J.M., van Teeffelen, S., Yakhnina, A.A., Gitai, Z., 2010. *Caulobacter* chromosome segregation is an ordered multistep process. Proc. Natl. Acad. Sci. USA 107, 14194–14198.
Shipley, K., Hekmat-Nejad, M., Turner, J., Moores, C., Anderson, R., Milligan, R., et al., 2004. Structure of a kinesin microtubule depolymerization machine. EMBO J. 23, 1422–1432.
Sindelar, C.V., Downing, K.H., 2010. An atomic-level mechanism for activation of the kinesin molecular motors. Proc. Natl. Acad. Sci. USA 107, 4111–4116.
Slep, K.C., 2010. Structural and mechanistic insights into microtubule end-binding proteins. Curr. Opin. Cell Biol. 22, 88–95.
Smrzka, O.W., Delgehyr, N., Bornens, M., 2000. Tissue-specific expression and subcellular localisation of mammalian delta-tubulin. Curr. Biol. 10, 413–416.
Snyder, J.P., Nettles, J.H., Cornett, B., Downing, K.H., Nogales, E., 2001. The binding conformation of Taxol in beta-tubulin: a model based on electron crystallographic density. Proc. Natl. Acad. Sci. USA 98, 5312–5316.

Song, Y.H., Mandelkow, E., 1993. Recombinant kinesin motor domain binds to beta-tubulin and decorates microtubules with a B surface lattice. Proc. Natl. Acad. Sci. USA 90, 1671–1675.

Sontag, C.A., Staley, J.T., Erickson, H.P., 2005. *In vitro* assembly and GTP hydrolysis by bacterial tubulins BtubA and BtubB. J. Cell Biol. 169, 233–238.

Sontag, C.A., Sage, H., Erickson, H.P., 2009. BtubA-BtubB heterodimer is an essential intermediate in protofilament assembly. PLoS One 4, e7253.

Sprang, S.R., 1997. G protein mechanisms: insights from structural analysis. Annu. Rev. Biochem. 66, 639–678.

Srivastava, P., Panda, D., 2007. Rotenone inhibits mammalian cell proliferation by inhibiting microtubule assembly through tubulin binding. FEBS J. 274, 4788–4801.

Staiger, C.J., Sheahan, M.B., Khurana, P., Wang, X., McCurdy, D.W., Blanchoin, L., 2009. Actin filament dynamics are dominated by rapid growth and severing activity in the Arabidopsis cortical array. J. Cell Biol. 184, 269–280.

Staiger, C.J., Poulter, N.S., Henty, J.L., Franklin-Tong, V.E., Blanchoin, L., 2010. Regulation of actin dynamics by actin-binding proteins in pollen. J. Exp. Bot. 61, 1969–1986.

Sui, H., Downing, K.H., 2006. Molecular architecture of axonemal microtubule doublets revealed by cryo-electron tomography. Nature 442, 475–478.

Sui, H., Downing, K.H., 2010. Structural basis of interprotofilament interaction and lateral deformation of microtubules. Structure 18, 1022–1031.

Sun, L., Veith, J.M., Pera, P., Bernacki, R.J., Ojima, I., 2010. Design and synthesis of *de novo* cytotoxic alkaloids by mimicking the bioactive conformation of paclitaxel. Bioorg. Med. Chem. 18, 7101–7112.

Sun, M., Wartel, M., Cascales, E., Shaevitz, J.W., Mignot, T., 2011. Motor-driven intracellular transport powers bacterial gliding motility. Proc. Natl. Acad. Sci. USA 108, 7559–7564.

Tadros, M., Gonzalez, J.M., Rivas, G., Vicente, M., Mingorance, J., 2006. Activation of the *Escherichia coli* cell division protein FtsZ by a low-affinity interaction with monovalent cations. FEBS Lett. 580, 4941–4946.

Tan, D., Rice, W.J., Sosa, H., 2008. Structure of the kinesin13-microtubule ring complex. Structure 16, 1732–1739.

Taylor, K.A., Reedy, M.C., Cordova, L., Reedy, M.K., 1989. Three-dimensional image reconstruction of insect flight muscle. II. The rigor actin layer. J. Cell Biol. 109, 1103–1123.

Tian, G., Bhamidipati, A., Cowan, N.J., Lewis, S.A., 1999. Tubulin folding cofactors as GTPase-activating proteins. GTP hydrolysis and the assembly of the alpha/beta-tubulin heterodimer. J. Biol. Chem. 274, 24054–24058.

Tojkander, S., Gateva, G., Schevzov, G., Hotulainen, P., Naumanen, P., Martin, C., et al., 2011. A molecular pathway for myosin II recruitment to stress fibers. Curr. Biol. 21, 539–550.

Toro, E., Shapiro, L., 2010. Bacterial chromosome organization and segregation. Cold Spring Harb. Perspect. Biol. 2, a000349.

Usui, T., Watanabe, H., Nakayama, H., Tada, Y., Kanoh, N., Kondoh, M., et al., 2004. The anticancer natural product pironetin selectively targets Lys352 of alpha-tubulin. Chem. Biol. 11, 799–806.

van den Ent, F., Löwe, J., 2000. Crystal structure of the cell division protein FtsA from *Thermotoga maritima*. EMBO J. 19, 5300–5307.

van den Ent, F., Amos, L.A., Löwe, J., 2001. Prokaryotic origin of the actin cytoskeleton. Nature 413, 39–44.

van den Ent, F., Moller-Jensen, J., Amos, L.A., Gerdes, K., Löwe, J., 2002. F-actin-like filaments formed by plasmid segregation protein ParM. EMBO J. 21, 6935–6943.

van den Heuvel, M.G., de Graaff, M.P., Dekker, C., 2008. Microtubule curvatures under perpendicular electric forces reveal a low persistence length. Proc. Natl. Acad. Sci. USA 105, 7941–7946.

Vaughan, S., Wickstead, B., Gull, K., Addinall, S.G., 2004. Molecular evolution of FtsZ protein sequences encoded within the genomes of archaea, bacteria, and eukaryota. J. Mol. Evol. 58 (1), 19–29. http://www.ftsz.bravehost.com/ftsz.htm.

Vitre, B., Coquelle, F.M., Heichette, C., Garnier, C., Chretien, D., Arnal, I., 2008. EB1 regulates microtubule dynamics and tubulin sheet closure *in vitro*. Nat. Cell Biol. 10, 415–421.

Voter, W.A., Erickson, H.P., 1979. Tubulin rings: curved filaments with limited flexibility and two modes of association. J. Supramol. Struct. 10, 419–431.

Wade, R.H., 2009. On and around microtubules: an overview. Mol. Biotechnol. 43, 177–191.

Wang, H.W., Nogales, E., 2005. Nucleotide-dependent bending flexibility of tubulin regulates microtubule assembly. Nature 435, 911–915.

Wang, H.W., Long, S., Finley, K.R., Nogales, E., 2005. Assembly of GMPCPP-bound tubulin into helical ribbons and tubes and effect of colchicine. Cell Cycle 4, 1157–1160.

Watts, N.R., Cheng, N., West, W., Steven, A.C., Sackett, D.L., 2002. The cryptophycin-tubulin ring structure indicates two points of curvature in the tubulin dimer. Biochemistry 41, 12662–12669.

Wegner, A., 1976. Head to tail polymerization of actin. J. Mol. Biol. 108, 139–150.

White, E.L., Ross, L.J., Reynolds, R.C., Seitz, L.E., Moore, G.D., Borhani, D.W., 2000. Slow polymerization of *Mycobacterium tuberculosis* FtsZ. J. Bacteriol. 182, 4028–4034.

Wickstead, B., Gull, K., 2007. Dyneins across eukaryotes: a comparative genomic analysis. Traffic 8, 1708–1721.

Wickstead, B., Gull, K., Richards, T.A., 2010. Patterns of kinesin evolution reveal a complex ancestral eukaryote with a multifunctional cytoskeleton. BMC Evol. Biol. 10, 110.

Widlund, P.O., Stear, J.H., Pozniakovsky, A., Zanic, M., Reber, S., Brouhard, G.J., et al., 2011. XMAP215 polymerase activity is built by combining multiple tubulin-binding TOG domains and a basic lattice-binding region. Proc. Natl. Acad. Sci. USA 108, 2741–2746.

Wilkes, D.E., Watson, H.E., Mitchell, D.R., Asai, D.J., 2008. Twenty-five dyneins in *Tetrahymena*: a re-examination of the multidynein hypothesis. Cell Motil. Cytoskeleton 65, 342–351.

Xu, K., Luduena, R.F., 2002. Interaction of nocodazole with tubulin isotypes. Drug Dev. Res. 55, 39–52.

Yan, K., Pearce, K.H., Payne, D.J., 2000. A conserved residue at the extreme C-terminus of FtsZ is critical for the FtsA-FtsZ interaction in *Staphylococcus aureus*. Biochem. Biophys. Res. Commun. 270, 387–392.

Yang, Y., Alcaraz, A.A., Snyder, J.P., 2009. The tubulin-bound conformation of paclitaxel: T-taxol vs "PTX-NY" J. Nat. Prod. 72, 422–429.

Yuan, A., Kumar, A., Peterhoff, C., Duff, K., Nixon, R.A., 2008. Axonal transport rates *in vivo* are unaffected by tau deletion or overexpression in mice. J. Neurosci. 28, 1682–1687.

Yutin, N., Wolf, M.Y., Wolf, Y.I., Koonin, E.V., 2009. The origins of phagocytosis and eukaryogenesis. Biol. Direct 4, 9.

Zanic, M., Stear, J.H., Hyman, A.A., Howard, J., 2009. EB1 recognizes the nucleotide state of tubulin in the microtubule lattice. PLoS One 4, e7585.

Zimmerman, S., Chang, F., 2005. Effects of {gamma}-tubulin complex proteins on microtubule nucleation and catastrophe in fission yeast. Mol. Biol. Cell 16, 2719–2733.